Volume 21, Number 4

October, 1966

SOVIET ATOMIC ENERGY

АТОМНАЯ ЭНЕРГИЯ
(ATOMNAYA ENERGIYA)

TRANSLATED FROM RUSSIAN

CONSULTANTS BUREAU

SOVIET ATOMIC ENERGY

Soviet Atomic Energy is a cover-to-cover translation of *Atomnaya Énergiya*, a publication of the Academy of Sciences of the USSR.

An arrangement with Mezhdunarodnaya Kniga, the Soviet book export agency, makes available both advance copies of the Russian journal and original glossy photographs and artwork. This serves to decrease the necessary time lag between publication of the original and publication of the translation and helps to improve the quality of the latter. The translation began with the first issue of the Russian journal.

Subscription (12 Issues): $95

Single Issue: $30
Single Article: $15

Order from:

CONSULTANTS BUREAU
227 West 17th Street, New York, New York 10011

SOVIET ATOMIC ENERGY

A translation of *Atomnaya Énergiya*

Volume 21, Number 4 October, 1966

CONTENTS

CONTENTS

(continued)

NOTE

The Table of Contents lists all material that appeared in the original Russian journal. Items originally published in English or generally available in the West are not included in the translation and are shown in brackets. Whenever possible, the English-language source containing the omitted items is given.

The Russian press date (podpisano k pechati) of this issue was 10/3/1966. Publication therefore did not occur prior to this date, but must be assumed to have taken place reasonably soon thereafter.

IN MEMORIAM: ACADEMICIAN V.I. VEKSLER

Vladimir Iosifovich Veksler, one of the most prominent of contemporary physicists, died on September 22. Soviet nuclear physics lost a brilliant scientist and a remarkable organizer.

V.I. Veksler was born in Zhitomir in 1907. In 1931 he was graduated from the Moscow Power Institute. While still a student V.I. Veksler began working at the All-Union Electrotechnical Institute. For many years prior to 1936 he was engaged in x-ray analysis. He developed a new method for making x-ray measurements by using a modified Geiger counter operating in the proportional region. Much of his work of this period was devoted to the development of methods for recording ionizing radiation. This work was later summarized in the monographs "Experimental Methods of Nuclear Physics" in collaboration with N.A. Dobrotin and L.V. Groshev in 1940, and "Ionization Methods in Radiation Research" written with L.V. Groshev and B.M. Isaev in 1949. In 1935 V.I. Veksler was awarded the academic degree of Candidate of Physical and Mathematical Sciences.

In 1936 Academician S.I. Vavilov invited V.I. Veksler to work at the Lebedev Physics Institute of the Academy of Sciences of the USSR. Here Vladimir Iosifovich studied cosmic rays. In the Elbrus expeditions of 1937-1940 V.I. Veksler's group used proportional counters to study the heavy, strongly ionizing particles in cosmic rays. Even the earliest experimental data argued strongly against the assumption that the penetrating component of cosmic rays consisted of protons. In 1940 V.I. Veksler defended his doctor's dissertation on "Heavy Particles in Cosmic Rays."

The war interrupted V.I. Veksler's work on cosmic rays. However, during the war years he was able to apply radio engineering methods used in cosmic ray physics to the solution of several important defense problems.

Beginning in 1944 V.I. Veksler led a cosmic-ray research group to Pamir. The most important results of this stage of the work was the discovery of a new type of shower, later called an electron-nuclear shower, in which electrons are formed along with secondary nuclear-active particles. The investigation of the properties of these showers and their production set the whole trend in cosmic-ray physics.

While carrying on his cosmic-ray research Vladimir Iosifovich was also for a long time seeking new methods for accelerating charged particles. After the construction of the cyclotron, a device which played an important role in nuclear physics, there occurred a lull in the development of particle accelerators. It seemed that the relativistic increase in mass of the particles set a limit on the energy which could be attained in a cyclotron. In 1944 V.I. Veksler conceived the principle of phase stability. This fruitful idea revolutionized accelerator technology and established the basis for all ultrahigh-energy accelerators in operation, under construction, or being designed. V.I. Veksler noticed that if the increase in mass is very large it is possible to construct a relativistic cyclotron. For if the increase in mass changes the period of revolution by a multiple of the period, resonance is not destroyed. An accelerator of this type was later called a microtron.

In developing the theory of the microtron V.I. Veksler discovered a remarkable property of resonance accelerators called phase stability. It turned out that the relativistic increase in mass with energy may be used to preserve resonance when there is a change in accelerator parameters. V.I. Veksler proposed a whole series of accelerators using the principle of phase stability. The most important of these were: a synchrotron

Translated from Atomnaya Énergiya, Vol. 21, No. 4.

accelerating electrons to ultrahigh energies, a phasotron or synchrocyclotron accelerating protons to 1000 MeV, and a synchrophasotron to accelerate protons to ultrahigh energies.

In 1947 a small 30 MeV synchrotron, under construction since late 1944 at the Physics Institute, was put into operation. This synchrotron, the first in the Soviet Union, has been used successfully for research in nuclear physics. In 1949 a 280 MeV synchrotron was started up.

For several years V.I. Veksler worked in the fields of photonuclear and photomeson physics where, under his leadership, much first-class research was performed, Among these projects were the proof of isotopic invariance in photomesonic reactions, the photodisintegration of the deuteron, the photoproduction of π^- mesons close to threshold, and the creation of π^0 mesons in deuterium. In the latter problem particles were selected by their time of flight in a magnetic field. This allows one to separate the effects of the photoproduction of π^0 mesons with and without the disintegration of the deuteron, and shows that the cross sections of the two processes are comparable.

As a result of the initiative of V.I. Veksler, S.I. Vavilov, and D.V. Efremov, the development of a large proton accelerator — the 10 GeV Dubna synchrophasotron – was begun in 1949. At the same time a model of this accelerator was constructed at the Physics Institute. At the present time it is being used to accelerate electrons to 700 MeV. During this period V.I. Veksler was devoting most of his attention to the construction of large accelerators, but he steadily continued his search for new accelerator methods.

In 1947 Veksler, Burshtein, and Kolomenski proposed a stochastic acceleration method where even in the absence of resonance it is possible to arrange conditions so that particles acquire large energies in a random fashion during a finite time interval.

The so-called coherent method of acceleration, differing in principle from all previously proposed methods was introduced in 1950. In ordinary accelerators the particles acquire energy from an external electromagnetic field which is synchronized with the motion of the particles. In the coherent method the particles themselves produce the accelerating field whose magnitude is proportional to the number of accelerated particles.

In research performed from 1950 to 1958 various schemes for coherent accelerators were studied: 1) the radiative acceleration of plasmoids; 2) the acceleration of proton clusters by electron clusters; and 3) the collisions of clusters and ring currents. Experimental tests of these methods have recently been started.

After the startup of the Dubna synchrophasotron in 1957 Veksler switched back to high-energy physics. After the discovery of the antisigma minus hyperon he focused his attention on the study of the creation of strange particles by high energy π^- mesons. Some important rules were established for these phenomena. The work on the investigation of resonance interactions of elementary particles was of great importance.

V.I. Veksler spent a good deal of his time working with students, many of whom are now leaders of large scientific establishments working in the fields of accelerators, cosmic rays, plasma physics, nuclear physics, and high-energy physics.

In 1947 Veksler was elected a Corresponding Member of the Academy of Sciences of the USSR and in 1958 he was made a member of the Academy. In 1963 he was elected Academic Secretary of the department of Nuclear Physics of the Academy of Sciences of the USSR. He was awarded the Lenin prize and other high scientific awards of the USSR for his work. V.I. Veksler's services in the field of scientific development in the USSR have been rewarded by three Orders of Lenin, an Order of the Red Banner, and medals.

V.I. Veksler organized many international conferences on high-energy physics and accelerators. He was active in organizing international cooperation in these fields of physics. For several years he was a member, and then chairman, of the International Commission on High-Energy Physics.

V.I. Veksler's contributions to science were not confined to his research, books, and inventions. He examined the work of students and colleagues with exceptional care, generously sharing ideas, discussing problems, making suggestions, and offering criticism.

By his modesty, his astonishing capacity for work, and his boundless love of science he inspired and

instructed his co-workers. Students were attracted to him, and he particularly enjoyed working with them.

The memory of V. I. Veksler, distinguished scholar and physicist, will always remain in the history of science and in the hearts of all who knew him.

SYNTHESIS OF SEVERAL ISOTOPES OF FERMIUM AND DETERMINATION OF THEIR RADIOACTIVE PROPERTIES

G. N. Akap'ev, A. G. Demin, V. A. Druin, É. G. Imaev, I. V. Kolesov, Yu. V. Lobanov, and L. P. Pashchenko

UDC 539.172.817:546.799

The article describes the results of experiments in which U^{238} and U^{235} were irradiated with accelerated ions of O^{16}, using an internal beam of the OIYaI 310-cm cyclotron. In the procedure used, the products of the nuclear reactions were collected by means of a stream of gas, and the α-decay was then recorded with (Si + Au) detectors. The excitation functions of the (O^{16}, xn) reactions were studied. Four isotopes of fermium, with mass numbers of 250, 249, 248, and 246, were investigated. Data on the energies and half-life periods of these isotopes were obtained.

Among the transuranium elements the products of nuclear reactions caused by heavy ions are, for the most part, relatively short-lived neutron-deficient isotopes. One of the principal modes of decay of these isotopes is α-decay. The cross section of formation of these isotopes decreases with increasing Z because of the strong competition from fission. In order to obtain information on new isotopes in this range, we need a rapid and highly efficient method which can also provide good energy resolution in the recording of the α-particles. These requirements are satisfied, in the main, by the method of collecting the reaction-product nuclei by adsorption from a stream of gas [1].

The purpose of the present study is to examine the α-decay of neutron-deficient isotopes of fermium by this method.

MEASUREMENT PROCEDURE

Figure 1 shows a diagram of the apparatus. A number of technical details of its design are taken from the work of V. L. Mikheev [2].

A beam of accelerated ions was passed through the aluminum foil of the chamber inlet window, the target, and the foil of the outlet window, hit the collector, and was recorded by means of a current integrator. The reaction-product nuclei knocked out of the target were slowed down in a helium-filled chamber and then carried off by a stream of gas through an approximately 0.5-mm diameter opening into the sampler. A hermetically sealed VN-1 vacuum pump was used to maintain the pressure drop between the chamber and the sampler. It continuously pumped the helium out of the sampler and through a system of traps, cooled with liquid nitrogen, into the chamber. The pressure in the chamber was selected on the basis of the path lengths of the reaction products.

The recoil nuclei caught by the stream of helium were deposited inside the sampler on special collectors consisting of discs 10 mm in diameter attached to the ends of a cross-shaped member. When the member was rotated through 90°, the accumulated activity to be recorded was transferred to a semiconductor detector. A Maltese cross was used for precise positioning of the member when the collector was exposed to the detector (during the measurement) and to the stream of helium (to collect the recoil nuclei) and to shift it rapidly from one position to the next (in about 0.12 sec). It was mounted on the same shaft with the cross-shaped member and driven by an electric motor and a transmission system.

The energy and time distributions of the pulses were analyzed as follows. The amplified pulses from the semiconductor detector passed through a linear network to an analog-digital converter if their amplitude exceeded the threshold of the discriminator. In the analog-digital converter the pulse

Translated from Atomnaya Énergiya, Vol. 21, No. 4, pp. 243-246, October, 1966. Original article submitted May 17, 1966.

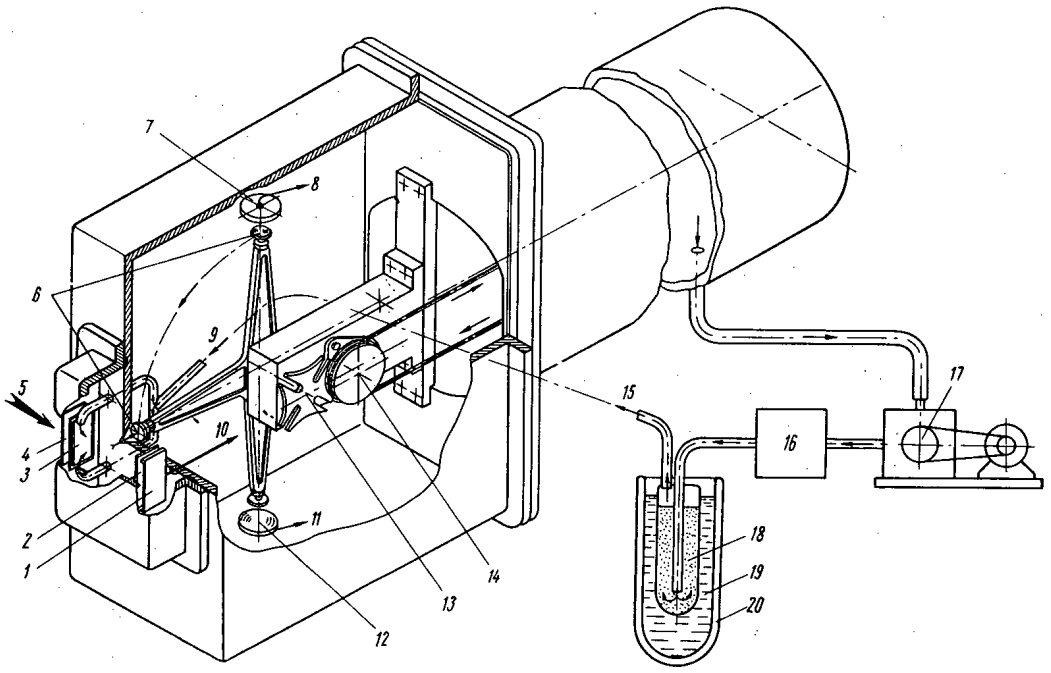

Fig. 1. Diagram of experimental apparatus: 1) ion collector; 2) outlet window (15 μ Al); 3) target (backing 6 μ Al, uranium layer 1 mg/cm^2), 4) inlet window (6μ Al); 5) ion beam; 6) recoil-nucleus collectors; 7) semiconductor detector; 8) to preamplifier; 9) helium; 10) to current integrator; 11) to preamplifier; 12) semiconductor detector; 13) Maltese cross; 14) pulley; 15) helium; 16) filter; 17) pump; 18) activated charcoal; 19) liquid nitrogen; 20) Dewar flask.

amplitude was converted into a series of standard pulses, which were then recomputed by means of a binary-decimal computer. The pulses, corresponding to the range of energies measured, were recorded by a digital printer designed on the principle of a telegraph instrument [3].

The system driving the Maltese cross was adjusted in accordance with the half-life of the activity measured and was fixed by an automatic circuit consisting of a chain of triggers which converted the pulses from the shaper and had a tracking frequency of 50 cps. The conversion factor of this chain determined the duration of one measurement-and-irradiation cycle and could be varied from 2^6 to 2^{12} (T_{cycle} = 1-800 sec).

When the system changed from irradiation to measurement, the motor was fed by means of a starting pulse from one of the triggers of the automatic circuit. After the cross-shaped member had turned 90°, the manipulator of the HF generator was shut off and the linear transmission network was opened.

The automatic control system determined the eight time intervals of the measuring process. The arrival time and amplitude of the reported pulse were marked by the telegraph instrument.

RESULTS OF THE EXPERIMENT

The fermium isotopes were synthesized in nuclear reactions in which targets of natural uranium and U^{235}, with a thickness of 1.5 mg/cm^2, were irradiated with accelerated O^{16} ions. The energy of the ions was measured in the 80-105 MeV range by shifting the sampler along a radius. This energy is enough to evaporate 4-6 neutrons from a compound nucleus.

When natural-uranium targets were irradiated, we observed activities with α-particle energies of 7.42 ± 0.03, 7.53 ± 0.02, and 7.88 ± 0.03 MeV and half-lives of 30 ± 3, 2.6 ± 0.7, and 0.60 ± 0.06 min, respectively.

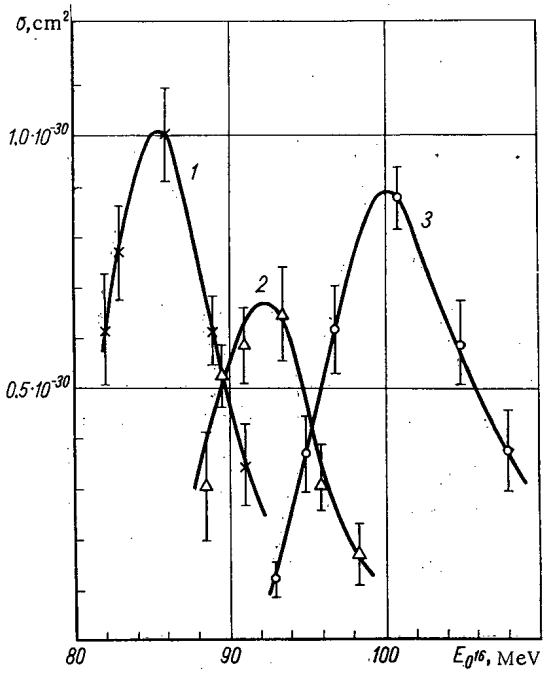

Fig. 2. Excitation functions of the reactions U^{238} (O^{16}, 4; 5; 6n) $Fm^{250-248}$ (curves 1, 2, and 3, respectively). The absolute values of the cross section were not measured; to convert to absolute values, we used known data on the U^{238} (O^{16}, 4n) Fm^{250} reaction [4]. The statistical errors are shown.

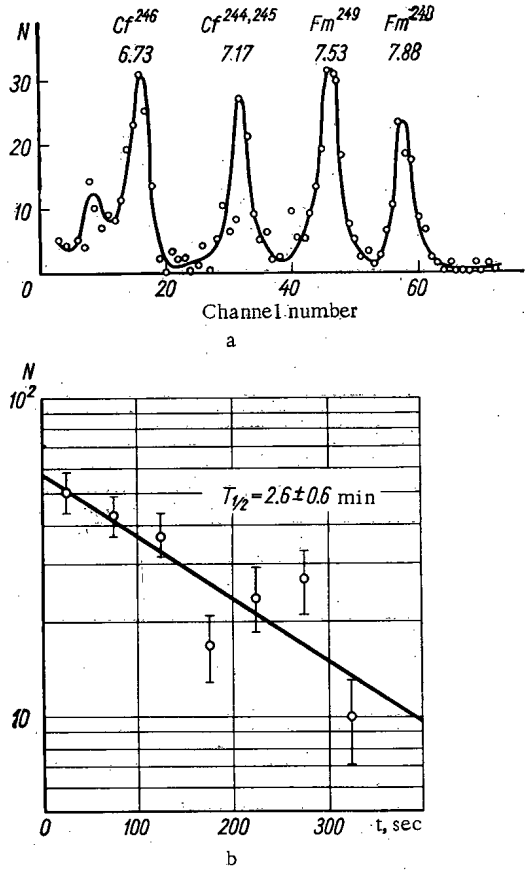

Fig. 3. α-particle spectrum measured when U^{238} targets were irradiated with O^{16} ions (a), and decay curve of Fm^{249} (b).

The yield of each of these activities as a function of the energy of the bombarding ions is shown in Fig. 2. Each curve has the characteristic shape for the excitation function of a reaction with neutron evaporation from a compound nucleus.

The α-particle energies and half-lives of the products of the (O^{16}, 4,6n) reactions agree with the known α-particle energy and half-life values for Fm^{250} and Fm^{248} [4-7].

Figure 3 shows the α-particle spectrum measured when U^{238} targets were irradiated*. The measuring time, equal to the irradiation time, was 400 sec. The group of α-particles with an energy of 7.53 MeV and a half-life of 2.6 min apparently belongs to Fm^{249} formed in the U^{238} (O^{16}, 5n) reaction.

In [8] the following values are given for the half-life and α-particle energy of Fm^{249}: $T_{1/2}$ = 150 sec, $E_\alpha = 7.9 \pm 0.3$ MeV. Since the α-particle energy in [8] was found by the photo-emulsion method, our value for the α-particle energy of Fm^{249} is more accurate. The α-particle energy of Fm^{249} is in good agreement with the classification given in [9]; its decay curve is shown in Fig. 3.

The half-life measurement results were analyzed by the method of least squares. The resulting value of $T_{1/2}$ is practically identical with the data of [8].

From studies dealing with excitation functions of similar nuclear reactions [10], it is known that the maximum cross section for a reaction in which five neutrons evaporate is much higher than the cross section for reactions in which four neutrons and six neutrons evaporate. This rule is a general one and must also hold for the reactions we used for synthesizing the isotopes of fermium.

* The data of a number of experiments with different O^{16} ion energies were added together.

The ratio we found for the maximum yields of Fm^{250}, Fm^{249}, and Fm^{248} α decay indicates that Fm^{249} decays by electron capture in a large percentage of cases.

It is useful to determine the ratio between α decay and electron capture when Fm^{249} disintegrates. It is a practical impossibility to determine this ratio by recording the α decay of the isotopes Es^{249} and Cf^{249} produced in the electron capture of Fm^{249}, since Es^{249} undergoes electron capture in 99.9% of the cases, while the half-life of the Cf^{249} is 360 years. However, the fraction of α decay may be estimated on the basis of the ratio we observed for the maximum yields of Fm^{249} and Fm^{248}; this ratio is approximately 0.8. If the fractions of α decay in the disintegration of Fm^{249} and Fm^{248} are denoted by α_1 and α_2 respectively, we obtain the following formula:

$$\alpha_1 \approx 0.8\alpha_2 \frac{\sigma_{\max}(O^{18}, 6n)}{\sigma_{\max}(O^{18}, 5n)}.$$

The ratio of the maximum cross sections of the U^{238} (O^{16}, 6n) Fm^{248} and U^{238} (O^{18}, 5n) Fm^{249} reactions should be close to the value of 0.5 obtained for the ratio of the maximum cross sections of the U^{238} (O^{16}, 6n) Fm^{250} and U^{238} (O^{18}, 5n) Fm^{251} in [10]. According to the classification, the value α_2 should be close to 100%.

Thus, the fraction of α decay in the disintegration of Fm^{249} (the fraction α_1) is approximately 40%. On the basis of this figure, we can state that the prohibition factor on the α decay of Fm^{249} is approximately unity.

In addition to these tests, we irradiated a target enriched with U^{235} (U^{235} content $\approx$ 90%). For O^{16} ion energies corresponding to the estimated values of the maxima of the excitation function of the U^{235} (O^{16}, 5n) reaction, we obtained an activity with $T_{1/2} = 1.4 \pm 0.6$ sec and an energy of $E_\alpha = 8.23 \pm 0.02$ MeV. These values are in good agreement with the values given in the classification for Fm^{246}. As the energy of the bombarding ions is increased, the yield of this activity decreases, in accordance with the behavior of the excitation function of a complete-fusion reaction with the evaporation of five neutrons. It must be assumed that this α activity belongs to Fm^{246}.

The authors are grateful to G. N. Flerov, Corresponding Member of the Academy of Sciences of the USSR, for his constant help and useful advice; to V. M. Plotko, G. Ya. Tsin Sun-yan, V. I. Krashonkin, and Yu. V. Poluboyarinov of their assistance in conducting the experiments; to the staff of the Radio Electronics Group for designing the apparatus; and to the staff of the Semiconductor Detector Group, who furnished us with silicon α-detectors.

LITERATURE CITED

1. R. Macfarlane and R. Griffioen, Nucl. Instrum. and Methods, 24, 461 (1963).
2. V. L. Mikheev, OIYaI Pre-print 2991 [in Russian]. Dubna (1965).
3. É. G. Imayev and L. P. Chelnokov, Rept. No. 148 at the Sixth Sci. and Tech. Conf. on Nuclear Electronics [in Russian]. Moscow, Atomizdat (1965).
4. V. V. Volkov et al., ZhÉTF, 37, 1207 (1959).
5. S. Amiel et al., Phys. Rev., 106, 553 (1957).
6. A. Ghiorso et al., Phys. Rev. Letters, 1, 18 (1958).
7. A. Ghiorso, Atomnaya Énergiya, 7, 338 (1959).
8. V. P. Perelygin, E. D. Donets, and G. N. Flerov, ZhÉTF, 37, 1559 (1959).
9. V. Viola and G. Seaborg, J. Inorg. Nucl. Chem., 28, 697 (1966).
10. E. D. Donets, V. A. Shchegolev, and V. A. Ermakov, Yadernaya fizika, 2, 1015 (1965).

MEASUREMENT OF THE FAST NEUTRON ALBEDO DOSE FOR DIFFERENT SHIELDS

L. A. Trykov, I. V. Goryachev, and V. I. Kukhtevich

UDC 621.039.58:539.125.52

The energy distribution of neutrons reflected from iron, soil, water, and polyethylene is measured with a monocrystal scintillation spectrometer for various angles of incidence of a beam of reactor neutrons at the surface of the medium being studied. The relationship is developed between the magnitude of the neutron albedo dose and the layer thickness for iron. The experimental data from this paper are compared with the results obtained by other authors.

A knowledge of the albedo is necessary in order to solve many applied problems of engineering physics; e.g., for calculating the passage of radiation through channels and slits in shielding, for calculating the dose intensity of scattered neutrons in closed shields, etc. Consequently, great attention has been paid recently to studying the characteristics of a reflected neutron field.

The numerical albedo of monoenergetic neutrons was measured in an experimental report [1] for paraffin and water in the case of a normally and obliquely incident beam at the surface of the reflector. The range of neutron energies of the original beam studied varied from thermal to 5 MeV.

A certain amount of work has been devoted to the calculation of the differential characteristics of the reflected neutron field by the Monte-Carlo method. In [2], on the basis of the calculated data from [3], empirical relationships are found which describe the angular distribution of the dose intensity of neutrons reflected from iron, concrete, and soils of different moisture content in the case of oblique incidence of monoenergetic neutrons, and neutrons with a fission spectrum, at the surface of the reflector. The numerical and dose albedos are calculated in [4] by the Monte-Carlo method for iron, aluminum, concrete, water, and hydrogen.

After completion of the present paper, a report [5] appeared concerning the experimental investigations of the differential albedo in the case of oblique incidence of reactor neutrons on samples of concrete, 180 × 180 mm and ~ 23 cm thick. A narrow unidirectional beam of neutrons was used for the measurements together with an isotope detector located at a sufficiently large distance from the illuminated spot on the shield. Fast neutron dosimeters were used as detectors.

In the present paper, we studied the energy distributions of fast neutrons reflected from iron, soil, water, and polyethylene in the case of normal and oblique incidence of a broad unidirectional beam of neutrons at the surface of the reflector. In addition, the dependence of the neutron albedo on the thickness of the plane layer of an iron reflector was studied. The measurements were made with an isotope detector located at the surface of the shield.

A zero-power reactor was used as the neutron source. The beams of neutrons were conducted through a cylindrical channel in the shielding with a diameter of 25 cm. The angular divergence of the primary neutron beam was not greater than 4°. (To a good approximation, the beam could be assumed to be parallel.) The neutron beams were directed onto the barrier being studied, which had cross-sectional dimensions of 1000 × 750 mm. The nonuniformity of the neutron beam at the surface of the reflecting medium was not greater than 10% at a diameter of 70 cm.

The experiment showed that for all the media studied and at angles of incidence of the beam at the barrier of up to 70°, the cross-sectional dimensions of the latter ensured complete collection of the reflected radiation; in other words, the condition for an infinitely-wide beam was fulfilled. The barriers and detector were oriented relative to the primary neutron beam by means of a special kinematic device.

Translated from Atomnaya Énergiya, Vol. 21, No. 4, pp. 246-254, October, 1966. Original article submitted April 5, 1966.

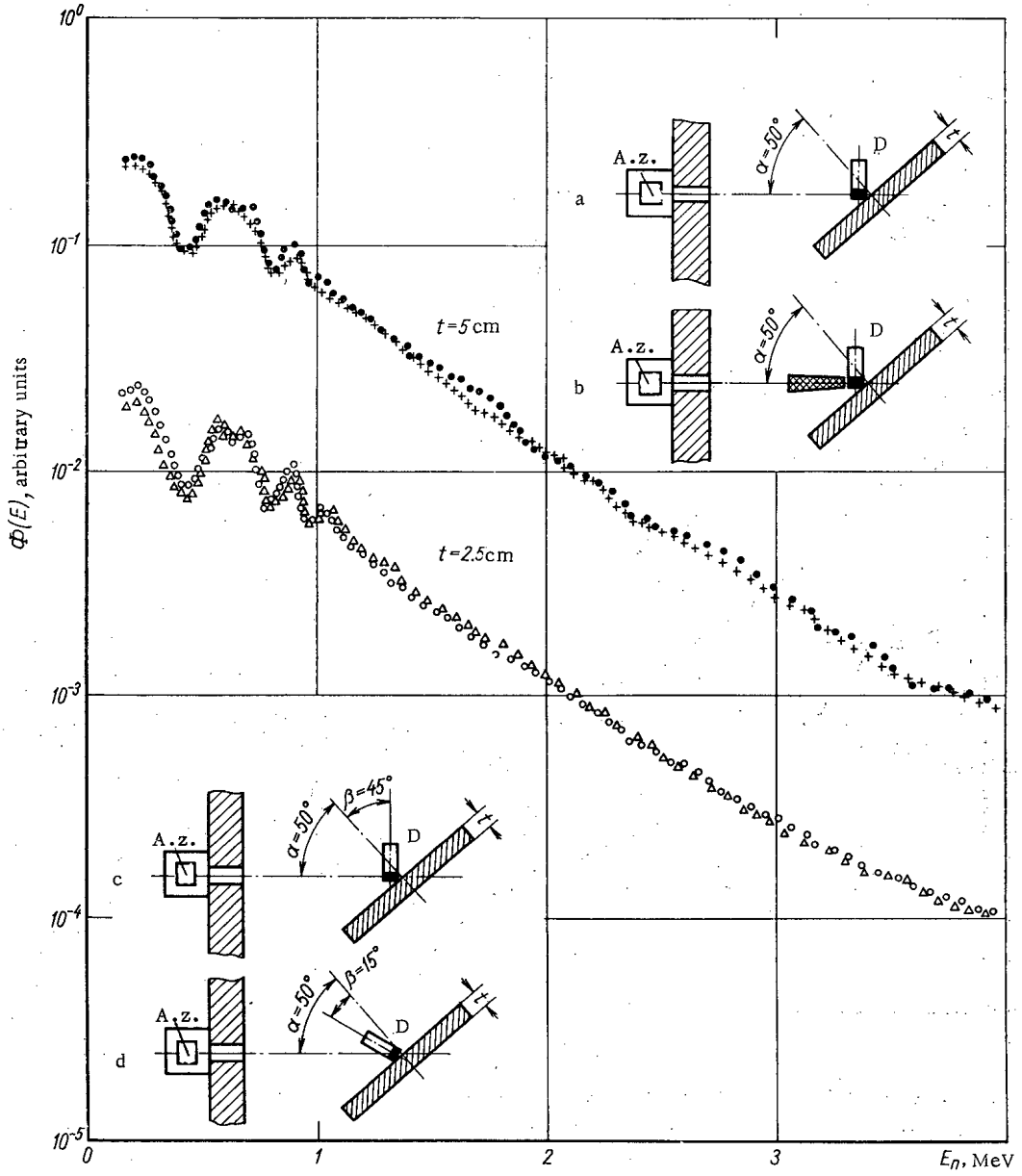

Fig. 1. Procedure for measuring the neutron albedo. a) (●) By the difference of effects at the detector; b) (+) with the conical shield; c) (Δ), d) (○) by the difference of effects at the detector for limiting position of the crystal relative to the screen. A.z. = active zone; D = detector.

A monocrystal scintillation neutron spectrometer was used as the neutron detector, with a γ-ray discrimination with respect to the time of luminescence similar to the spectrometer described in [6]. This was mounted on a type FÉU-13 photomultiplier with a monocrystal of stilbene, 30×20 mm. The spectroscopic recording threshold for neutrons, as a result of cooling the photomultiplier to -5° C was 0.1 to 0.15 MeV for a γ-ray discrimination factor of $\sim 2 \times 10^{-3}$.

If required (for measuring the albedo with hydrogeneous media) the degree of γ-ray discrimination was fixed at $\sim 4 \times 10^{-4}$ and in this case the spectroscopic threshold was 0.2-0.3 MeV. The amplitude distributions were transformed into energy spectra by the method of channelled smoothing differentiation [6].

The total mean-square error of the measurements was 15% in the worst case; for water and polyethylene, and for iron and soil it was not greater than 10%.

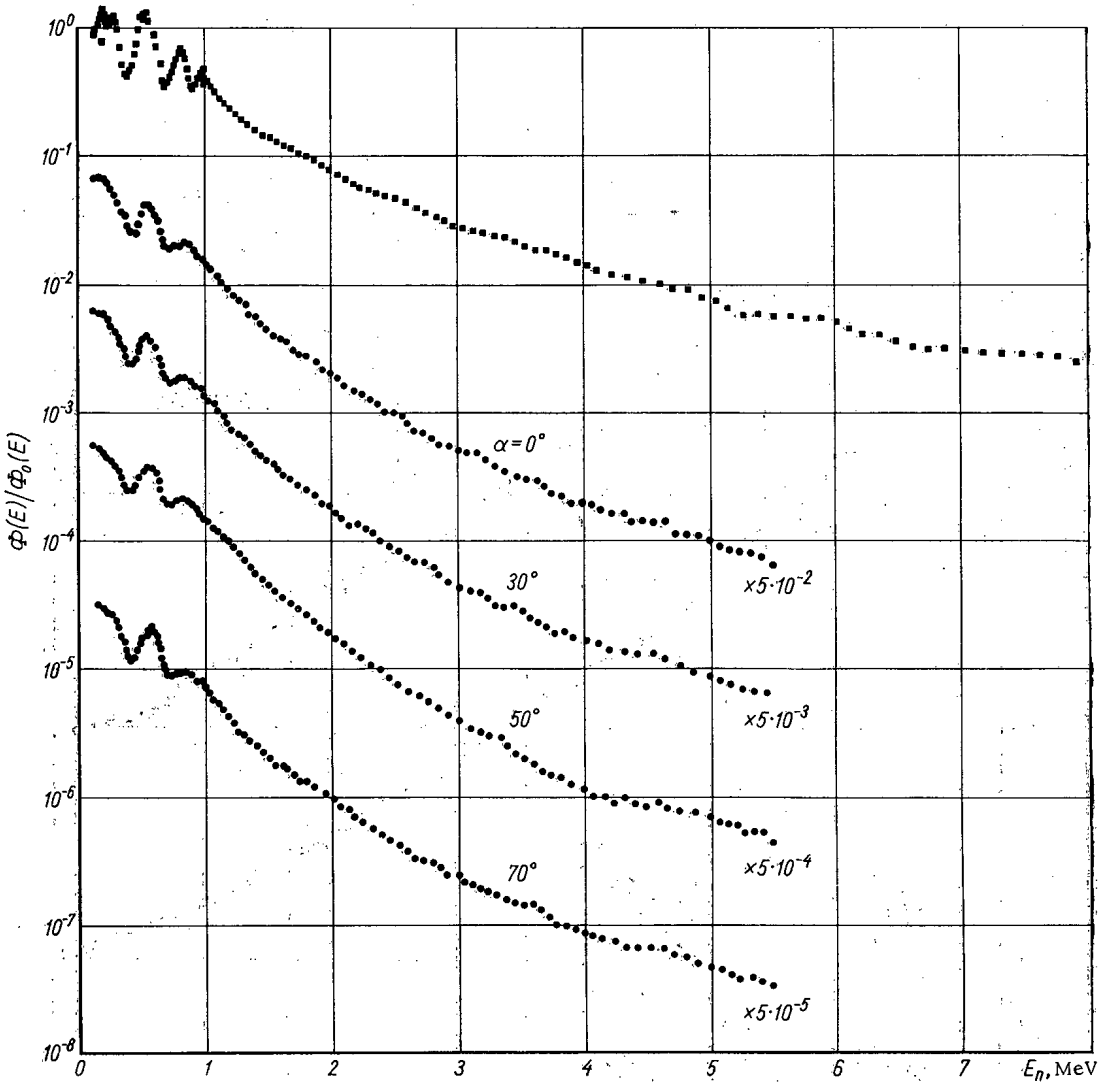

Fig. 2. Spectra of neutrons reflected from iron with a thickness of 19 cm at various angles of incidence of the beam on the shield (here and in Figs. 3-6, the reactor neutron spectrum is shown by the points ■).

The flux of neutrons reflected from the layers of iron was measured by two methods (Fig. 1). In the first case (see Fig. 1a), the number of reflected neutrons was recorded on the background of the primary radiation, i.e., by the difference method. In the second case (Fig. 1b), the nonscattered neutrons were suppressed by the shield cone. Each method has obvious advantages and disadvantages, but the second is preferable from the point of view of the time of measurement. The completely satisfactory agreement in the albedo values (not worse than 10%) measured by both these methods confirms that the shield cone does not introduce any significant discrepancies into the measurement results.

Figure 2 shows the total energy distributions of neutrons reflected from iron 19 cm thick at different angles of beam incidence on the screen (the angle of incidence of the α beam on the screen is measured from the normal to the surface of the screen). In the case of reflection of fast neutrons, this thickness of iron is almost equivalent to a semiinfinite medium [2]. In Fig. 2, the differential albedo is plotted along the axis of ordinate, determined as the flux of reflected neutrons at the surface of the scatterer over the energy range from E to E+dE, relative to the neutron flux in the original beam at the same point over the same energy range. The spectra of the incident neutrons are shown in the same figure.

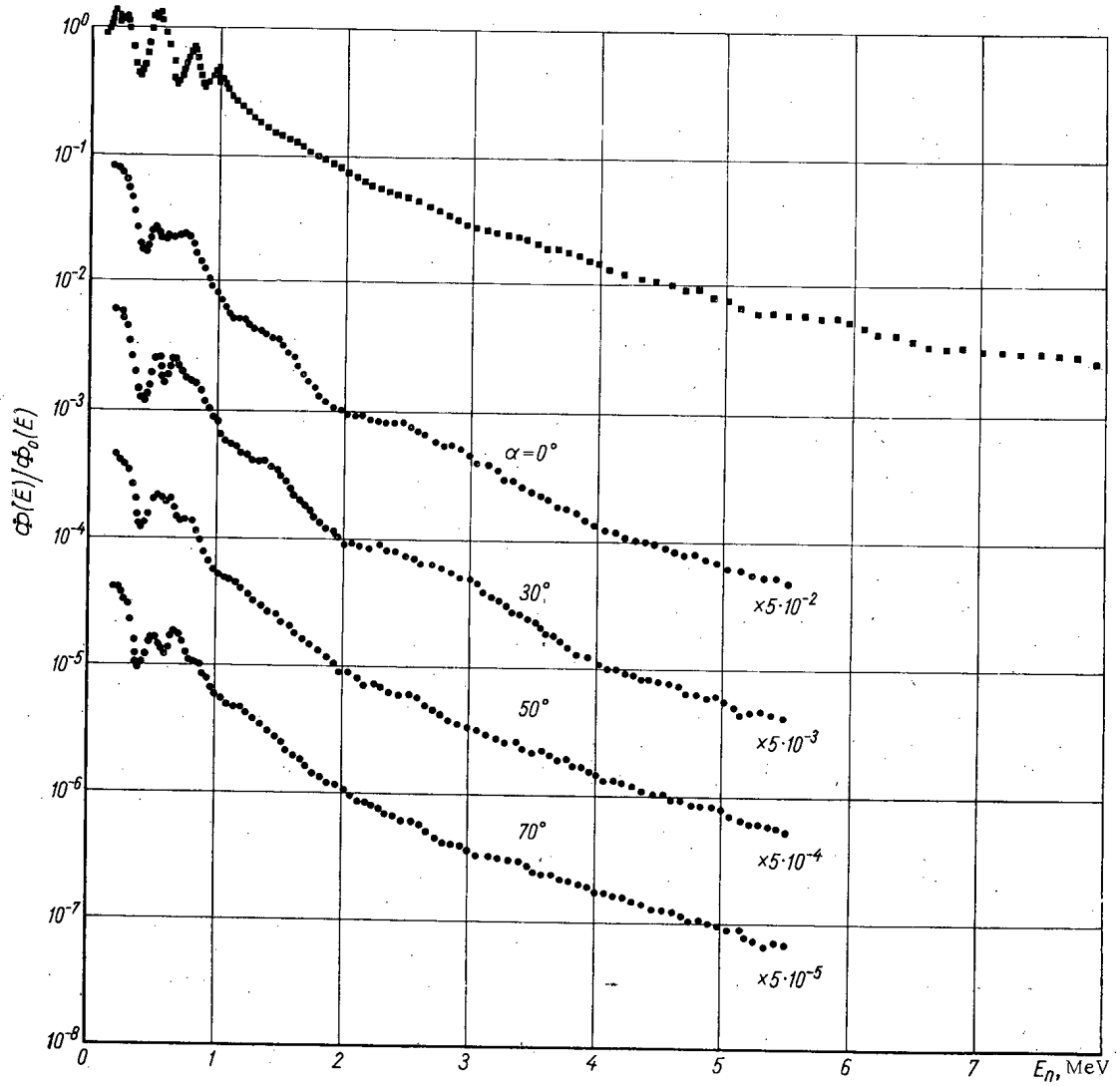

Fig. 3. Energy distribution of neutrons reflected from soil.

It can be seen from the plotted data that in the energy region below ~ 2 MeV, a certain relative buildup of neutrons occurs in the spectrum of the reflected neutrons, which leads to a soft spectrum of the reflected neutrons in comparison with the incident spectrum.

At a neutron energy of $E_n > 2-3$ MeV, the form of the spectrum remains approximately the same as for the initial energy distribution. This behavior of the spectrum can be explained by the fact that in the region of energies greater than ~ 3 MeV, the inelastic neutron scattering cross section is almost independent of the energy, and for $E_n < 3$ MeV, it is reduced sharply with decreasing energy. The energy losses by elastic interactions with iron nuclei are small. This is due to the relative buildup of the number of neutrons in the energy region of less than 1 MeV.

Figure 3 shows the total energy distribution of neutrons reflected from a layer of soil 30 cm thick (equivalent to a semiinfinite medium [2]). The soil density was 1.65 g/cm³. The chemical composition of the soil used in the experiment is as follows:

Element	Content, wt.%
Hydrogen	1.02
Oxygen	54.68
Silicon	41.0
Aluminum	1.30
Iron	1.13
Calcium	0.87

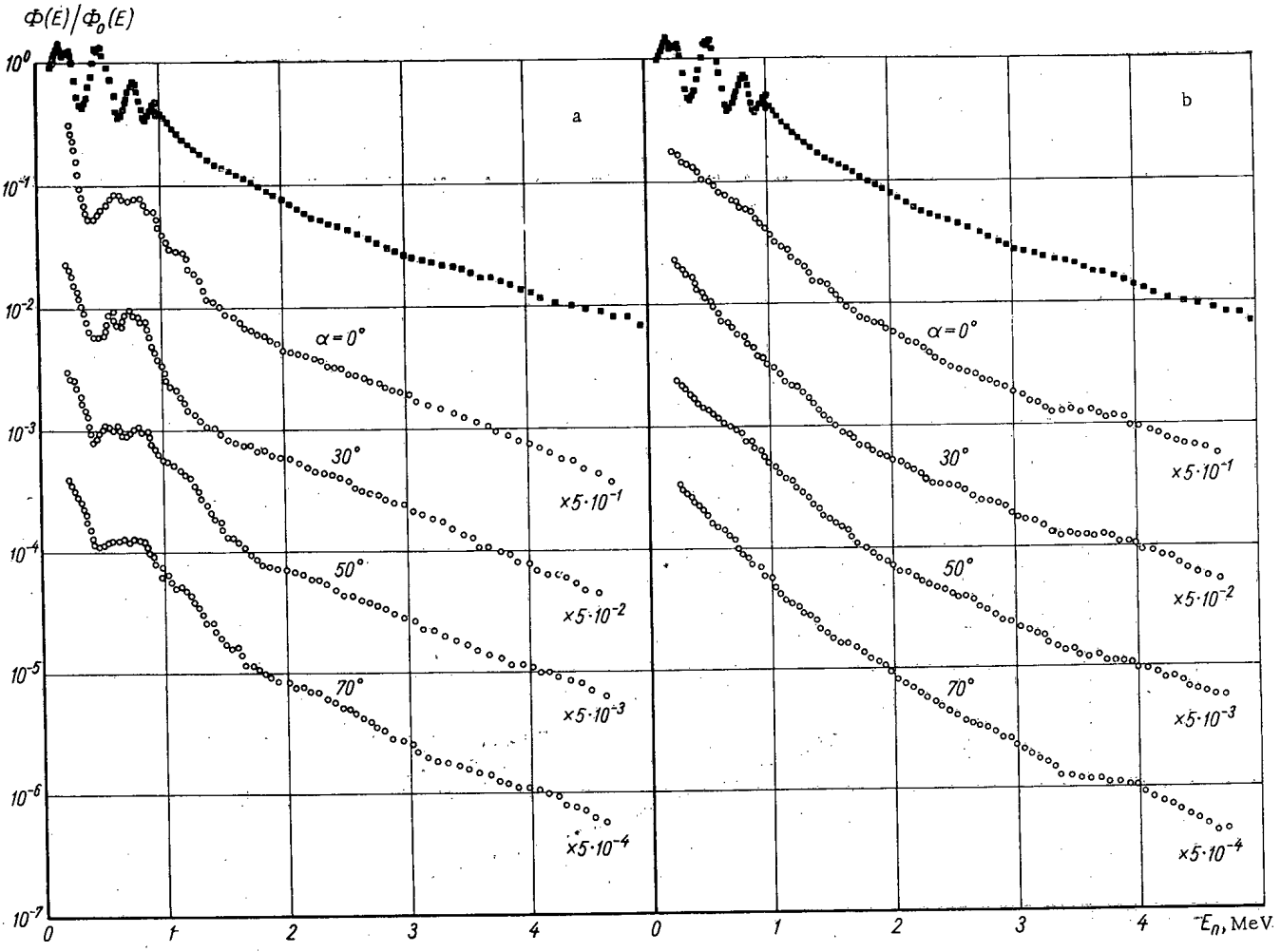

Fig. 4. Spectra of neutrons reflected from layers of water (a) and polyethylene (b).

Since the soil is composed of elements from the middle portion of Mendeleev's Periodic Table of the Elements, the general nature of the neutron interactions with nuclei of these elements is almost the same as for iron.

Figure 4 shows the total spectra of neutrons reflected from water and polyethylene of identical thickness (10 cm) for various angles of incidence of the beam at the surface of the medium. They differ from one another in the irregularities due to the nature of the total neutron cross sections in hydrogen and carbon. In the spectra of neutrons reflected from water, irregularities are noticed in the region of energies of ~ 1 and 2 MeV, due to peculiarities in the neutron cross sections in oxygen nuclei at these energies. The considerable increase of the spectrum of neutrons reflected from polyethylene in the region of 3-5 MeV is due to irregularities in the energy-dependence of the total neutron cross sections in carbon nuclei.

The energy distributions obtained enabled us to find the relationship between the magnitude of the neutron albedo dose and the angle of incidence of the beam on the medium. In order to convert the neutron energy distributions to dose intensity, the conversion factors for flux to dose intensity given in [7] were used.

Figure 5 shows the dependence of the magnitude of the neutron albedo dose for iron (19 cm thick), soil (30 cm), and water (10 cm) on the angle of incidence of the beam at the surface of the reflector. The calculated results of the neutron albedo from iron are plotted in the same figure. These were obtained specially for this experiment by the Monte-Carlo method. The agreement between the calculated results and the experimental data is very satisfactory and is within the limits of experimental and computational accuracy.

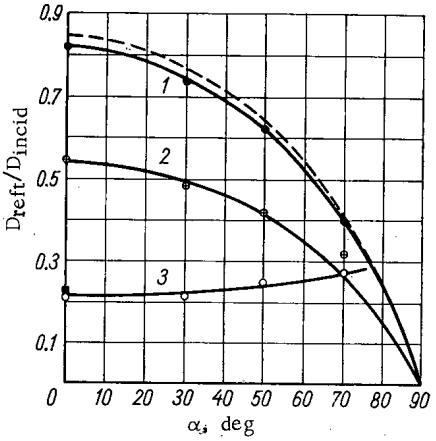

Fig. 5. Dependence of the magnitude of the neutron albedo dose on the angle of incidence of the beam on the medium. 1) Iron, 2) soil, and 3) water.

It can be seen from Fig. 5 that the dependence of the magnitude of the neutron albedo dose on the angle of incidence of the beam at the iron shield agrees with the conclusions of [2] and is accurately described by the expression

$$A(\alpha) = A_0 \cos^{2/3}\alpha, \quad (1)$$

where A_0 and $A(\alpha)$ are the values of normal and oblique incidence (at an angle α) on the shield of given thickness.

The neutron albedo for water as a function of the angle α is entirely different. It can be seen from Fig. 5 that the neutron albedo dose for water increases slightly with increase of the angle α (up to 70°) and can be described by the relationship

$$A(\alpha) = A_0 \cos\alpha + 0.30(1 - \cos\alpha). \quad (2)$$

This dependence of the albedo on the angle of incidence is explained by the singularity of the scattering of neutrons by

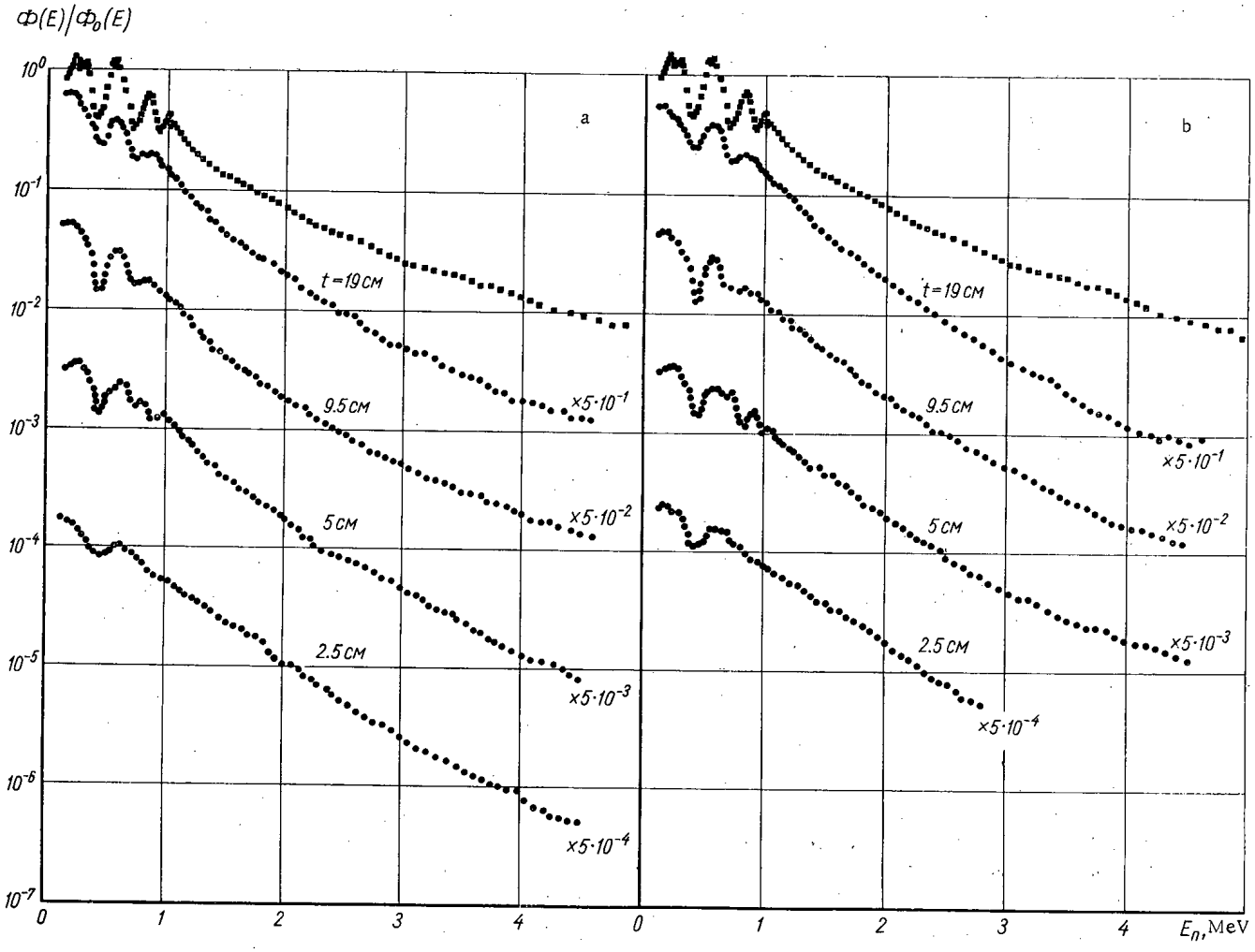

Fig. 6. Spectral distribution of neutrons reflected from layers of iron of different thicknesses. a) $\alpha = 0°$; b) $\alpha = 50°$.

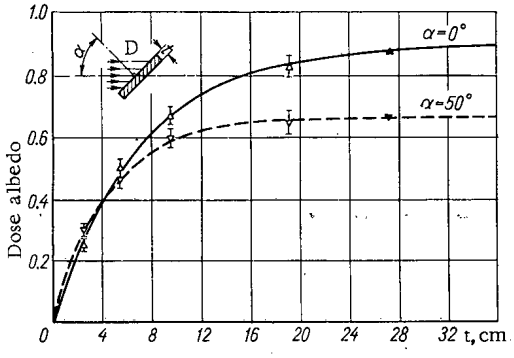

Fig. 7. Dependence of the magnitude of the neutron albedo dosage on the iron thickness. ▲, ▼ - data from [2].

hydrogen nuclei (in comparison with iron). The scattering of neutrons by hydrogen nuclei is directed predominantly "forward." Therefore, by increasing the angle of incidence of the beam at the surface of the scatterer with decreasing values of the scattering angles of the neutrons in an elementary event, removal of neutrons at the surface being illuminated increases the probability for a neutron to proceed in the direction of the source with small loss of energy. This fact, together with an increase of the probability of a neutron being reflected in view of the reduction of the distance from the centers of scattering to the surface – resulting from an increase of the angle – covers the tendency towards reduction of the magnitude of the albedo because of the reduction of the neutron flux through the surface being illuminated as a result of increasing the "grazing" of the beam incidence at the surface of the scatterer. The data obtained for $\alpha = 90°$ are in good agreement with the results of]2] and [4], although in the latter paper this value was calculated only for neutrons with an initial energy equal to 3 MeV.

The value of the albedo dosage of neutrons for iron, in the case of normal incidence of the beam on the shield, was found to be 0.82; this agrees well with the data of [2, 4]. The close equivalence of a 19-cm thick iron plate to a semiinfinite medium is verified by the results obtained in this paper of the study of the relationship between the albedo and the thickness of the reflector; these results are presented in Figs. 6 and 7.

It can be seen from Fig. 7 that by increasing the thickness of the reflector, the magnitude of the albedo dosage can be made to increase, and asymptotically approach a certain limiting value corresponding to the magnitude of the albedo for a semiinfinite medium. It can be seen from this figure that when $\alpha = 50°$, the increase of the magnitude of the albedo with increase of the normal reflector thickness takes place somewhat more rapidly than for $\alpha = 0°$, which agrees well with the conclusions of [5].

In the general case, the magnitude of the neutron albedo dose as a function of the thickness of the iron reflector and the angle of incidence α of the neutron beam on its surface can be described by the expression

$$A(t, \alpha) = A_m \cos^{2/3}\alpha \left(1 - e^{-0.14 \frac{t}{\cos \alpha}}\right), \quad (3)$$

where A_m is the magnitude of the neutron albedo from a semiinfinite medium of iron, equal to 0.90.

The magnitude of the total neutron albedo dose for soil, in the case of normal incidence on its surface of the neutron beam, obtained in this paper is 0.54, which agrees very well (~ 5%) with the data of [4, 5] and somewhat less (~ 15%) with that of [2] for very similar chemical compositions of the soil.

Analysis of the results of [2, 4, and 5] and the data from the present paper show the generality of the values obtained for the albedo dosage for the media studied, since they depend weakly on the form of the spectrum of the neutrons emerging from the reactor.

LITERATURE CITED

1. A. M. Kogan et al., Atomnaya Énergiya, 7, 351 (1959).
2. R. French and M. Wells, Nucl. Sci. and Engng, 19, 441 (1964).
3. F. Allen et al., BRL Rapport No. 1189, 1190, 1199, 1204 (1963).
4. M. Leimdörfer, FOA-4, Rapport A 4365-411, Stockholm, (1966).
5. R. Maerker and F. Muckenthaler, Nucl. Sci. and Engng, 22, 455 (1965).
6. Yu. A. Kazanskii et al., Atomnaya Énergiya, 20, 143 (1966).
7. G. Gol'dshtein, Principles of Reactor Shielding. Moscow, Gosatomizdat (1961).

APPLICATION OF NOMOGRAMS OF EQUIVALENT POINTS IN THE KINEMATICS OF NUCLEAR REACTIONS

G. N. Potetyunko

UDC 539.107.1:518.3

The representation of kinematic relations in nuclear reactions at nonrelativistic energies by nomograms of equivalent points is considered. Working nomograms enabling all kinematic problems in reactions involving the yield of two particles and some extremely important problems (transformation of cross sections and continuous spectra from the laboratory system of coordinates into the center-of-mass system) for reactions involving the yield of three or more particles to be solved are presented. The nomograms not only mechanize a great deal of the calculations, but also provide a picture of the physical aspects of scattering following from kinematical considerations and show how measuring errors affect the error in determining the remaining kinematic parameters.

The nomograms under consideration are extremely convenient for practical use, since they are quite simple and give high accuracy; a particularly important point is that they also give a clear geometric representation of all the special features in the functional relationships being studied.

The authors of [1, 2] published a nomogram for the system of equations [3]

$$\operatorname{ctg}\vartheta_1=\frac{\rho_1+\cos\vartheta}{\sin\vartheta};\quad \operatorname{ctg}\vartheta_2=\frac{\rho_2-\cos\vartheta}{\sin\vartheta}, \tag{1}$$

describing the interrelation between the escape angles of the products of nuclear reaction I + II - 1 + 2* in the laboratory or L system (ϑ_1 and ϑ_2), the escape angle in the center-of-mass or C system (ϑ), and the beam energy E_I. The quantities $\rho_{1\,(2)}$ constitute the ratio of the translational velocity to the velocities of particles 1 and 2 in the C system and are calculated from the formulas [3]

$$\left.\begin{aligned}\rho_{1(2)}&=\sqrt{\frac{A_{1(2)}E_I}{E_I+QB}};\quad A_{1(2)}=\frac{m_{1(2)}m_I}{m_{2(1)}m_{II}};\\ B&=1+\frac{m_I}{m_{II}};\quad \frac{\rho_1}{m_1}=\frac{\rho_2}{m_2}.\end{aligned}\right\} \tag{2}$$

A weak point of the nomogram given in [2] is the fact that values of $\vartheta_{1\,(2)}$ close to 0 and π do not appear on the $\vartheta_{1\,(2)}$ scale. Figure 1 (a and b) presents nomograms obtained from those mentioned by a projective transformation effected by means of formula (6) (see [1]) with $\lambda = 1/\sqrt{24}$ (Fig. 1a) and $\lambda = 1/\sqrt{1{,}25}$ (Fig. 1b). Values of $\vartheta_{1\,(2)}$ close to $\pi/2$ do not appear on these nomograms. Thus the nomograms of [2] supplement those derived in the present paper. The advantage of these is not only that they mechanize the computing process but also that they reflect some of the aspects of the reaction in a clear geometric form. This aspect is fully treated in [4], and we shall therefore here concentrate mainly on aspects omitted from the earlier paper.

Let us first consider the critical points of the nomogram, the intersections of its scales. In our case the scales intersect at $\rho_1=1$ and $\rho_2=1$. These values of ρ_1 and ρ_2 correspond to the following values of beam energy, which we shall call critical:

$$E_{I\,cr}^{(1)}=\frac{m_2Q}{m_I-m_2};\quad E_{I\,cr}^{(2)}=\frac{m_1Q}{m_I-m_1}. \tag{3}$$

* Subsequently index 1 means the light reaction product and index 2 the heavy reaction product. On this condition $\rho_1 \leq \rho_2$.

Translated from Atomnaya Énergiya, Vol. 21, No. 4, pp. 254-262, October, 1966. Original article submitted February 16, 1966.

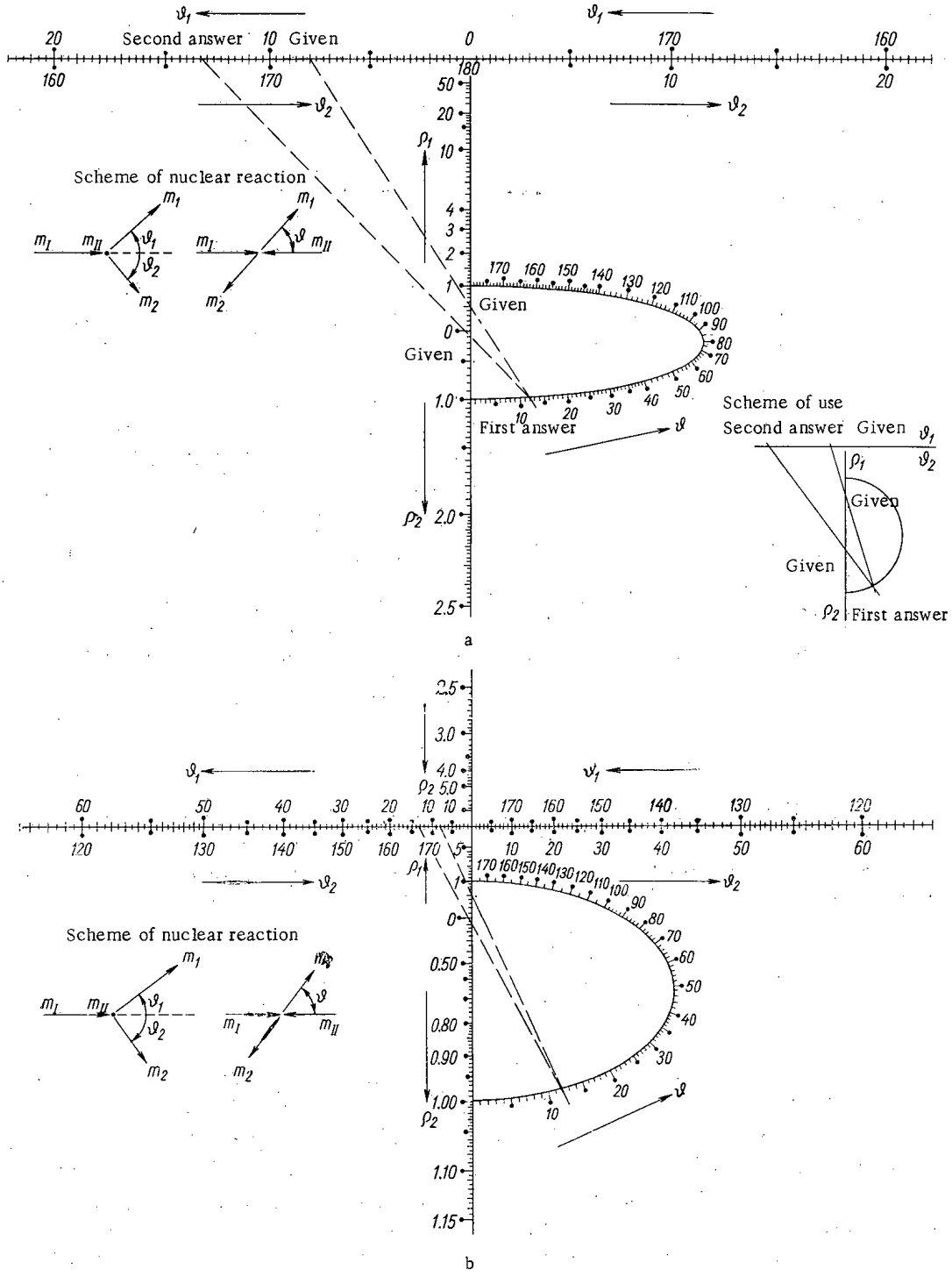

Fig. 1. Nomograms for equation system (1). Example. Given $\vartheta_1=8°, \rho_1=0.5$; $\rho_2=0.1$. We find $\vartheta_2=166°\ 40'$; $\vartheta=12°$.

The values $\rho_1=1$ and $\rho_2=1$ separate single- and double-valued regions in the relation between angles ϑ_1 and ϑ_2. For $\rho_1<1$ and $\rho_2<1$, the relationship between the angles ϑ_1 and ϑ_2 is mutually single-valued or unambiguous. For $\rho_1<1$ and $\rho_2>1$ to one escape angle ϑ_1 of the light reaction product there corresponds one escape angle ϑ_2 of the heavy reaction product, but to one angle ϑ_2 there correspond two angles ϑ_1. For $\rho_1>1$ and $\rho_2>1$ the relationship between ϑ_1 and ϑ_2 is mutually double-valued. The relations between ρ_1 and ρ_2 for various conditions are shown in Tables 1 and 2.

TABLE 1. Conditions of Various Relations Between ρ_1 and ρ_2 for $Q > 0$

Relation between ρ_1 and ρ_2	$m_1>m_I$; $m_2>m_I$	$m_1<m_I$; $m_2>m_I$	$m_1<m_I$; $m_2<m_I$
$\rho_1<1$; $\rho_2<1$	$0<E_I<\infty$	$E_I<\frac{m_1Q}{m_I-m_1}$	$E<\frac{m_1Q}{m_I-m_1}$
$\rho_1<1$; $\rho_2>1$	—	$E_I>\frac{m_1Q}{m_I-m_1}$	$\frac{m_1Q}{m_I-m_1}<E_1<\frac{m_2Q}{m_I-m_2}$
$\rho_1>1$; $\rho_2>1$	—	—	$E_I>\frac{m_2Q}{m_I-m_2}$

TABLE 2. Conditions of Various Relations Between ρ_1 and ρ_2 for $Q < 0$

Relation between ρ_1 and ρ_2	$m_1>m_I$; $m_2>m_I$	$m_1<m_I$; $m_2>m_I$	$m_1<m_I$ $m_2<m_I$
$\rho_1<1$; $\rho_2<1$	$E_I>\frac{m_1Q}{m_I-m_1}$	—	—
$\rho_1>1$; $\rho_2>1$	$\frac{m_2Q}{m_I-m_2}<E_I<\frac{m_1Q}{m_I-m_1}$	$\frac{MQ}{m_I-M}<E_1<\frac{m_2Q}{m_I-m_2}$	—
$\rho_1>1$; $\rho_2>1$	$\frac{MQ}{m_I-M}<E_I<\frac{m_2Q}{m_I-m_2}$	$E_I>\frac{m_2Q}{m_I-m_2}$	$0<E_I<\infty$

It should be noted that all the peculiarities in the relationship between angles ϑ_1 and ϑ_2 have already been indicated in the literature relating to the kinematics of nuclear reactions (see, e.g., [3]), but in the nomogram these appear in an obvious geometrical form.

The nomograms considered above were originally intended for studying the interrelation between the angles ϑ_1, ϑ_2, and ϑ described by equation system (1). More detailed consideration, however, shows that other kinematic problems also reduce to equation system (1), and this greatly widens the possible scope of the nomograms.

Let us first consider the problem of finding the energy $E_{1\,(2)}$ of the escaping particles in the L system. The corresponding system of equations has the form

$$\left.\begin{aligned}\sqrt{2m_IE_I}&=\sqrt{2m_1E_1}\cos\vartheta_1+\sqrt{2m_2E_2}\cos\vartheta_2;\\ 0&=\sqrt{2m_1E_1}\sin\vartheta_1-\sqrt{2m_2E_2}\sin\vartheta_2.\end{aligned}\right\} \tag{4}$$

From (4) we find

$$\operatorname{ctg}\vartheta_2=\frac{\sqrt{m_IE_I/m_1E_1}-\cos\vartheta_1}{\sin\vartheta_1}. \tag{5}$$

Thus we have obtained the second equation of system (1) with $\rho_2=\sqrt{\frac{m_IE_I}{m_1E_1}}$. Hence we have the following order for finding energy E_1 from the nomogram: 1) From the rules given in [1, 2] we find angles ϑ_2; 2) without changing the position of the point on the ϑ_2 scale representing the ϑ_2 value so found, we obtain the angle ϑ_1 from the curvilinear scale and find $\sqrt{m_IE_I/m_1E_1}$ on the ρ_2 scale, after which we calculate E_1. For convenience in use, we recommend superimposing an E_I/E_1 scale or its reciprocal on the ρ_2 scale.

Now let us consider another kinematic problem, that of converting continuous spectra from the L system to the C system in reactions of the form $I+II=1+2+3+\ldots+n$ $(n>2)$. The system of equations describing the interrelation between the L and C systems for the i-th escaping particle has the form

$$\left.\begin{aligned}v_i\cos\theta_i&=v_i'\cos\theta_i'+V;\\ v_i\sin\theta_i&=v_i'\sin\theta_i'.\end{aligned}\right\} \tag{6}$$

Here v_i and v_i' are the velocity of the i-th escaping particle in the L and C systems, θ_i and θ_i' are the escape angles of the i-th particle in the L and C systems, and V is the translational velocity.

It follows from (6) that

$$\operatorname{ctg}\theta_i'=\frac{\cos\theta_i-\rho_i}{\sin\theta_i};\quad \rho_i=\frac{\sqrt{m_Im_i}}{m_I+m_{II}}\sqrt{\frac{E_I}{E_i}}; \tag{7a}$$

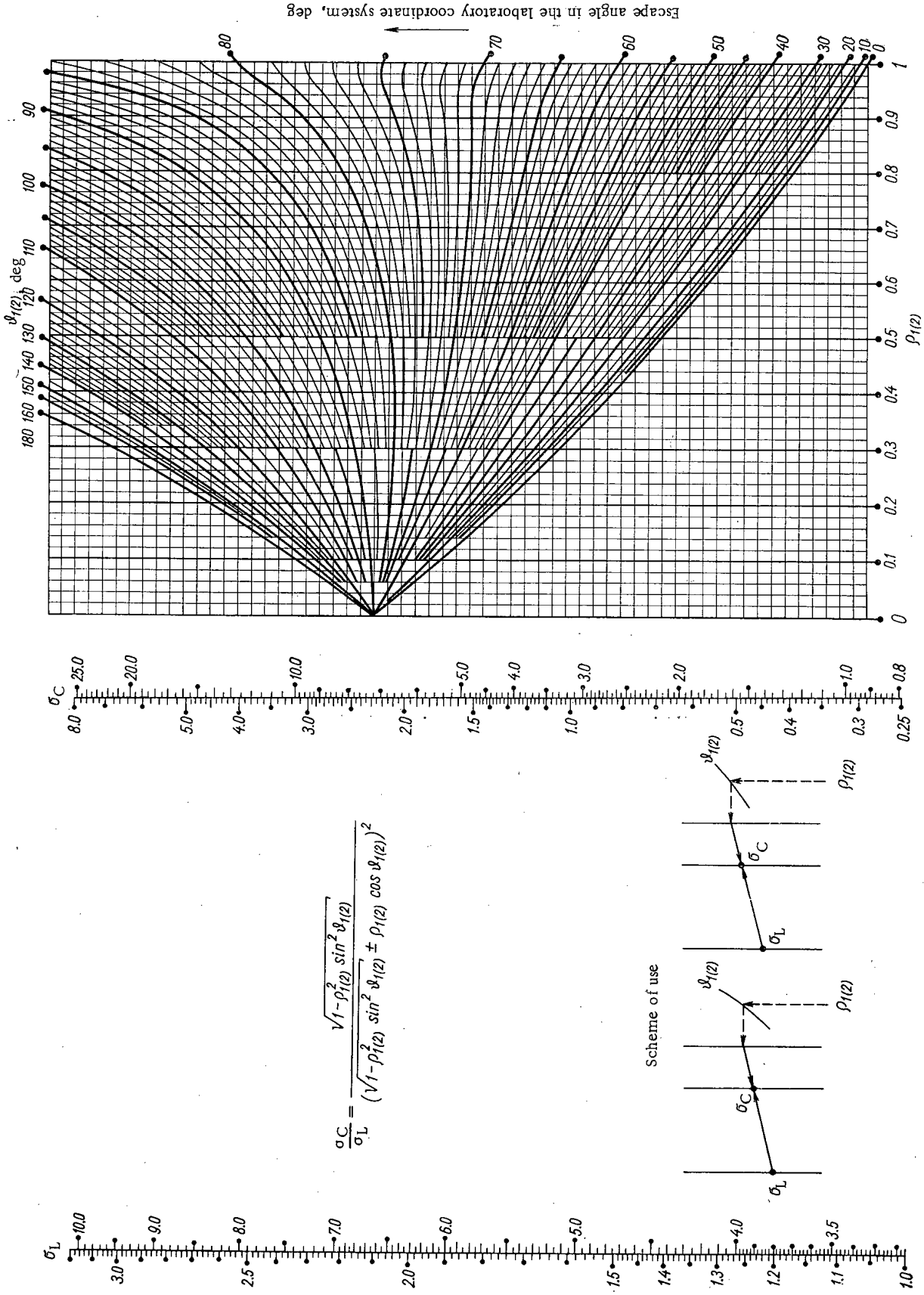

Fig. 2. Nomogram for converting cross sections from the laboratory system of coordinates to the center-of-mass system.

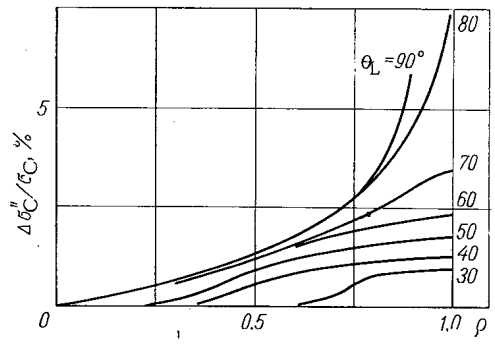

Fig. 3. Values of $\Delta\sigma''_C/\sigma_C$ as a function of ρ for $\Delta\vartheta_{1\,(2)} = \pm 1°$.

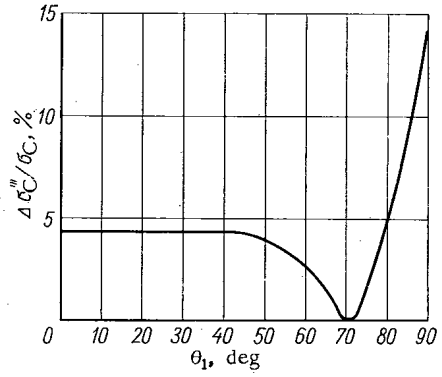

Fig. 4. Values of $\Delta\sigma'''_C/\sigma_C$ as a function of ϑ_1 for the escape of deuterons from the reaction Li^7 (He^4, d) Be^9 with $E_I = 13$ MeV, $\Delta E_I/E_I = 1$, $Q = 7.152$ MeV.

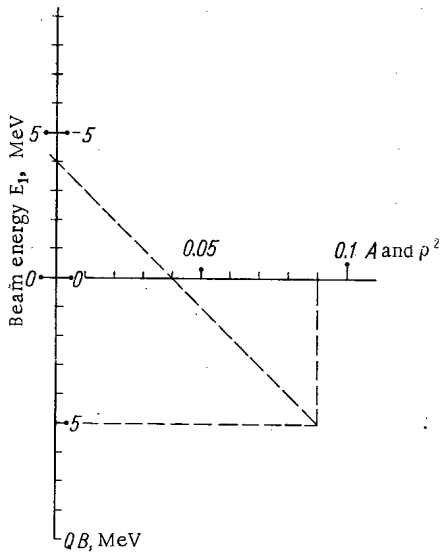

Fig. 5. Nomogram for finding the values of $\rho_{1\,(2)}$ from formula (2). Example. Given $E_I = 4$ MeV, $A = 0.09$; $QB = 5$ MeV. We find: $\rho^2 = 0.04$; $\rho = 0.2$.

$$\operatorname{ctg}\theta_i = \frac{\cos\theta'_i + \rho'_i}{\sin\theta'_i}\,; \quad \rho'_i = \frac{\sqrt{m_I m_i}}{m_I + m_{II}}\sqrt{\frac{E_I}{E'_i}}\,. \tag{7b}$$

Here E_i and E'_i are the energy of the i-th particle in the L and C systems.

Thus once more we obtain equations of type (1). Let us assume that we know the continuous spectra for the following values of laboratory angle: $\theta_i = \theta_i^{(0)}$; $\theta_i^{(1)}$; ...; $\theta_i^{(n)}$. We wish to determine the continuous spectrum in the C system for an angle θ'_i. By comparing equation (7) with equation (1) we find the following order for solving this problem from the nomograms: 1) We note the given angle ϑ_1 on the θ'_i scale angle $\theta_i^{(0)}$ on the curvilinear scale, and find ρ_i from the ρ_2 scale [i. e., we solve equation (7a)], after which we calculate E_i; 2) we mark the angle $\theta_i^{(0)}$ on the ϑ_1 scale and θ'_i on the curvilinear scale and find ρ'_i on the ρ_1 scale [i.e., we solve equation (7b)], after which we calculate E'_i; 3) we repeat these operations for all values of laboratory angle θ_i.

For convenience in using the nomogram we recommend superimposing an E_I/E_i scale or its reciprocal on the ρ_2 scale, and an E_I/E'_i scale or its reciprocal on the ρ_1 scale. The critical points of the nomogram $\rho_i = 1$ and ρ'_i are reflected by critical energies of the escaping particles:

$$E_{i\,cr} = E'_{i\,cr} = \frac{m_I m_i}{(m_I + m_{II})^2} E_I. \tag{8}$$

The nomogram clearly reveals the following special features: 1) Only those particles escaping at angles $\theta_i < \theta'_i$ in the L system can escape at θ'_i in the C system; 2) for particles with supercritical energies in the L system, angles θ_i and θ'_i have a single-valued relative correspondence; 3) for particles with subcritical energies in the L system to one θ'_i there correspond two θ_i, but to one θ_i there correspond only one θ'_i; 4) particles with supercritical energies in the L system can escape in either the front or rear hemisphere in the C system; 5) particles with subcritical energies in the L system can only escape in the rear hemisphere in the C system.

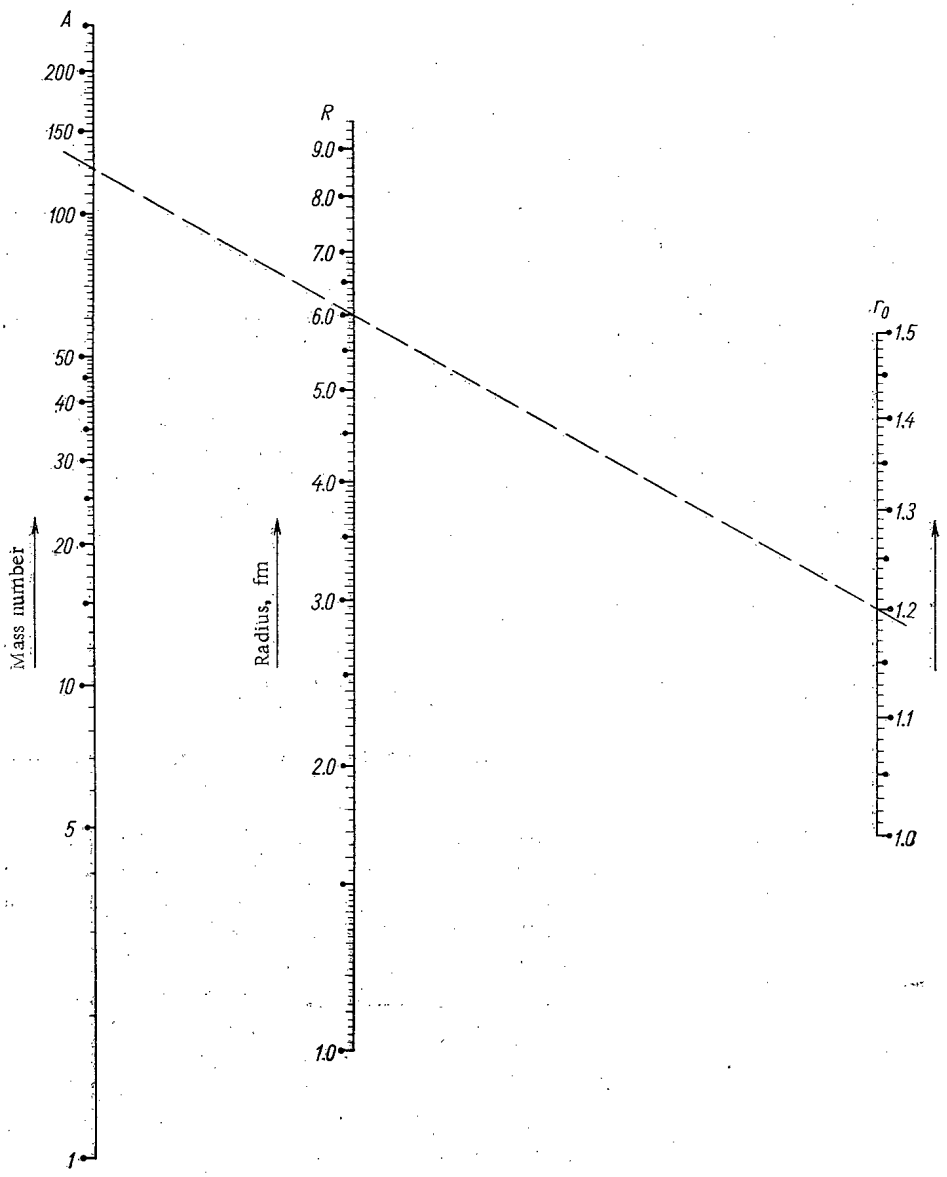

Fig. 6. Nomogram for determining the radius of the nucleus from the formula $R = r_0 A^{1/3}$. Example. Given $A = 125$; $r_0 = 1.2$. We find $R = 6$ fm.

Let us now consider the problem of converting the cross sections from the L system into the C system. For reactions $I + II = 1 + 2$ the corresponding formula has the form [5]

$$\frac{\sigma_C}{\sigma_L} = \frac{\sqrt{1-\rho_{1(2)}^2 \sin^2 \vartheta_{1(2)}}}{(\sqrt{1-\rho_{1(2)}^2 \sin^2 \vartheta_{1(2)}} \pm \rho_{1(2)} \cos \vartheta_{1(2)})^2}. \quad (9)$$

We take only the plus sign for $\rho_1^{(2)} < 1$, but both signs for $\rho_1^{(2)} > 1$. For reactions of the form $I + II = 1 + 2 + 3 + \ldots + n$ $(n > 2)$, the ratio of the cross sections is expressed by the same formula (9), but instead of $\rho_1^{(2)}$ and $\vartheta_1^{(2)}$ we have to substitute ρ'_i and θ_i.

Formula (9) may be presented in the form of a nomogram of equivalent points on rectilinear carriers with a single binary scale. Unfortunately, in this case it is inconvenient to embrace the whole range of the variables with one or two nomograms, since the accuracy would then be very low, and a series of nomograms has therefore to be plotted. One of these is shown in Fig. 2. The scale of σ_L is plotted over a range of 1 to 10 arbitrary units and is divided into two sections. The section from 1 to 3.162 is placed

on the left and that from 3.162 to 10 on the right of the carrier. Correspondingly the σ_C scale is also divided into two sections (left and right corresponding to the left and right of the σ_L system) and is given in the same units. The scheme for using the nomogram is obvious from Fig. 2.

By using the nomogram we can obtain a fairly exact numerical estimate of the error $\Delta\sigma_C$, which is affected by the following factors: the error $\Delta\sigma_L$ in the measurement of σ_L, the error $\Delta\vartheta_{1\,(2)}$ characterizing the apparatus and that committed in measuring the angles $\theta_{1\,(2)}$ (or θ_i), and the error ΔE_I in the beam energy. The error ΔE_I is made up of two quantities: the error committed in measuring the beam energy and the error introduced by the energy spread of the beam particles. Thus $\Delta\sigma_C$ may be expressed as the sum of three terms

$$\Delta\sigma_C = \Delta\sigma'_C(\Delta\sigma_L) + \Delta\sigma''_C(\Delta\vartheta_{1(2)}) + \Delta\sigma'''_C(\Delta E_I). \quad (10)$$

The first term depends on the error $\Delta\sigma_L$. The value of this may be found from the nomogram (see Fig. 2). Here $\Delta\sigma_L$ is counted along the σ_L scale and $\Delta\sigma_C$ along the σ_C scale. The second term depends on the value of $\Delta\vartheta_{1\,(2)}$ (or $\Delta\theta_i$). Figure 3 shows $\Delta\sigma''_C/\sigma_C$ as a function of ρ for various values of $\vartheta_{1(2)}$ over the range $\rho = 0$ to 1. The third term depends on ΔE_I. The quantity $\Delta\sigma'''_C$ enters into the nomogram by way of $\Delta\rho$. The value of $\Delta\sigma'''_C$ must be estimated separately in each specific case. Figure 4 shows $\Delta\sigma'''/\sigma_C$ as a function of the escape angle in the L system for deuterons from the Li^7 (He^4, d) Be^9 reaction, on the assumption that $E_I = 13$ MeV, $\Delta E_I/E_I = 1\%$, $Q = -7.152$ MeV. Here $\rho = 0.967 \pm 0.030$.

The quantities ρ_1 and ρ_2 enter into all the nomograms considered as one of the scales; these quantities depend in a fairly complicated manner on the beam energy and the mass of the particles taking part in the reaction. For calculating ρ_1 and ρ_2 there is an extremely simple nomogram, the principle of which appears in Fig. 5. The basis of this nomogram is a sheet of ordinary millimeter paper. The method of plotting the nomogram on the mm mesh and the method of applying it are obvious from Fig. 5. We merely note that the scales marked off along each straight line must be equal (i.e., the scales of E_I and QB along the vertical line and the scales of A and ρ^2 along the horizontal line).

The nomogram for finding the values of ρ_1 and ρ_2 may conveniently be used in order to plot double scales for the $\rho_{1(2)} = f(E_I)$ relationship [6, 7]. These scales are, first, very convenient in use, and, secondly, they give a clear indication of the extent to which the error ΔE_I affects the errors in determining the remaining kinematic characteristics. In addition to this, such scales enable us to establish the acceptable error ΔE_I, i.e., the value which has no effect on the errors in the remaining kinematic characteristics. In some cases (e.g., $|Q|B \ll E_I$), the acceptable error ΔE_I is quite large (sometimes of the order of several hundred keV's), while in other cases (e.g., in reactions with $Q < 0$ for $E_I/|Q|B = 1$ to 3) it is quite small (of the order of a few keV's), so that the errors in the kinematic characteristics arising from the ΔE_I may reach quite large values.

In conclusion, we present a nomogram for determining the radius of the nucleus from the formula $R = r_0 A^{1/3}$ (Fig. 6).

The author takes this opportunity to offer sincere thanks to Corresponding Member of the Academy of Sciences of the USSR G. N. Flerov and S. S. Vasil'ev for organizing his contributions to the Seminars in the Nuclear-Reactions Laboratory of the United Institute of Nuclear Research (Dubna) and the Scientific-Research Institute of Nuclear Physics, Moscow State University, to the delegates of both Seminars for useful discussion, to V. V. Volkov and G. S. Khovanskii for constant interest in the work and for useful comments, and also to N. A. Vlasov for setting some extremely important problems for nomogram treatment.

LITERATURE CITED

1. G. N. Potetyunko, Atomnaya Énergiya, 13, 588 (1962).
2. G. N. Potetyunko, Atomnaya Énergiya, 16, 349 (1964).
3. A. M. Baldin et al., Kinematics of Nuclear Reactions [in Russian]. Moscow, Fizmatgiz (1959).
4. G. N. Potetyunko, Nomographic Handbook [in Russian]. Moscow, Izd. VTs AN SSSR (1966).
5. H. Bethe and M. Livingston, Rev. Mod. Phys., 9, 245 (1936).
6. B. A. Nevskii, Handbook of Nomography [in Russian], Ch. 5. Moscow-Leningrad, Gostekhteorizdat (1951).
7. G. S. Khovanskii, Nomographic Methods [in Russian]. Moscow, Izd. VTs AN SSSR (1964).

NEUTRON PENETRATION IN AIR

P. A. Yampol'skii, V. F. Kokovikhin, A. I. Golubkov, N. A. Kondurushkin, and A. V. Bolyatko

UDC 539.125.52

A Monte-Carlo calculation of the neutron distribution arising from monoenergetic isotropic point sources in an infinite homogeneous medium of normal density is presented. Initial neutron energies of 0.001; 0.025; 0.025; 0.2; 0.8; 2; 5; 10; and 14 MeV are considered. The space-energy and time neutron distribution at distances of 10 to 1300 m from the source are obtained. The results are compared with certain of the authors' experimental data.

In view of the wide use of neutron sources in various fields of popular economy, the question of ensuring the protection of the operators from radiation hazard assumes prime importance. It is very essential to know the neutron distribution in the air at various distances from the sources. The experimental solution of this problem is beset with considerable technological difficulties. Published calculations disagree seriously among themselves.

In this paper we shall present calculations carried out on the ÉVM M-20 computer; these relate to the air penetration of neutrons from an isotropic point source providing monoenergetic neutrons with energies between 1 keV and 14 MeV.

COMPUTING METHOD

We used the statistical-test, or Monte-Carlo, method of calculation; this enabled the physical process of neutron penetration to be represented in mathematical form [1]. The whole history of neutrons passing through air was traced from the given initial energy to a final energy of 0.2 eV. The density of the air was taken as $1.293 \cdot 10^{-3}$ g/cm^3, comprising 76% nitrogen and 23% oxygen [2] (other constituents not considered). The characteristics of the interactions taking place between the neutrons and the oxygen and nitrogen atoms were taken from [3-5]. All possible forms of neutron interaction contributing at least 3% to the total neutron cross section were taken into account.

The calculations were carried out for an isotropic point source of neutrons with initial energies 1; 25; 200 and 800 keV; and 2; 5; 10, and 14 MeV. The passage of the neutrons through 15 concentric spheres surrounding the source at distances of 10 to 1300 m was recorded. At each intersection, the neutron energy and time of propagation were determined. For each of the 15 distances from the source, the total neutron flux (number of neutrons penetrating the sphere in question, referred to its area), the energy distribution of the neutrons, and the average time for a neutron to reach the distance in question were obtained.

In determining the energy spectrum of the neutrons, the energy range 0.2 to 14 MeV was divided into 20 intervals. The subdivision of the range was carried out with the intention of obtaining the greatest possible accuracy when using the data to determine neutron doses. The average time for a neutron to reach a given distance was obtained by averaging over all neutron intersections relating to the sphere in question, independently of the direction in which the neutrons were moving. The number of neutron histories traced in different cases varied between 7000 and 20,000.

RESULTS

The spatial distribution of neutrons belonging to various energy groups in air are shown in Figs. 1 to 8. The results are normalized to a single neutron emitted from the source. The average times for a neutron to reach a given distance are shown in Fig. 9.

Translated from Atomnaya Énergiya, Vol. 21, No. 4, pp. 262-266, October, 1966. Original article submitted May 18, 1966.

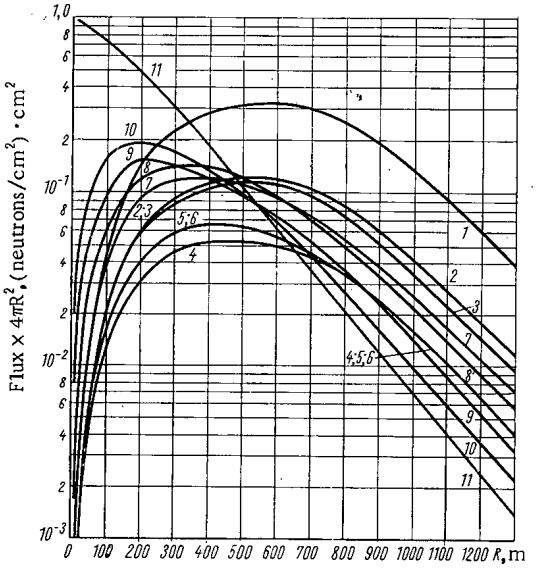

Fig. 1. Spatial distribution of neutrons belonging to various energy groups in air for a source energy of $E_0 = 14$ MeV. 1) 0.2 eV - 1 keV; 2) 1 - 10 keV; 3) 10 - 50 keV; 4) 50 - 100 keV; 5) 100 - 200 keV; 6) 200 - 500 keV; 7) 0.5 - 1 MeV; 8) 1 - 2 MeV; 9) 2 - 4 MeV; 10) 4 - 8 MeV; 11) 8 - 14 MeV.

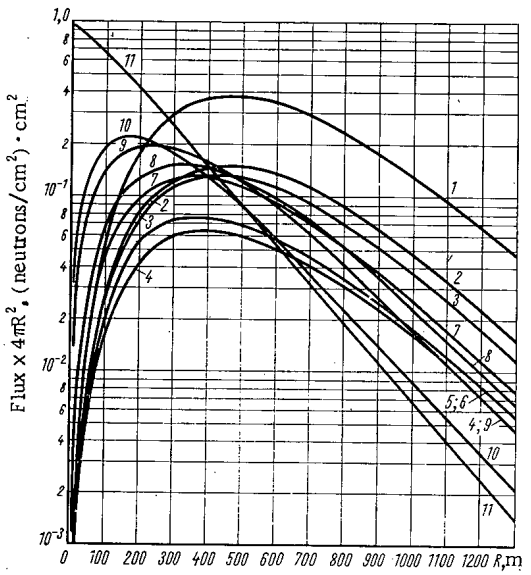

Fig. 2. Spatial distribution of neutrons belonging to various energy groups in air for $E_0 = 10$ MeV (notation is explained in Fig. 1).

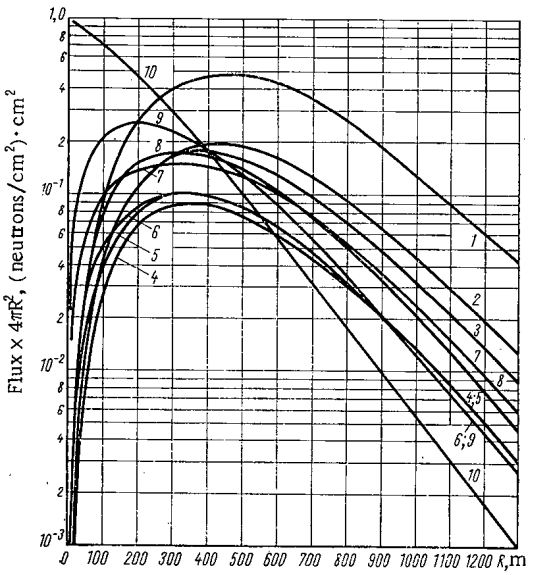

Fig. 3. Spatial distribution of neutrons belonging to various energy groups in air for $E_0 = 5$ MeV (explanation of curves in Fig. 1).

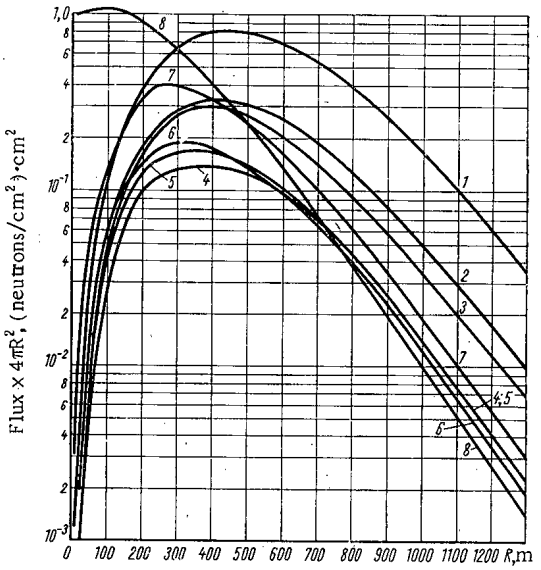

Fig. 4. Spatial distribution of neutrons belonging to various energy groups in air for $E_0 = 2$ MeV (explanation of curves in Fig. 1).

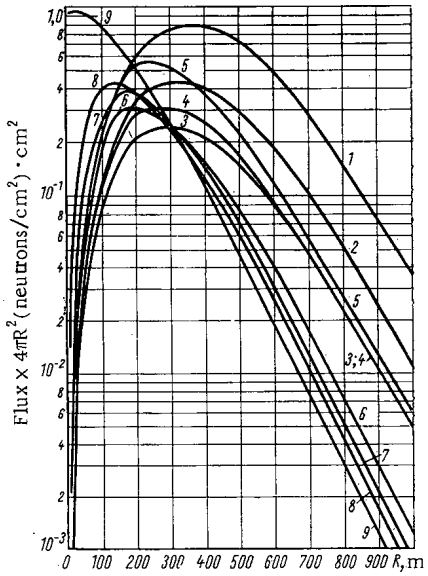

Fig. 5. Spatial distribution of neutrons belonging to various energy groups in air for E_0 = 800 keV: 1) 0.2 eV - 0.1 keV; 2) 0.1 - 1 keV; 3) 1 - 3 keV; 4) 3 - 10 keV; 5) 10 - 50 keV; 6) 50 - 100 keV; 7) 100 - 200 keV; 8) 200 - 500 keV; 9) 500 - 800 keV.

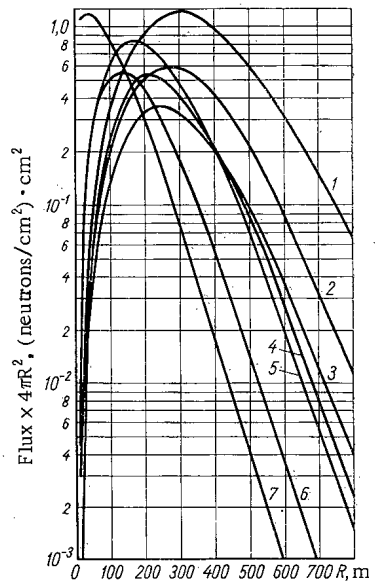

Fig. 6. Spatial distribution of neutrons belonging to various energy groups in air for E_0 = 200 keV (explanations of curves in Fig. 5).

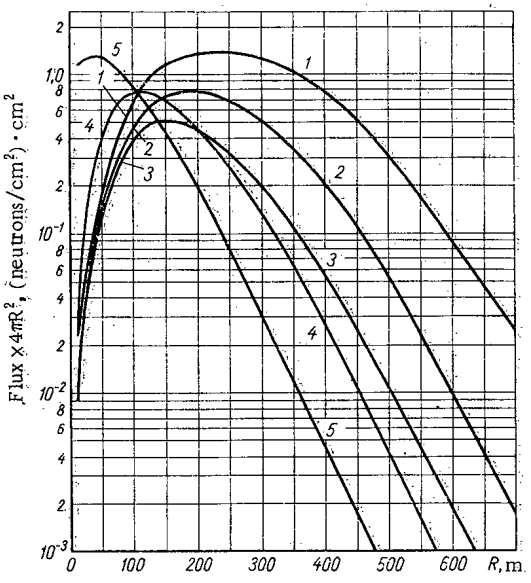

Fig. 7. Spatial distribution of neutrons belonging to various energy groups in air for E_0 = 25 keV (explanation of curves in Fig. 5).

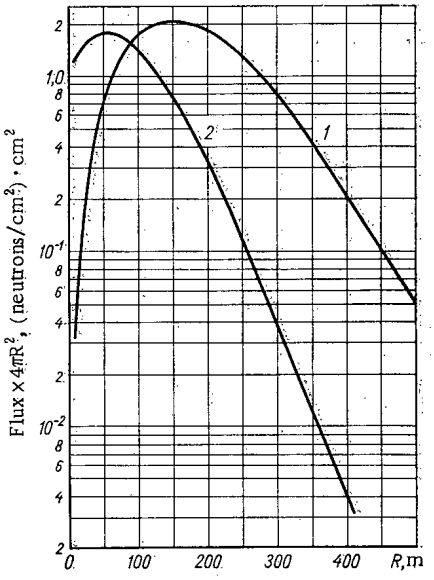

Fig. 8. Spatial distribution of neutrons belonging to various energy groups in air for E_0 = 1 keV (explanation of curves in Fig. 5).

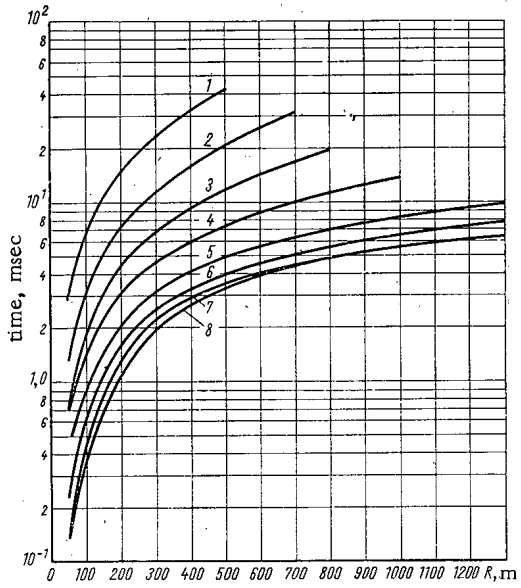

Fig. 9. Average time for neutrons to reach a given distance for various initial neutron energies: 1) 0.001; 2) 0.025; 3) 0.2; 4) 0.8; 5) 2; 6) 5; 7) 10; 8) 14 MeV.

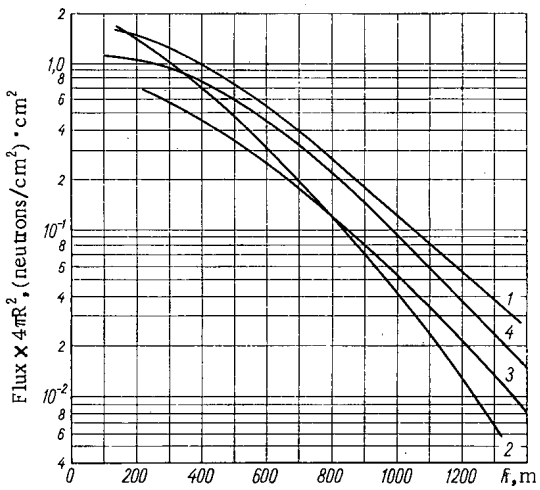

Fig. 10. Neutron flux (for energies exceeding 0.2 MeV) in air for an isotropic point source with an initial neutron energy of 14 MeV: 1) - 3) Data of [6] (1 = Los Alamos; 2) Rand; 3) General Dynamics); 4) our own data.

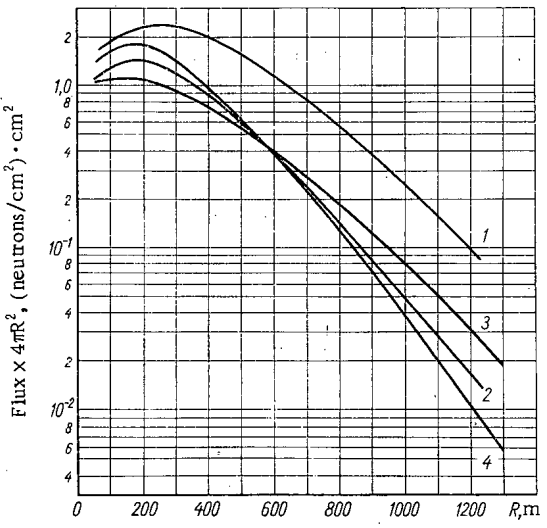

Fig. 11. Neutron flux (for energies exceeding 0.2 MeV) in air for isotropic point sources with various initial neutron energies: 1), 2) Data taken from [6] for energy 3 MeV (1 = Sandia, 2 = General Dynamics); 3) our own data for energy 5 MeV; 4) our own data for energy 2 MeV.

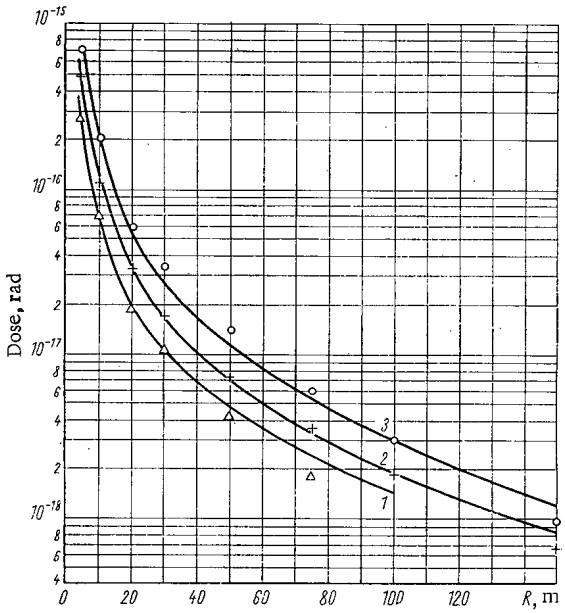

Fig. 12. Neutron dose from a point source in air: 1), 2), 3) Calculation for neutron energies 25, 200, and 800 keV respectively; △, +, ○ experiment with sources having mean energy 25, 220, and 830 keV respectively.

The neutron-penetration calculations were compared with the calculations given in [6] and with our own experimental data.

The author of [6] compares a number of Monte-Carlo calculations of neutron flux at various distances from monoenergetic neutron sources (3 to 14 MeV) in air; these calculations were carried out by

various laboratories in the United States: Sandia, General Dynamics, Rand, and Los Alamos. The calculations carried out at Sandia and General Dynamics related to an isotropic point source in an infinite air medium, and those carried out at Rand and Los Alamos to air-earth geometry (source at 91.5 m above the Earth's surface). The neutron fluxes were calculated over a range extending from the energy of the source neutrons to 0.2 MeV.

Figure 10 compares our own results with data taken from [6] for neutron source of energy 14 MeV; Fig. 11 shows data for neutrons with an initial energy of 3 MeV [6], together with our own results for neutrons starting at 2 and 5 MeV. The results obtained in [6] for an air density of $1.11 \cdot 10^{-3}$ g/cm^3 have been converted to an air density of $1.293 \cdot 10^{-3}$ g/cm^3.

The absorbed neutron tissue dose was calculated from the space-energy distribution of neutrons in air for initial energies of 25, 200, and 800 keV. The relation between the maximum tissue dose and the neutron energy given in [7, 8] was employed. For a distance of 5 m from the source (for which the neutron flux was not calculated), the dose was determined by direct radiation, without considering scattered neutrons.

Figure 12 shows the computed dose, together with the authors' experimental values for the dose in air (source and detector at 10 m above the Earth's surface). For these experiments we used photoneutron sources with an average initial energy of 25, 220, and 830 keV. The tissue dose was measured with dosimetric detectors based on the principle of preliminary retardation of the neutrons [9]. The energy dependence of the detector sensitivity lay within 25% of the dose curve given in [7, 8], which was used for the dose calculation.

The authors wish to thank O. I. Leipunskii for useful discussions.

LITERATURE CITED

1. N. P. Buslenko et al., Method of Statistical Tests (Monte-Carlo Method) [in Russian]. Moscow, Fizmatgiz, (1962).
2. W. Childs, Physical Constants, 5th Ed., Wiley (1958).
3. D. Hughes and R. Schwartz, Neutron Cross Sections. N. Y., BNL (1958).
4. M. Goldberg, V. May, and J. Stehen, BNL-400. 2nd Ed., Vol.1, Brookhaven (1962).
5. I. V. Gordeev et al., Nuclear-Physics Constants [in Russian]. Moscow, Gosatomizdat (1963).
6. M. Wells, Health Physics, 8, 543 (1962).
7. A. M. Kogan et al., Atomnaya Énergiya, 7, 351 (1959).
8. W. Snyder and J. Neufeld, Brit. J. Radio., 28, 342 (1955).
9. Kh. D. Androsenko and G. N. Smirenkin, Pribory i tekhnika éksperimenta, No. 5, 64 (1962).

STABILITY OF A CIRCULATING FUEL REACTOR NEGLECTING DELAYED NEUTRONS

V. D. Goryachenko

UDC 621.039.56:621.039.514

The stability of a nuclear reactor with circulating fuel is investigated by neglecting delayed neutrons but taking into account the distribution of variables through the core. The condition for stability in the small is obtained. Using a simplified description of the delayed neutrons it is shown that they increase the stability. The possibility of applying the Welton criterion is examined and it is shown that this criterion does not determine whether a reactor with distributed parameters is stable.

Let us consider a circulating fuel reactor shown schematically in Fig. 1. The fissionable material (fuel) circulates around a closed loop consisting of the reactor core and the heat exchanger. If the rate of circulation is large, the probability of emission of a delayed neutron in the core is given approximately $\tau_1/(\tau_1+\tau_2)$, where τ_1 and τ_2 are respectively the residence times of the fuel inside and outside the core. In certain cases of practical interest $\tau_2 \gg \tau_1$ and consequently the importance of the delayed neutrons will be small. In this connection it is appropriate to consider the limiting case where $\tau_1/(\tau_1+\tau_2)=0$. It is clear that if this relation is satisfied exactly or only approximately, the reactor cannot be controlled by conventional means and the question of self-regulation becomes particularly important. To settle this question it is first necessary to solve the problem of the stability of a circulating fuel reactor neglecting delayed neutrons.

This question is treated in several reports [1-5]. From the point of view of investigating stability, the most valuable articles are those by Ergen based on the following assumptions: 1) the fuel temperature at the core inlet is constant; 2) the fuel is incompressible; 3) the rate of consumption of fuel is constant; 4) there are no delayed neutrons. The effect of delayed neutrons is taken into account only for certain very simple cases of temperature feedback. In these reports the stability of very simple lumped parameter models is discussed in adequate detail but the investigation of the stability of a reactor with distributed parameters cannot be regarded as satisfactory. As a matter of fact it is concluded in [4, 5] that satisfying the Welton criterion is a sufficient condition for the stability of a reactor with distributed parameters. It will be shown below that the Welton criterion is not satisfied for the most common case of a sinusoidal variation of neutron density through the reactor. Therefore, even under the simplifying assumptions listed above, the stability question remains unresolved. In addition the assumption of constant core inlet temperature made by all the authors [1-5] is not always applicable in practice.

This article is devoted to the investigation of the stability in the small or a reactor model with distributed parameters, taking account of changes in fuel temperature at the core inlet in order to fill in, to some extent, the gaps pointed out above.

Basic Assumptions and the Mathematical Model

In setting up the mathematical model of the core it is supposed that: 1) the reactor has a negative temperature coefficient of reactivity insuring self-regulation; 2) there are no delayed neutrons; 3) the fuel is incompressible; 4) the rate of consumption of the fuel is constant; 5) the density and specific heat of the fuel are constant; 6) the heat released in the core is proportional to the neutron density; 7) the reactivity depends only on the fuel temperature; 8) in the energy balance for the fuel it is sufficient to take into account only the changes in thermal energy. In addition we limit ourselves to a discussion

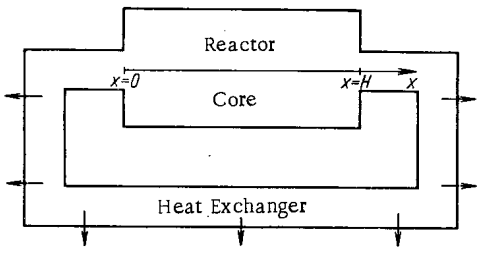

Fig. 1. Schematic diagram of the arrangement.

Translated from Atomnaya Énergiya, Vol. 21, No. 4 pp. 267-271, October, 1966. Original article submitted April 27, 1966.

of the one-dimensional problem and suppose that the spatial distribution of neutrons may be characterized by its first harmonic F (x).

Under these assumptions the core is described by the equations

$$\frac{dN}{dt} = \frac{kN}{l^*}; \tag{1}$$

$$k = -\varepsilon' \int_0^H [T(x, t) - T_0(x)]\, \Phi(x)\, dx; \tag{2}$$

$$\frac{\partial T}{\partial t} + w\frac{\partial T}{\partial x} = AN(t)\, F(x), \quad 0 \leqslant x \leqslant H \tag{3}$$

with the boundary condition

$$T(0, t) = T_{\text{in}}(t), \tag{4}$$

where N is the amplitude of the first harmonic of the spatial distribution of neutron density; k is the reactivity; l^* is the neutron lifetime; T (x, t) is the fuel temperature at cross section x of the core; T_{in} ε' is a constant characterizing the temperature coefficient of reactivity, being positive for a negative temperature coefficient; H is the core length; A is a positive constant of proportionality; T_{in} (t) is the fuel temperature at the core inlet (the heat exchanger outlet). The subscript 0 refers to steady state values.

Henceforth we will suppose that the neutron density distribution through the core is

$$F(x) = \sin\frac{\pi x}{H}. \tag{5}$$

This is true for reactors in the form of slabs, cylinders, and parallelepipeds. In the latter two cases we will understand by T (x, t) the fuel temperature averaged over the cross section of the core. On the basis of the seven assumptions the function Φ(x) will be the square of the neutron density distribution [7]

$$\Phi(x) = F^2(x) = \sin^2\frac{\pi x}{H}. \tag{6}$$

We make the same assumptions about the heat exchanger as in [8]. We will suppose that the heat exchanger is an arbitrary linear distributed system satisfying the conditions

$$\psi(t) \geqslant 0; \tag{7}$$

$$\int_0^\infty \psi(t)\, dt < 1, \tag{8}$$

where ψ (t) is the change in fuel temperature at the heat exchanger outlet due to a temperature pulse at its inlet, i.e., T (H, t) - T_0 (H) = δ (t).

The Characteristic Equation of the Linearized System

To analyze stability in the small it is necessary to linearize the original equations in the vicinity of the equilibrium state and to set up the characteristic equation of the linearized system. To do this we introduce the dimensionless coordinates

$$\tau = \frac{t}{\tau_1}, \quad y = \frac{x}{H}, \tag{9}$$

the variables

$$u(\tau) = \frac{N - N_0}{N_0}; \quad v(y, \tau) = T - T_0;$$
$$v_{\text{in}}(\tau) = T_{\text{in}} - T_{\text{in}\,0} \tag{10}$$

and the parameters

$$\nu = \frac{l^*}{\varepsilon' H \tau_1}; \quad \alpha = AN_0\tau_1 = \frac{\pi}{2}(T_{\text{out}\,0} - T_{\text{in}\,0}),$$

where T_{out} is the fuel temperature at the core outlet.

If we assume that the difference (10) is small, elementary transformations of Eqs. (1) - (6) lead to the linearized core equations

$$\nu \frac{du}{d\tau} = -\int_0^1 v(y, \tau) \sin^2 \pi y \, dy; \tag{11}$$

$$\frac{\partial v}{\partial \tau} + \frac{\partial v}{\partial y} + \alpha u(\tau) \sin \pi y \tag{12}$$

with the boundary condition

$$v(0, \tau) = v_{in}(\tau). \tag{13}$$

The function $\nu_{in}(\tau)$ is obtained from the solution of the linear equations of the heat exchanger and may be written as

$$v_{in}(\tau) = \int_0^\tau \psi(\tau - \xi) v(1, \xi) \, d\xi, \tag{14}$$

where the kernel ψ satisfies the inequalities (7) and (8) and $\nu(1,\xi)$ is the change in fuel temperature at the heat exchanger inlet (the core outlet). Equations (11) - (14) comprise a complete system of linearized equations for the model considered.

Let us take the Laplace transforms of the linearized system with respect to the variable τ for zero initial conditions, and solve Eq. (12) subject to the boundary condition (13). Then, after the necessary transformations we obtain the characteristic equation of the linearized system

$$ap + \frac{[1 + \Psi(p)](1 - e^{-p})}{p(p^2 + \pi^2)(p^2 + 4\pi^2)[1 - \Psi(p)e^{-p}]} + \frac{2p}{3\pi^4 (p^2 + \pi^2)} = 0, \tag{15}$$

where

$$a = \frac{l^*}{\tau_1 \varepsilon \pi^4 (T_{out\ 0} - T_{in\ 0})}; \tag{16}$$

$\varepsilon = \varepsilon' H$; $\Psi(p)$ is the transfer coefficient of the heat exchanger with respect to temperature and is equal to the Laplace transform of the kernel $\psi(\tau)$; and p is the Laplace transform variable.

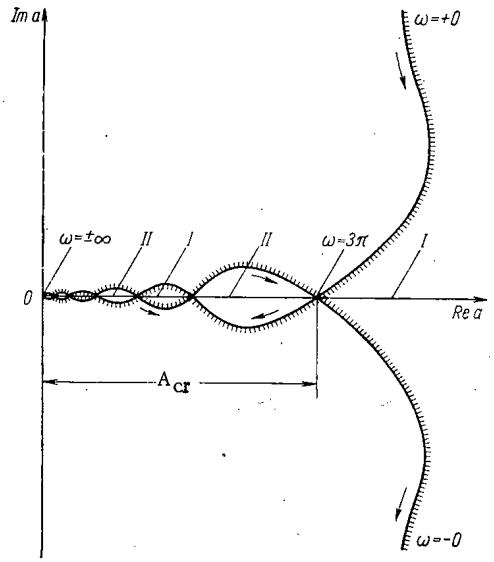

Fig. 2. Characteristics of the D-partition (I, II - stable and unstable operation respectively).

Investigation of Stability in the Small

Let us examine the stability of the steady-state operation of the model using the characteristic Eq. (15). To do this we construct the D-partition [9] of the plane of the complex variable

$$a = -\frac{[1 + \Psi(p)](1 - e^{-p})}{p^2(p^2 + \pi^2)(p^2 + 4\pi^2)[1 - e^{-p}\Psi(p)]} - \frac{2}{3\pi^4 (p^2 + \pi^2)}. \tag{17}$$

Setting $p = j\omega$ in (17) and separating the real and imaginary parts we obtain the equations of the D-curve

$$\left.\begin{aligned} Re\, a(j\omega) &= -\frac{2}{3\pi^4 (\pi^2 - \omega^2)} \\ &+ \frac{(1 - \cos\omega)[1 + 2\,\mathrm{Re}\,\Psi(j\omega) + |\Psi(j\omega)|^2] - 2\sin\omega\,\mathrm{Im}\,\Psi(j\omega)}{\omega^2(\pi^2 - \omega^2)(4\pi^2 - \omega^2)\{1 + |\Psi(j\omega)|^2 - 2\,\mathrm{Re}[e^{-j\omega}\Psi(j\omega)]\}}; \\ Im\, a(j\omega) &= \frac{(1 - |\Psi(j\omega)|^2)\sin\omega}{\omega^2(\pi^2 - \omega^2)(4\pi^2 - \omega^2)\{1 + |\Psi(j\omega)|^2 - 2\,\mathrm{Re}[e^{-j\omega}\Psi(j\omega)]\}}. \end{aligned}\right\} \tag{18}$$

The real variable ω takes on all values from $-\infty$ to $+\infty$.

From the inequalities (7) and (8) it is clear [8] that $|\Psi(j\omega)| < 1$ and therefore the expressions $1 - |\Psi|^2, |+|\Psi|^2 - 2\mathrm{Re}(\Psi e^{-j\omega})$ and $1 + |\Psi|^2 + 2\mathrm{Re}\,\Psi$, entering (18) are positive and bounded. Taking this important fact into account it is easy to see that the D-partition will have the form shown in Fig. 2.

Let us denote by a_{cr} the value of Re a at $\omega = 3\pi$. Then as follows from Eq. (18) and Fig. 2, the steady-state reactor operation will be stable in the small for any system parameters for which $a > a_{cr}$. If $a < a_{cr}$, then depending on the actual magnitude of a, the system may be either stable or unstable. Thus the inequality $a > a_{cr}$ may be considered as a sufficient condition of stability. Evaluating Re a ($j\omega$) at $\omega = 3\pi$ and using Eq. (16) for a we obtain the inequality $a > a_{cr}$ in the form

$$\frac{\varepsilon\tau_1 (T_{\text{cut 0}} - T_{\text{in 0}})}{l^*} < \frac{45\pi^2}{4}. \tag{19}$$

As may be seen from the formulas for the D-partition, Eqs. (18), the stable region in the range $0 < a < a_{cr}$ is small and decreases in size as the region approaches the origin in the a plane. Therefore choosing the system parameters within any such region must be regarded as undesirable, since for a small change in parameters—and such changes are unavoidable in practice—the reactor may become unstable. Let us note also that the instability will result in oscillations, as follows from the formulas for the D-partition Eqs. (18) and Fig. 2. An aperiodic instability arises only for a positive temperature coefficient of reactivity (cf. Fig. 2)

The sufficient condition (19) may not be satisfied: 1) for large negative reactivity coefficients; 2) for a large temperature drop of the fuel in the core; 3) for a long residence time of the fuel in the core. In these cases the steady-state operation of the reactor without delayed neutrons may be unstable.

The Effect of Delayed Neutrons on Stability

We shall show that the inequality (19) continues to be a sufficient condition for stability even when delayed neutrons are taken into account. We employ an approximate description of the delayed neutrons. Without altering the heat balance Eq. (3) or the assumptions about the heat exchanger we write the kinetic equations in the form

$$\frac{dN}{dt} = \frac{k-\beta}{l^*} N + \lambda C; \tag{20}$$

$$k = k_0 - \varepsilon' \int_0^H [T(x, t) - T_0(x)] \sin^2 \frac{\pi x}{H}\, dx; \tag{21}$$

$$\frac{dC}{dt} + \lambda C = \frac{\beta_{\text{eff}}}{l^*} N, \tag{22}$$

where C is the concentration of delayed neutron sources with the equivalent decay constant $\lambda \cong 0.1\ \text{sec}^{-1}$; $\beta_{\text{eff}} = \beta - k_0$ - is the effective delayed neutron fraction. For simplicity we here take into account only one (equivalent) group of delayed neutrons.

Thus the approximate accounting of delayed neutrons leads to a mathematical model of a reactor characterized by Eqs. (3) and (20) - (22) with the boundary condition (4) and the requirements (7) and (8) with regard to the heat exchanger. Let us consider the stability of this model in the small. After linearizing the equations and making all the necessary transformations we obtain the characteristic equation of the linearized system differing from Eq. (15) only in the presence of the added term $bp/(p + \sigma)$ on the left-hand side of the equation where

$$b = \frac{\beta_{\text{eff}}}{\varepsilon\pi^4 (T_{\text{out 0}} - T_{\text{in 0}})}; \quad \sigma = \lambda\tau_1. \tag{23}$$

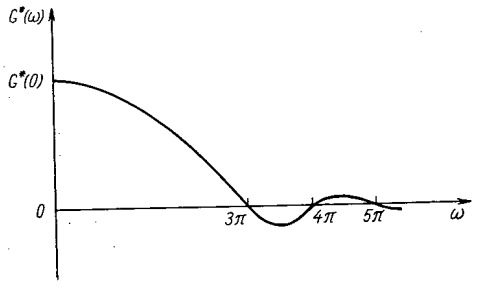

Fig. 3. Graph of the function G* (ω).

Let us consider the D-partition of the plane of the complex variable a when $b \neq 0$. In this case instead of the vector a ($j\omega$) given by Eqs. (18), it is necessary to use the vector sum of a ($j\omega$) from (18) and $-b\sigma/(\sigma^2 + \omega^2) + j \cdot b\omega/(\sigma^2 + \omega^2)$. Since $b > 0$ and $\sigma > 0$, the addition of this last vector to a ($j\omega$) leads to a displacement of the D-curve shown in Fig. 2* to the left and upward. It is clear that the magnitude of this displacement is proportional to b and depends on ω. As a result of this shift the first intersection of the D-curve with the axis of abscissas is displaced

* We are considering the branch of the D-curve corresponding to positive values of ω.

to the left, toward the origin. This means a decrease in the length of the interval over which the alternating regions of stability and instability occur. In addition, for large enough b, a case may arise in which the displacement of the D-curve in the upper half-plane will be so substantial that the whole D-curve for $\omega > 0$ will lie in the upper half-plane and will not interesect the axis of abscissas. In this case the system will be stable for any positive values of the parameter a. Since the parameter b, which is proportional to β_{eff}, characterizes the importance of delayed neutrons, it follows from the above discussion, first that the presence of delayed neutrons increases reactor stability and second that inequality (19) is still a sufficient condition even when delayed neutrons are taken into account, but this condition becomes more and more stringent as the neutron importance increases.

The Application of the Welton Criterion

We shall show that the Welton criterion, when applied to our reactor model does not determine whether the reactor is stable. As a matter of fact the transfer function G (p) from power to minus the reactivity will have the form

$$G(p) = \frac{1}{p^2+\pi^2}\left\{\frac{2\pi^3(1-e^{-p})[1+\Psi(p)]}{p(p^2+4\pi^2)[1-\Psi(p)e^{-p}]}+\frac{4p}{3\pi}\right\}. \qquad (24)$$

Substituting $p = j\omega$ into this expression, and taking the real part of G ($j\omega$), we find that, to within positive factors,

$$\mathrm{Re}\,G(j\omega) = G^*(\omega) = \frac{\sin\omega}{\omega(\pi^2-\omega^2)(4\pi^2-\omega^2)}. \qquad (25)$$

The function G* is shown graphically in Fig. 3.

According to Welton [6] the sufficient condition for reactor stability is $G^*(\omega) > 0$ for all $\omega > 0$. However, in our case the function G* oscillates in sign, and therefore the Welton criterion does not solve the stability question. This raises a doubt as to the practical value of that part of [4, 5] devoted to the stability of circulating fuel reactors with distributed parameters.

Thus, as shown in [8], a circulating fuel reactor whose core is a lumped-parameter unit is stable for any physically realizable system parameters, even in the absence of delayed neutrons. In contrast to the reactor discussed in [8], a reactor with distributed parameters may be unstable for small importance of the delayed neutrons. The main reasons for instability are: an extremely large negative value of the temperature coefficient of reactivity or a temperature drop in the fuel in the core or somewhere else.

A sufficient condition for stability in the small is expressed by the inequality (19) which, it appears, may be ensured in many practical cases.* The presence of delayed neutrons increases the stability of steady-state reactor operation. We note that this last conclusion is based on a simplified accounting of delayed neutrons. The exact quantitative characteristics of their effect on stability may be obtained only after investigating the dynamics of the distributed parameter reactor model with a rigorous description of delayed neutron emitters in terms of a system of partial differential equations. However, this is an independent problem and is not discussed here.

The author sincerely thanks N. A. Zheleztsov and E. F. Sabaev for their valuable comments and their interest in the work.

LITERATURE CITED

1. L. Fleck, BNL-357, USA (1955).
2. R. de Figueuredo, Paper No. 1815, Presented by Portugal at the Second International Conference on the Peaceful Uses of Atomic Energy, Geneva (1958).
3. T. A. Welton, Reactor Physics, Materials from the International Conference on the Peaceful Uses of Atomic Energy, Geneva 1955. Vol. 5, Moscow, Izd-vo AN SSSR, p. 454 (1958).
4. W. Ergen, J. Appl. Phys, 25, 702 (1954).
5. W. Ergen and A. Weinberg, Physica, 20, 413 (1954).
6. H. Smets, J. Appl. Phys., 30, 1623 (1959).
7. A. D. Galanin, The Theory of Thermal Neutron Reactors, Moscow, Atomizdat, [in Russian] (1957).
8. V. D. Goryachenko, Atomnaya Énergiya, 21, 3 (1966).
9. Yu. I. Neimark, The Stability of Linearized Systems, Leningrad, Izd. Leningrad Air Force Engineering Academy [in Russian], (1949).

* Thus for $1^* = 10^{-4}$ sec, $\varepsilon = 10^{-4}$/deg C, $\tau \cong 1$ sec, nominal reactor operation will surely be stable for $T_{out^0} - T_{in^0} \lesssim 100°C$.

NEUTRON DIFFUSION TENSOR IN A HETEROGENEOUS PERIODIC SYSTEM WITH AN ARBITRARY SCATTERING LAW

V. M. Novikov

UDC 621.039.512.4

A general expression for the diffusion coefficient tensor in a heterogeneous periodic system with an arbitrary scattering law is obtained in terms of quadratures. In contrast to a homegeneous system where anisotropic scattering affects the diffusion length only through the average value of the cosine of the scattering angle, in a heterogeneous medium the diffusion length is determined also by the higher angular moments of the scattering index. Using as an example a medium containing voids, it is shown that taking account of anisotropic scattering leads to expressions for L_i^2 which differ from the familiar Behrens formulas. The possibility of testing the theory experimentally is discussed.

In solving many problems connected with the diffusion of neutrons in heterogeneous periodic media, it frequently turns out to be useful to reduce the heterogeneous system to an equivalent homogeneous medium. In this procedure it is necessary to calculate the effective diffusion characteristics of the equivalent homogeneous medium. This problem has been solved by many authors for isotropic neutron scattering in all components of the medium. Ordinarily for an arbitrary scattering law it is assumed that anisotropic scattering in a heterogeneous medium may be taken into account in the same way as in a homogeneous medium, by replacing all scattering cross sections by transport cross sections in the expression for the diffusion coefficient tensor D_i [1-4]. However, this analogy is not generally valid. In this connection there arises the question of the correct evaluation of the effective diffusion parameters of a heterogeneous periodic system with an arbitrary scattering law. The solution of the problem is presented below.

The General Expression for the D_i Tensor for a Medium with an Arbitrary Scattering Law

The diffusion tensor in a heterogeneous periodic system may be conveniently calculated by using the integral form of the transport equation. As is shown in [5], this method is completely equivalent to the mean-free-path method used in [1, 2]. We write the transport equation for the neutron distribution function $f(\mathbf{r}, \Omega)$ for the diffusion of monoenergetic neutrons in a weakly absorbing medium ($\mu_s \approx \mu$) far from the source

$$f(\mathbf{r}, \Omega) = \int_0^\infty dR \mu_s(\mathbf{r}') e^{-\widetilde{\mu R}} \times \int_{(4\pi)} d\Omega' c(\mathbf{r}', \Omega\Omega') f(\mathbf{r}', \Omega'), \quad (1)$$

where $\mu_s(\mathbf{r})$ and $\mu(\mathbf{r})$ are respectively the macroscopic scattering and total cross sections at point r; $\widetilde{\mu R} = \int_r^{r'} \mu(\mathbf{r}'')\, dr''$ is the "optical" neutron path between points r and r'; Ω' and Ω are unit vectors characterizing the direction of the neutron velocity before and after scattering at point r'; $c(\mathbf{r}'\ \Omega\ \Omega')$ is the scattering index at point r' as a function of the cosine of the scattering angle. The arrangement of vectors is shown in Fig. 1.

To separate out the diffusion along the i-th axis of symmetry of an elementary cell of the medium, we will suppose, as was done in [2], that there is an infinite plane source of neutrons at right angles to the unit vector i which is directed along axis i. In such a system the neutron flux may be written as the sum of two terms. The first term $f_0(\mathbf{r})$ describes the overall decrease in flux along axis i; for sufficiently weak absorption it will be a linear function of x. The second term characterizes the "microstructure" of the flux within each cell and takes into account the effect of the

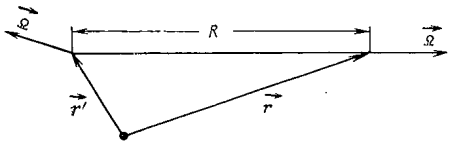

Fig. 1. Arrangement of the Vectors.

Translated from Atomnaya Énergiya, Vol. 21, No. 4, pp. 272-276, October, 1966. Original article submitted May 23, 1966.

heterogeneous nature of the system on the flux. This term is clearly a periodic function of coordinates with a period equal to the period of the cell.

$$f(\mathbf{r}, \Omega) = f_0(\mathbf{r}) - \left(\frac{\partial f_0}{\partial x_i}\right)_0 F_i(\mathbf{r}, \Omega), \tag{2}$$

where the factor $-(\partial f_0/\partial x_i)_0$ is introduced for convenience. Since the quantity $f_0(\mathbf{r})$ is determined to within a constant, it may be supposed that the volume average of the microflux over any cell is zero, i.e.,

$$\left\langle \int\limits_{(4\pi)} F_i(\mathbf{r}, \Omega)\, d\Omega \right\rangle = 0, \tag{3}$$

where $\langle \ldots \rangle$ denotes the average over the volume of an arbitrary cell of the medium.

The homogenization of a heterogeneous periodic system consists in replacing it by an equivalent homogeneous system for which the neutron flux and current are equal to the averages over the volume of a cell of the corresponding exact flux and current in the heterogeneous medium. Let us denote the flux in the equivalent homogeneous medium by $\Psi(\mathbf{r})$. Then

$$\left.\begin{aligned} -D_i \left\langle \frac{\partial \Psi}{\partial x_i} \right\rangle &= \int\limits_{(4\pi)} d\Omega\, (\Omega \cdot \mathbf{i}) \langle f(\mathbf{r}, \Omega) \rangle; \\ \langle \Psi \rangle &= \int\limits_{(4\pi)} d\Omega \langle f(\mathbf{r}, \Omega) \rangle. \end{aligned}\right\} \tag{4}$$

Using Eqs. (2) and (3) we obtain from (4) the expression for the diffusion tensor

$$D_i = \int\limits_{V_{ce}} \frac{d^3r}{V_{ce}} \int\limits_{(4\pi)} \frac{d\Omega}{4\pi} (\Omega \cdot \mathbf{i}) F_i(\mathbf{r}, \Omega). \tag{5}$$

To calculate the function F_i we substitute (2) into Eq. (1) and use the fact that the flux $f_0(\mathbf{r})$ falls off linearly along the i axis, i.e., $f_0(\mathbf{r}') = f_0(\mathbf{r}) - (\partial f/\partial x_i)_0 R(\Omega \cdot \mathbf{i})$. After some simple transformations we obtain the inhomogeneous integral equation for F_i

$$F_i(\mathbf{r}, \Omega) = (\Omega \cdot \mathbf{i})\, l(\mathbf{r}, -\Omega) - \int\limits_0^\infty dR \mu(\mathbf{r}')\, e^{-\tilde{\mu}R} \times \int\limits_{(4\pi)} d\Omega' c(\mathbf{r}', \Omega \cdot \Omega') F_i(\mathbf{r}', \Omega'), \tag{6}$$

where $l(\mathbf{r}, -\Omega) = \int\limits_0^\infty R e^{-\tilde{\mu}R} \mu(\mathbf{r}')\, dR$ is the mean free path of a neutron from point r in a direction opposite to Ω. Equation (6) may be solved by the method of successive approximations. It is easy to see that the series for F_i converges, since in the limiting case of a homogeneous medium this procedure gives the series expansion of the solution in terms of the average value of the cosine of the scattering angle α. Thus the diffusion tensor in an arbitrary heterogeneous periodic system may be written as a series involving integrals of the mean free path $l(\mathbf{r}, \Omega)$ and the scattering index $c(\mathbf{r}, \Omega \cdot \Omega')$.

Let us discuss the general calculational scheme by using a homogeneous medium as an example. In a homogeneous medium with spherically symmetric scattering the solution for the function F_i has the form $F_i(\mathbf{r}, \Omega) = (\Omega \cdot \mathbf{i})\mu^{-1}$. If this expression is substituted into Eq. (6) it is easy to see that the integral term vanishes. When the quantity $(\Omega \cdot \mathbf{i})\, \mu^{-1}$ is substituted for F_i in the case of an arbitrary scattering law, the integral term becomes equal to $\alpha (\Omega \cdot \mathbf{i}) \mu^{-1}$ where $\alpha = \int\limits_{(4\pi)} d\Omega c (\Omega \cdot \Omega') (\Omega \cdot \Omega')$ is the mean value of the cosine of the scattering angle. Therefore applying the method of successive approximations to Eq. (6) we obtain $F_i = (\Omega \cdot \mathbf{i}) \mu^{-1} \times (1 + \alpha + \alpha^2 + \ldots) = \frac{\Omega \cdot \mathbf{i}}{\mu(1-\alpha)}$. Substituting F_i into Eq. (5) we obtain the familiar result for a homogeneous medium: $D_i = (1/3)\mu_{tr}$. Let us now consider a heterogeneous medium. If the heterogeneous system has axial symmetry the diffusion tensor has two different components: $D_\parallel$ for diffusion along the axis of symmetry and $D_\perp$ for diffusion perpendicular to the axis. If scattering in all the components of the medium is spherically symmetric, the exact solution for the function $F_\parallel$ has the form $F_\parallel = (\Omega \cdot \mathbf{i}_\parallel)\, 1 \times (\mathbf{r}, \Omega)$. Actually in this case $c = 1$ and the integral $\int\limits_{(4\pi)} d\Omega\, (\Omega \cdot \mathbf{i}_\parallel)\, l(\mathbf{r}, \Omega)$ vanishes because of the symmetry

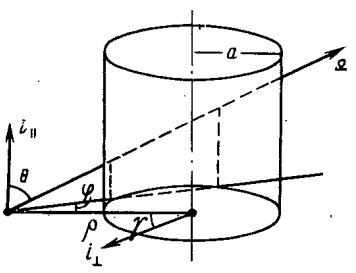

Fig. 2. Diagram for a medium with cylindrical channels.

of the problem. The neutron mean free path upward along $i \parallel$ is equal to the corresponding mean free path downward (Fig. 2). Therefore for spherically symmetric scattering the exact expression for $D \parallel$ has the form

$$D_{\parallel} = D_{\parallel}^{(0)} = \int\limits_{(4\pi)} \frac{d\Omega}{4\pi} (\Omega \cdot i)^2 \langle l(r, \Omega) \rangle. \tag{7}$$

For the function $F_{\perp}$ there is no such symmetry of the mean free paths and therefore even for spherically symmetric scattering the expression for $F_{\perp}$ does not reduce to a result analogous to (7). In this case the quantity $D_{\perp}^{(0)} = \int\limits_{(4\pi)} \frac{d\Omega}{4\pi} (\Omega \cdot i_{\perp})^2 \times \langle l(r, \Omega) \rangle$ corresponds to the first approximation to the solution of the integral equation (6). For spherically symmetric scattering, taking account of higher approximations to the function $F_{\perp}$ corresponds to taking account of the microstructure of the flux for diffusion in the transverse direction [2, 4]. For an arbitrary scattering law the quantity $\int\limits_{(4\pi)} d\Omega' (\Omega \cdot i)\, c(r, \Omega \cdot \Omega')\, l(r, \Omega')$ is different from zero for any direction. In the linear approximation to the scattering index the function F_i has the form

$$F_i(r, \Omega) = (\Omega \cdot i)\, l(r, -\Omega) - \int\limits_0^{\infty} dR \mu(r') e^{-\mu \tilde{R}} \times \int\limits_{(4\pi)} d\Omega' (\Omega' \cdot i)\, c(r, -\Omega \cdot \Omega')\, l(r', \Omega'). \tag{8}$$

Substituting this value into Eq. (5) and interchanging the order of integration over r and r', we obtain, after some simple transformations,

$$D_i = \int\limits_{(4\pi)} \frac{d\Omega}{4\pi} (\Omega \cdot i)^2 \langle l(r, \Omega) \rangle - \int\limits_{(4\pi)} \frac{d\Omega}{4\pi} (\Omega \cdot i) \int\limits_{(4\pi)} \frac{d\Omega'}{4\pi} \times (\Omega' \cdot i) \langle 4\pi \mu(r)\, c(r, -\Omega \cdot \Omega')\, l(r, \Omega)\, l(r, \Omega') \rangle. \tag{9}$$

The second term in Eq. (9) takes into account the contribution to D_i of the averages, over the volume of a cell, of the angular correlations between two successive free paths of a neutron in a heterogeneous medium with an arbitrary scattering law. Similarly it can be shown that taking into account the next approximation to the solution of Eq. (6) reduces to calculating averages over a cell of the angular correlations between two free paths separated by one arbitrary intermediate free path etc.

Neutron Diffusion in a Medium Containing Voids

Let us consider an application of the general formula (9) to the description of neutron diffusion in a homogeneous medium with empty channels of circular cross section. We shall assume that the channels are far enough apart so that a single free path intersects no more than one of them. The first term in Eq. (9) leads to the familiar result of Behrens [1] for a system with isotropic scattering

$$D_i^0 = \frac{1}{3\mu} \cdot \frac{1 + 2p + \mu a p Q_i}{1 + p}, \tag{10}$$

where p is the ratio of the volume of a channel to that of the moderator in a cell; a is the radius of the channel; the coefficient Q_i is equal to two for $D_{\parallel}$ and to unity for $D_{\perp}$. The presence of the factor $\mu(r)$ in the second term of Eq. (9) reduces the averaging over the volume of a cell to an integration over the volume of the moderator in the cell. It is convenient to separate out of this term the part which corresponds, in the linear approximation in α, to replacing the scattering cross section in the first term by the transport cross section. To do this we write the quantity $l(r, \Omega)$ in the form $l(r, \Omega) = \mu^{-1} + \delta l(r, \Omega)$, where the term δl takes into account the fraction of the free path connected with the intersection of the boundaries of separation of the components of the heterogeneous medium. Then the product of free paths may be written as a sum

$$l(r, \Omega)\, l(r, \Omega') = \frac{1}{\mu} [l(r, \Omega) + l(r, \Omega)] - \frac{2}{\mu^2} + \delta l(r, \Omega)\, \delta l(r, \Omega'). \tag{11}$$

Values of Coefficients δQ_i A_i and B_i for $\mu a \gg 1$

Direction of i axis	δQ_i	A_i	B_i
Along axis of channel ($\parallel$)	0	0.3	0.28
Perpendicular to axis of channel ($\perp$)	0.23	0.39	0.24

It should be noted that each of the first two terms of Eq. (11) depends on a single angle variable. When (10) is subsitituted into (9) this fact allows us to integrate over one angle variable in each of the first two terms. Then by applying the same calculational procedure as used in obtaining (10) we find

$$-4\pi \int\limits_{(V_{mod})} \frac{d^3r}{V_{ce}} \int\limits_{(4\pi)} \frac{d\Omega}{4\pi}(\Omega\cdot i) \int\limits_{(4\pi)} \frac{d\Omega'}{4\pi}(\Omega'\cdot i)\, c(-\Omega\cdot\Omega')\left[l(r,\Omega)+l(r,\Omega')-\frac{2}{\mu}\right]=\frac{\alpha}{3\mu}\cdot\frac{1+2p}{1+p}. \tag{12}$$

It is easy to see that in the linear approximation in α the addition of (12) to (10) effectively reduces to replacing the scattering by transport cross section in (10). Therefore, in the linear approximation in the scattering index, the diffusion tensor D_i for systems with voids may be written in the form

$$D_i=\frac{1}{3\mu_{tr}}\cdot\frac{1+2p+\mu_{tr}apQ_i}{1+p}-\int\limits_{(4\pi)}\frac{d\Omega}{4\pi}(\Omega\cdot i)\int\limits_{(4\pi)}\frac{d\Omega'}{4\pi}(\Omega'\cdot i)\int\limits_{V_{mod}}\frac{d^3r}{Vce}4\pi c(-\Omega\cdot\Omega')\,\delta l(r,\Omega)\,\delta l(r,\Omega'). \tag{13}$$

In contrast to the first term, the second term in (13) is determined not only by terms proportional to α, but also by higher moments in the expansion of the scattering index in Legendre polynomials. For simplicity we henceforth limit ourselves to the first three terms of the expansion

$$4\pi c(\Omega\cdot\Omega')=1+3\alpha(\Omega\cdot\Omega')+5\beta P_2(\Omega\cdot\Omega'), \tag{14}$$

where The quantity δl may be determined from the geometry of the system (cf. Fig. 2)

$$\delta l(r,\Omega)=\frac{2a}{\sin\theta}\sqrt{1-\left(\frac{\rho}{a}\right)^2\sin^2\varphi}\exp\times\left\{-\frac{\mu a}{\sin\theta}\left[\frac{\rho}{a}\cos\varphi-\sqrt{1-\left(\frac{\rho}{2}\right)^2\sin^2\varphi}\right]\right\}, \tag{15}$$

where ρ is the distance from the point under consideration to the axis of the channel; θ, φ are the polar angles of the vector Ω, $|\varphi|\leq\sin^{-1}\rho/(\rho+a)$.

Let us consider the case where $\mu a \gg 1$ which is the most interesting practically. It is easy to show that in this case the integration over r in Eq. (13) does not depend on Ω. Finally we obtain

$$-4\pi\int\limits_{(4\pi)}\frac{d\Omega}{4\pi}(\Omega\cdot i)\int\limits_{(4\pi)}\frac{d\Omega'}{4\pi}(\Omega'\cdot i)\int\limits_{(V_{mod})}\frac{d^3r}{Vce}c(-\Omega\cdot\Omega')\,\delta l(r,\Omega)\,\delta l(r,\Omega')=\frac{aQ_i}{3\mu(1+p)}(-\delta Q_i+\alpha A_i-\beta B_i), \tag{16}$$

where the coefficients δQ_i, A_i, and B_i are given by

$$\delta Q_i-\alpha A_i+\beta B_i=\frac{3}{4\pi^3 Q_i}\int\limits_0^{2\pi}d\gamma\int\limits_0^{\pi}\int d\theta\,d\theta'\int\limits_{-\pi/2}^{\pi/2}\int d\varphi\,d\varphi'$$

$$\times\frac{\cos^2\varphi\cos^2\varphi'\sin\theta\sin\theta'}{\sin\theta\cos\varphi+\sin\theta'\cos\varphi'}(\Omega\cdot i)(\Omega'\cdot i)[1-3\alpha(\Omega\cdot\Omega')+5\beta P_2(\Omega\cdot\Omega')]. \tag{17}$$

Thus for anisotropic scattering the diffusion tensor in a medium with voids has form

$$\frac{D_i}{D_0}=\frac{1+2p+\mu apQ_i(1-\delta Q_i+\alpha A_i-\beta B_i)}{1+p}. \tag{18}$$

If we use the expression $\langle\mu_a\rangle=\frac{\mu_a}{1+p}$ for the average absorption cross section in a medium containing voids we can then obtain from Eq. (18) the tensor for the square of the diffusion length

$$\frac{L_i}{L_0^2}=1+2p+\mu apQ_i(1-\delta Q_i+\alpha A_i-\beta B_i). \tag{19}$$

This expression differs from Behrens' formula [1] and that of Benoist [4] in containing terms proportional to α and β.

The values of the coefficients δQ_i, A_i and B_i listed in the table correspond to the condition $\mu a \gg 1$. In general when this condition is not satisfied Eqs. (17) and (18) still hold but the coefficients depend on the parameter μa. However, even for $\mu a \gtrsim 2$ these coefficients differ only slightly from the values given in the table.

In the next approximation to Eq. (6), terms proportional to α^2 and β^2 appear in Eqs. (17) and (18). These correspond to the angular correlations of two free paths separated by one arbitrary intermediate path. It can be shown that taking account of higher approximations in the solution of (6) reduces to replacing $\delta Q_i - \alpha A_i + \beta B_i$ in (17) and (18) by a more general expression which may be written as the series $\sum_{k=1}(\delta Q_{ik} - \alpha^k A_{ik} + \beta^k B_{ik})$. It should be noted that for longitudinal diffusion all the δQ_{ik} vanish by symmetry.

Thus taking account of anisotropic scattering in a heterogeneous medium leads to the appearance of new terms in the expression for the diffusion coefficient tensor which have no analogues in the corresponding expression for a homogeneous medium.

The dependence of the diffusion length in a heterogeneous medium on higher angular moments of the scattering index allows one in principle to determine the mean square value of the cosine of the scattering angle by comparing the diffusion length in a continuous medium with that in a medium containing voids.

We note that although Eqs. (9) and (10) were obtained under the assumption of weak absorption, they may be applied also to neutron multiplying systems. As a matter of fact the assumption of small neutron absorption was used only to justify the small change in neutron flux over an elementary cell of the medium, a condition which is clearly satisfied in many reactor systems.

CONCLUSIONS

Let us estimate the contributions to the expression for the D_i tensor made by the new terms derived here. The most interesting part is $D_\parallel$ for which $\delta Q_{11,k} = 0$. It is clear that for $\mu a \gg 1$ the last term in (19) may be much larger than the sum of the first two terms. For hydrogen the quantities α and β are 2/3 and 1/4 respectively, and therefore $\alpha A_\parallel - \beta B_\parallel \approx 0.11$. Taking account of terms quadratic in α can only increase this result. Therefore on the whole one must expect that for $\mu a \gg 1$ these terms will amount to about 10 to 20% of the terms of the corresponding Behrens formula. For the diffusion of thermal neutrons in water $\alpha \approx 1/3$ and therefore the above estimate is in principle still valid.

For diffusion in the transverse direction the contribution of terms depending on α is appreciably less. This is due to the fact that, unlike for the case of diffusion in the longitudinal direction, in this case there appear terms proportional to α due to taking account of higher approximations in the solution of Eq. (6) and their contribution will have a sign opposite that of $\alpha A_\perp$ calculated by Eq. (6). The higher order approximations for $L_\perp^2$ are particularly important in a slab lattice. In this case it can be shown that $1 - \sum_k (\delta Q_{\perp k} - \alpha A_{\perp k} + \beta^k B_{\perp k}) = 0$, and therefore for a slab lattice $L_\perp^2 / L_0^2 = 1 + 2p$. For a lattice with cylindrical channels of circular cross section the corresponding quantity, while not zero, makes an essentially smaller contribution than for diffusion in the longitudinal direction.

Thus taking account of anisotropic scattering leads to still larger anisotropies in neutron diffusion in heterogeneous media. The experimental data of I. S. Grigor'ev [6] on the diffusion of thermal neutrons in water containing voids reliably indicate a difference between $L_\parallel^2 / L_0^2$ and the value given by the Behrens formula. This difference is in satisfactory agreement with the above estimate of the contribution of the new terms in $L_\parallel^2$.

From the point of view of the experimental investigation of the effect it is interesting to measure the neutron age in water containing voids using a source energy of no more than a few hundred kilovolts. This condition is desirable since in this region the scattering cross section does not depend on energy. For comparison it is interesting to measure $L_\parallel^2 / L_0^2$ for the same parameter μ_{tr} ap in graphite and water containing voids ($\alpha_C \approx 0$, $\alpha_{H_2O} \approx 1/3$).

We note that in a two-component slab lattice, when one of the components scatters neutrons weakly, the contribution of the new terms to $L_\parallel^2$ may be larger than in a system with cylindrical voids. Later we propose to calculate similar corrections to the diffusion tensor for arbitrary two-component media.

LITERATURE CITED

1. D. Behrens, Proc. Phys. Soc., A62, 607 (1949).
2. N. I. Laletin, Proceedings of the Second International Conference on the Peaceful Uses of Atomic Energy, Vol. 2, Moscow, Atomizdat, p. 634, [in Russian] (1959).
3. J. Ferziger et al., Nucl. Sci. and Eng. 10, 285 (1961).
4. P. Benoist, React. Sci., A13, 97 (1961).
5. V. M. Novikov, Atomnaya Énergiya, 20, 520 (1966).
6. I. S. Grigor'ev and V. M. Novikov, Diffusion of Neutrons in Heterogeneous Media, Moscow, Atomizdat [in Russian] (1966).

USE OF RADIOACTIVE CATALYSTS FOR DEHYDRATING ALCOHOLS

Vikt. I. Spitsyn and N. E. Mikhailenko

UDC 541.128.3:553.76

The authors show that catalytic processes can be influenced by radioactive radiation. The addition of radioactive material to a catalyst greatly changes the velocity and apparent activation energy of the process, and sometimes changes the direction of a heterogeneous-catalytic reaction. It is shown that radioactive radiations produce qualitative changes in the catalyst and have a marked effect on the adsorbed layer of molecules on the catalyst surface which become polarized, the degree of polarization depending on the structure of the reacting molecule.

In the USSR the properties of radioactive catalysts have been studied since 1957 [1, 2]. The principal results of these investigations are given in [3-8]. Research in other countries includes work at Oak Ridge [9-12], University of Illinois, and in France [13].

The present paper is a detailed study of the dehydration of alcohols over different catalysts (magnesium sulfate containing S^{35} [14, 15], tricalcium phosphate with Ca^{45} or P^{32} [16], and aluminum oxide with various additives [17]). The radioactive catalysts were prepared by introducing the radioactive isotope during the chemical reaction of the initial reagents, or by irradiating the catalyst in a nuclear reactor.

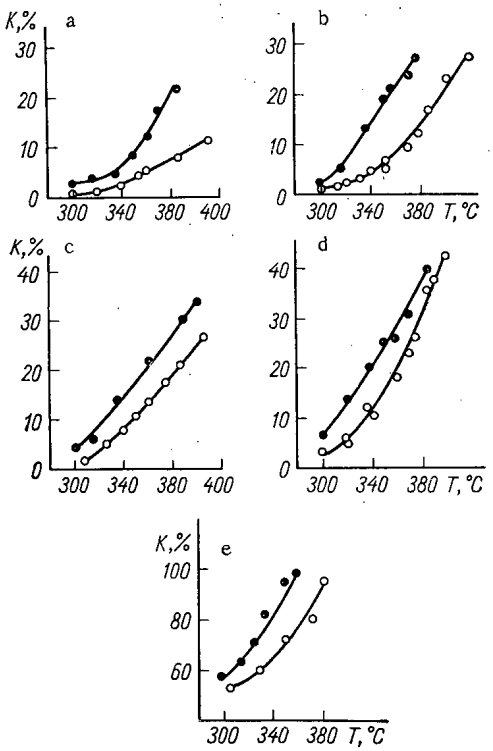

Fig. 1. Degree of conversion of alcohol K, plotted vs. temperature over radioactive MgSO4. a) n-Amyl alcohol; b) n-hexyl alcohol; c) n-decyl alcohol; d) n-dodecyl alcohol; e) cyclohexanol; ○) nonradioactive; ●) radioactive MgSO4, activity 103-105 mCi/g.

Figure 1 plots the yield of olefin (the reaction product of alcohol dehydration) versus temperature on a magnesium sulfate catalyst containing S^{35} [$E(\beta)_{max}$ = 0.167 MeV]. The catalyst's specific activity was 100 mCi/g. The increase in the degree of conversion at 350°C was as follows: for n-amyl alcohol 200%; n-hexyl alcohol 121%; n-decyl alcohol 42%; n-dodecyl alcohol 26%; total conversion of cyclohexanol begins at a temperature 40°C lower.

Figure 2 plots the yield of propylene vs. temperature over tricalcium phosphate catalyst containing Ca^{45} [$E(\beta)_{max}$ = 0.255 MeV] or P^{32} [$E(\beta)_{max}$ = 1.70 MeV]. The increase in the degree of conversion for these two isotopes is 400 and 700% respectively. It will be seen from Figs. 1 and 2 that the reduction in the optimum process temperature may reach 100-120°C.

We made a detailed study of the dehydration of alcohols of different composition on magnesium sulfate catalyst versus the radioactive isotope content. Magnesium sulfate was made by the method in [5] and contained 0.95% H_2O, so its composition was $MgSO_4 \cdot 0.06\ H_2O$. The specific activity of these catalysts was in the range 15-160 mCi/g. The specific surface, determined by adsorption of krypton or air at the temperature of liquid

Translated from Atomnaya Énergiya, Vol. 21, No. 4, pp. 277-281, October, 1966. Original article submitted July 8, 1965; revised May 23, 1966.

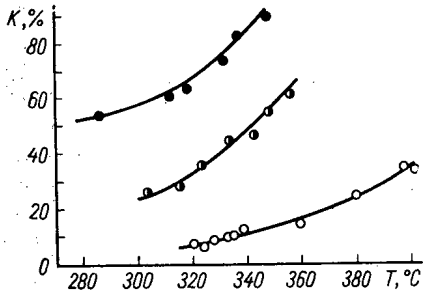

Fig. 2. K vs. temperature over radioactive catalyst $Ca_3(PO_4)_2 \cdot H_2O$. ○) nonradioactive; ◐) radioactive with respect to calcium, activity 58,1 mCi/g; ●) radioactive with respect to phosphorus, activity 52.2 mCi/g.

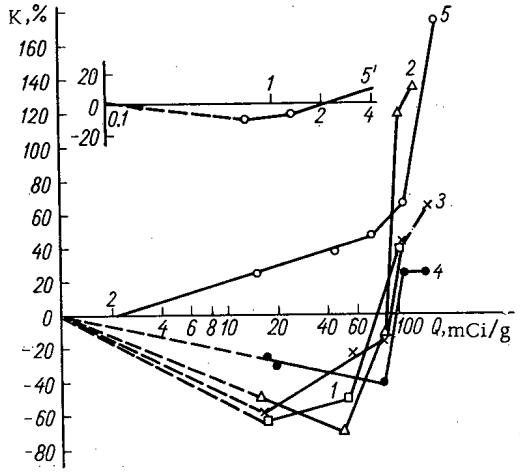

Fig. 3. Degree of conversion of alcohol K, plotted versus specific radioactivity of magnesium sulfate Q at 375°C. 1) n-Amyl alcohol; 2) n-hexyl alcohol; 3) n-decyl alcohol; 4) n-dodecyl alcohol; 5) cyclohexanol.

nitrogen, was 4-7 m^2/g. To calculate the apparent activation energy at zero order of the reaction, we selected conditions on a nonradioactive catalyst for which the degree of alcohol dehydration would not exceed 30%.

Figure 3 plots the degree of conversion of alcohol at 375°C versus the logarithm of the catalyst's specific radioactivity. The appearance of a minimum on these curves can be attributed to the change in the limiting stage of the process on the radioactive catalyst's surface. Alcohol dehydration probably has a carbonium-ionic mechanism:

$$C_nH_{2n+1}OH \xrightarrow{+H^+} C_nH_{2n+1}OH_2^+ \xrightarrow{-H_2O} C_nH_{2n+1}^+ \xrightarrow{-H^+} C_nH_{2n}.$$

As a result of bombardment by β particles, $MgSO_4$ becomes positively charged. This intensifies the adsorption of alcohol molecules on the catalyst's surface and assist their protonization. The next stage of the reaction, the removal of a molecule of water, is slower, as was observed in the case of catalysts with low specific activities. At higher specific activities of magnesium sulfate, polarization of the adsorbed intermediate products and dehydration of the ROH_2^+ ion are intensified. This explains why in the specific radioactivity range 80-100 mCi/g the dehydration velocities of all these aliphatic alcohols displayed a marked increase on radioactive magnesium sulfate. A further increase in specific radioactivity to 120-160 mCi/g does not produce such a marked increase in catalytic activity, and in the case of n-dodecanol the activity becomes constant. This was attributable to the attainment of equilibrium in these two stages of the process. In the case of cyclohexanol dehydration, minimum catalytic activity of $MgSO_4$ was observed for a catalyst with specific activity 0.7 mCi/g (see curve 5 in Fig. 3).

In the case of aliphatic alcohols the range of increased catalytic activity of $MgSO_4$ is 80-160 mCi/g, but is much wider in the case of cyclohexanol (2.5-160 mCi/g). This is evidently due to the different orientations of the alcohol molecules on the catalyst's surface [18, 19] and to the fact that cyclic molecules display greater polarization than molecules of aliphatic alcohols.

It will be seen from Fig. 4 that for all these alcohols the activation energy of the catalytic process at different specific activities of $MgSO_4$ can be calculated from the Arrhenius equation.

Figure 5 plots the apparent activation energy E_K vs. the specific radioactivity of $MgSO_4$ for each alcohol. With increasing number of carbon atoms in the aliphatic alcohol chain the E_K of dehydration over nonradioactive $MgSO_4$ decreases and reaches a minimum in the case of n-dodecanol. In accordance with its structure, cyclohexanol has an even lower E_K.

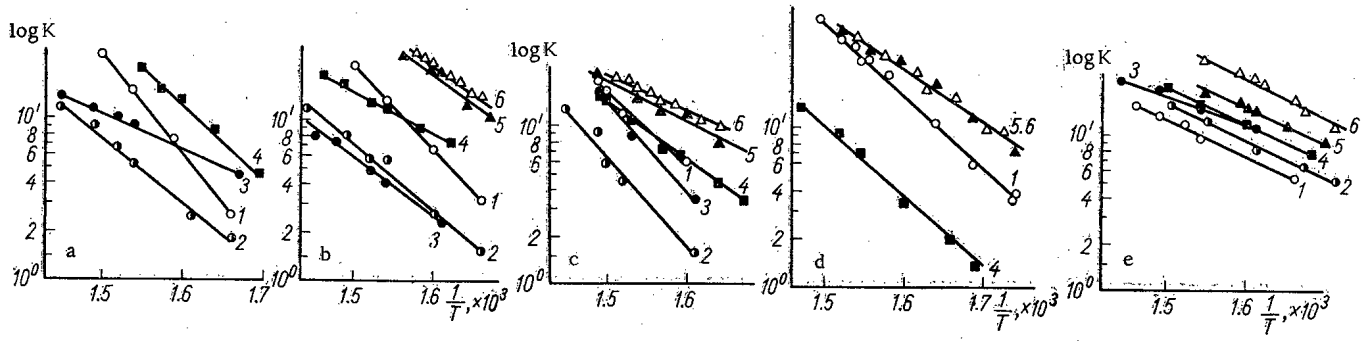

Fig. 4. Log of the reaction rate plotted versus 1/T. a) n-Amyl alcohol; b) n-hexyl alcohol; c) n-decyl alcohol; d) n-dodecyl alcohol; e) cyclophexanol. Catalyst: $MgSO_4$: 1) nonradioactive; 2) activity 15-16 mCi/g; 3) 45-54 mCi/g; 4) 73-86 mCi/g; 5) 103-105 mCi/g; 6) 130-160 mCi/g.

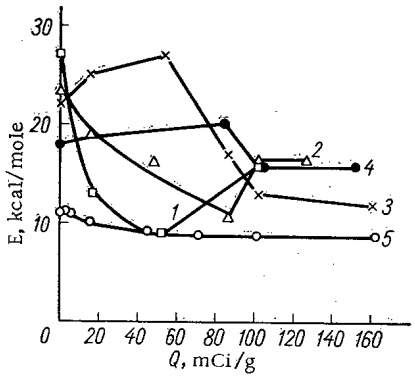

Fig. 5. E_K of alcohol dehydration, plotted vs. specific radioactivity Q of the catalyst. 1) n-Amyl alcohol; 2) n-hexyl alcohol; 3) n-decyl alcohol; 4) n-dodecyl alcohol; 5) cyclohexanol.

In most cases E_K decreases with increasing content of radioactive isotope. A fairly simple relation between E_K and the isotope content is observed only in the case of cyclohexanol, for which E_K decreases slowly with increasing specific radioactivity and then remains constant. This agrees with data obtained for catalysts with the compositions $MgSO_4 + Na_2SO_4$ and $Ca_3(PO_4)_2 \cdot H_2O$.

A more complex relation was observed for aliphatic alcohols: in the case of n-amyl and n-hexyl alcohols an increase in the specific radioactivity of $MgSO_4$ > 100 mCi/g increases the activation energy somewhat, but it remains below the value for a nonradioactive catalyst. For n-decyl and n-dodecyl alcohols, at high specific radioactivities of $MgSO_4$ the value of E_K increases, as opposed to its decrease in activity range 85-100 mCi/g. On catalysts with activity 100-160 mCi/g the E_K of all these alcohols becomes virtually constant ($\sim$ 12-16 kcal/mole). It should be noted that in the temperature range of the experiments, the yield of olefin from alcohol dehydration decreases, despite the fall in E_K above radioactive catalysts.

The complex relation between the E_K of the catalytic process and the catalyst's absolute radioactivity indicates changes due to radiation. The latter must also affect the adsorbed layer of molecules which participate in the reaction on the catalyst's surface.

For a more detailed study of the changes in structure and composition of sulfate catalysts, we employed infrared spectroscopy [20], nuclear magnetic resonance and thermography [21]. The first phase in this part of the investigation was a study of the infrared spectra of K_2SO_4 specimens subjected to different doses due to the different initial specific radioactivities with respect to S^{35}. At the time the measurements were performed, the K_2SO_4 specimens had very weak residual radioactivities (0.01-0.02 mCi/g).

Figure 6 shows the infrared spectra of K_2SO_4 with initial specific radioactivity 3, 40, 50, and 94 mCi/g. The dose received by the specimens was $6 \cdot 10^{19}$, $9 \cdot 10^{20}$, $1 \cdot 10^{21}$ and $2.2 \cdot 10^{22}$ eV/g respectively. The absorption spectra of specimens containing radioactive isotopes are characterized by splitting of the valence vibration absorption band (1100-1200 cm^{-1}) and increased intensity of the bands at 1200 and 1000 cm^{-1}. These changes in the SO_4 group may be due to a change in the charge of this group, namely the loss of a monovalent electron and therefore a change in the electron cloud of the group.

The infrared spectra of highly radioactive magnesium sulfate displayed a slight shift (+10 cm^{-1}) in the deformation vibration absorption band (687 cm^{-1}). It must be borne in mind that magnesium sulfate crystals are less symmetrical than K_2SO_4 crystals. It is more difficult to detect slight changes in the spectra of less symmetrical radioactive specimens. There are grounds for assuming that ions of

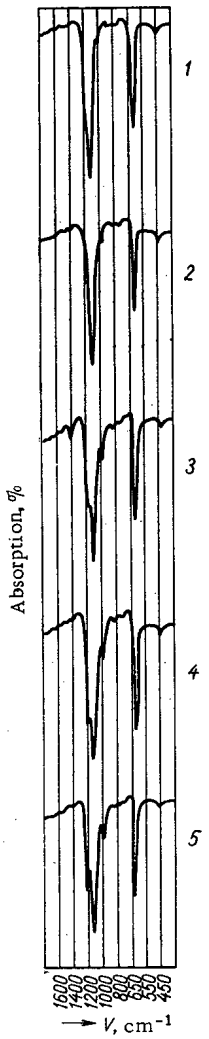

Fig. 6. Infrared absorption spectra of K_2SO_4 specimens. 1) Nonradioactive with initial specific activity; 2) 3 mCi/g; 3) 40.0 mCi/g; 4) 49.7 mCi/g; 5) 90.3 mCi/g; (V is the wave number).

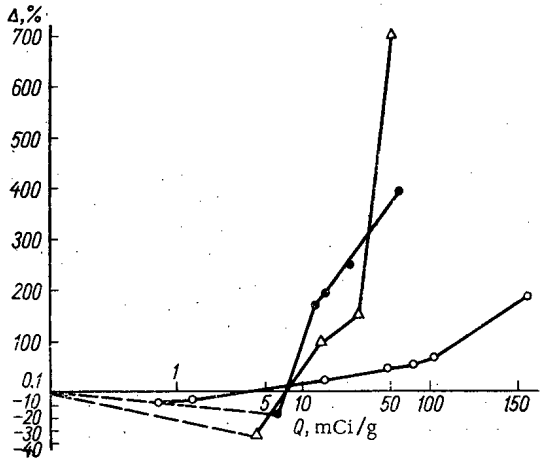

Fig. 7. Change in the degree of conversion of cyclohexanol and isopropyl alcohol on radioactive catalyst: ○) $\overset{\times}{MgSO_4}$; ●) $\overset{\times}{Ca_3(PO_4)_2}\cdot H_2O$; △) $Ca_3(\overset{\times}{PO_4})_2\cdot H_2O$.

anomalous valence (SO_4^- type) are also formed in radioactive $MgSO_4$. In fact, the authors of [22], who used the EPR method, found that radioactive specimens of sulfate of group 2 elements also contain SO_4^- ion-radicals. It may be supposed that the increase in catalytic activity depends on the formation of ions of anomalous valence or ion-radicals.

Our study of the dehydration of different alcohols showed that if one portion of catalyst (composition $MgSO_4\cdot 0.06\ H_2O$) is used at 300-400°C for 2-3 h, reproducible results are obtained and the catalytic activity is retained. However, after a series of experiments had been performed, the catalyst's weight increased by 5-6% to $MgSO_4\cdot 0.3$-$0.4\ H_2O$. It was therefore of interest to study the composition of the $MgSO_4$ hydrates formed and the bonding character of this water. For this purpose we used thermography and proton magnetic resonance. Thermographic analysis showed that crystal hydrates of $MgSO_4$ are formed during the catalytic reaction. The spectra obtained by nuclear magnetic resonance confirmed that the water in spent magnesium sulfate catalyst is water of crystallization, and not merely adsorbed. Hydroxyl groups were not detected in the spent catalyst. If the prepared catalyst is heated at 800°C, its catalytic activity is greatly reduced. It is therefore very important to know the content and bond character of the water in a magnesium sulfate catalyst.

The following conclusions may be drawn from this investigation. Isotopes with low radiation energies are more effective in the case of catalysts with low absolute activities. However, at high absorption doses the yield of the reaction products increases markedly on catalysts containing radioactive isotopes with high radiation energies (Fig. 7).

The reduction in the optimal reaction temperatures indicates that it is essentially possible to make practical use of radioactive catalysts.

LITERATURE CITED

1. A.A. Balandin et al., Dokl. AN SSSR, 121, 495 (1958); 137, 628 (1961); 86, 299 (1964).
2. Vikt. I.Spitsyn, Izv. AN SSSR, Otd. khim. nauk., No. 11, 1296 (1958).
3. R. Coekelbergs, A. Crucq, and A. Frenet, Advances in Catalysis, 13, 55 (1962).
4. V.G. Baru, Uspekhi khimii, 32, 1340 (1963).
5. V. Spitsyne. Nucleus, 4, 284 (1963).
6. V. Spitsyne. Z. phys. Chem., 226, 360 (1964).
7. D. Wagnerova. Chem. listy, 58, 133 (1964).
8. P.L. Gruzin, Report No, 298, Presented by the USSR Delegation to the 3rd International Conference on the Peaceful Uses of Atomic Energy (Geneva, 1964).
9. Nucl. Sci. Abstr., 24A, 3296 (1960).
10. N. Krohn, H. Smith. J. Phys. Chem., 65, 1919 (1961).
11. N. Krohn, R. Wymer. Paper CN-14/17 Presented on IAEA Conference on the Application of Harge Radiation Sources in Industry, Salzburg, Austria, (1963).
12. N. Krohn, H. Smith. J. Phys. Chem., 67, 1497 (1963).
13. P. Traynard and L. Orsini, Compt. rend., 252, 873 (1961).
14. Vikt. I. Spitsyn, I.E. Mikhailenko, and O.M. Petrova, Zh. fiz. khim., 39, 478 (1965).
15. Vikt. I. Spitsyn, I.E. Mikhailenko, and O.M. Petrova, Kinetika i kataliz, 6, 735 (1965).
16. Vikt. I. Spitsyn et al., Dokl. AN SSSR, 146, 1128 (1962).
17. V. Spitzin et al. J. prakt. Chem., 25, 160 (1964).
18. M.P. Maksimova, V.E. Vasserberg, and A.A. Balandin, Izv. AN SSSR, Otd. khim. nauk, 17, No.1, 17 (1963).
19. V.E. Vasserberg, A.A. Balandin, and M.P. Maksimova, Zh. fiz. khim., 35, 858 (1961).
20. M.V. Akhmanova and I.E. Mikhailenko, Zh. fiz. khim, 39, 2273 (1965).
21. Vikt. I. Spitsyn, I.E. Maikhailenko, and V.F. Chubaev, Dokl. AN SSSR. 162, 1346 (1965).
22. Vikt. I. Spitsyn, V.V. Gromov, and L.G. Karaseva, Dokl. AN SSSR, 159, 178 (1964).

All abbreviations of periodicals in the above bibliography are letter-by-letter transliterations of the abbreviations as given in the original Russian journal. *Some or all of this periodical literature may well be available in English translation.* A complete list of the cover-to-cover English translations appears at the back of the first issue of this year.

RADIATION-CHEMICAL STABILITY OF TBP IN SOLUTIONS OF HYDROCARBONS

E. P. Barelko, I. P. Solyanina, and Z.I. Tsvetkova

UDC 541.15:547.27

The radiolysis of binary mixtures containing tributyl phosphate (TBP) and ali-phatic or aromatic hydrocarbons is discussed. The radiation-chemical stability of the irradiated systems was measured according to the yields of the acid esters (di- and monobutyl phosphate) and gaseous products, as well as according to the change in the distribution coef ficients of plutonium and zirconium between the irradiated organic phase and an aqueous solution containing 2M nitric acid and the nitrates of these metals.

The concentration dependence of the radiation chemical yields of gaseous and acid radiolysis products gives evidence of a deviation from the additivity rule and of a transfer of energy from the aliphatic hydrocarbon to TBP. As a result of replacement of the aliphatic hydrocarbon by an aromatic hydrocarbon, the yields of the radiolysis products are sharply reduced. The influence of aromatic hydrocarbons upon the radiation-chemical stability of TBP is confirmed by data on the distribution coefficients of plutonium and zirconium, the values of which are determined to a considerable degree by the content of dibutyl phosphate—the basic product of the radiolysis of TBP.

It is known that tri-n-butyl phosphate (TBP) is chemically rather stable. However, under definite conditions, for example, under the action of concentrated solutions of acids or radioactive radiations, it is subjected to decomposition – dealkylation; as a result of these processes, acid phosphates arise, chiefly dibutyl phosphate (DBP), which form stronger complexes with certain metal ions than does TBP, which promotes their extraction from aqueous solutions into the organic phase.

The investigation of the effects of radiation on the decomposition of pure TBP was the subject of [1-7], in which the nature and radiation chemical yields of the basic radiolysis products of TBP are considered. Until recently, however, the question of the radiation-chemical stability of TBP in solutions of hydrocarbons, in particular, aliphatic hydrocarbons, had not been sufficiently clarified. And yet, it is well known that precisely such systems are widely used in the technological utilization of extraction processes [8]. According to the data of Burger and MacClanahan [1], the radiation chemical yield of the decomposition of TBP does not depend upon the degree of its dilution by octane. Wagner et al. [2] have shown that aliphatic hydrocarbons appreciably influence the radiation stability of this ester, lowering the stability of TBP.

Data on the influence of an aliphatic diluent upon the stability of TBP, recently published [5, 7], show that at a low TBP concentration in the mixture, the radiation chemical yield of acid esters exceeds the value which follows from the additivity rule.

At the same time, a substantial increase in the stability of TBP in solutions of aromatic hydrocarbons is noted in comparison with aliphatic hydrocarbons [7]. Analogous results were obtained several years ago by the authors of this work.

This work was devoted to an investigation of the quantitative principles of the process of radiation chemical decomposition of TBP in solutions of aliphatic and aromatic hydrocarbons and to the change in the extraction properties of such solutions.

Translated from Atomnaya Énergiya, Vol. 21, No.4, pp.281-285, 1966. Original article submitted April 16, 1966.

EXPERIMENTAL PROCEDURE

The samples were irradiated in glass ampoules under vacuum and in the presence of air. The radiation source was Co^{60}. The dose rate was varied within the range 71-590 R/sec. The maximum radiation dose was $6.7 \cdot 10^{20}$ eV/ml.

TBP was thoroughly freed of traces of acid esters by shaking with a dilute solution of potash, followed by redistillation under vacuum. The middle fraction, with boiling point 125°C at the pressure 1 mm Hg, was collected for the work. Dodecane and the investigated aromatic hydrocarbons were purified by treatment with sulfuric acid and redistillation on a highly efficient column under vacuum. The concentration of the acid esters was measured by conductometric titration with a 0.01 N solution of sodium hydroxide. The sample was mixed with 20 volumes of water before titration; the equivalence point was calculated according to the titration curves.

A volumetric method was used to measure the total amount of gas liberated during radiolysis. The yield of the polymer formed from TBP was determined by vacuum distillation of the irradiated sample (at the temperature 130-140°C). The still residue, nonvolatile under these conditions, was a mixture of the polymer and acid esters. The amount of the latter, found preliminarily by conductometric titration, was deducted from the weight of the nonredistilled residue. The difference obtained was taken as the weight of the polymer.

The distribution coefficients K_p between the organic and nitric acid (2 M) aqueous phases of Pu^{239} and Zr^{95} nitrates were used as the characteristics of the extraction properties of the investigated systems. The Pu^{239} concentration was determined according to the α-activity, Zr^{95} according to the γ-activity.

DISCUSSION OF RESULTS

The results of the radiolysis of pure TBP under vacuum, obtained by the authors of this work during irradiation of TBP within the dose range $1.39 \cdot 10^{20} - 1.39 \cdot 10^{21}$ eV/ml, are presented in Table 1 in the form of the summary radiation chemical yields of the gaseous, acid, and polymer products and butanol. The table simultaneously presents the literature data for comparison.

From Table 1 it can be concluded that the decomposition of TBP occurs according to a nonchain mechanism. The differences in the values of the yields are most likely due to errors of dosimetry and analysis by individual authors and they should not be explained by the different effects of β- and γ-radiation. From the data of an investigation of trialkyl phosphates by the method of electron impact [9], it follows that the alkylation of compounds of this kind, forming an acid ester, may occur practically in the primary process.

Figure 1 presents the curves of the dependence of the yield of acid esters and gaseous products (considering the energy absorbed by the mixture) on the TBP concentration in dodecane solution. It can be seen that the two curves show evidence of a deviation from additivity. With increasing fraction of dodecane in the mixture, the yield of acid esters, characterizing the rate of decomposition of TBP,

TABLE 1. Radiation Chemical Stability of TBP

Type of radiation	Yield, molecules/100 eV				Literature
	gaseous products	DBP	polymer	butanol	
Co^{60}, γ	2.7	2.1	0.91	0.70	[1]
Co^{60}, γ	2.54	2.64	-	-	[2]
Electrons, 1.66 MeV	3.1	2.58	-	-	[3]
Electrons, 1 MeV..	1.1	1.67	-	-	[4]
The same	1.85	1.76 + 0.08	-	-	[5]
Co^{60}, γ	-	2.35	-	-	[6]
Co^{60}, γ	-	2.4	-	-	[7]
Co^{60}, γ	1.5	1.86	1.0	0.78	Data of this work

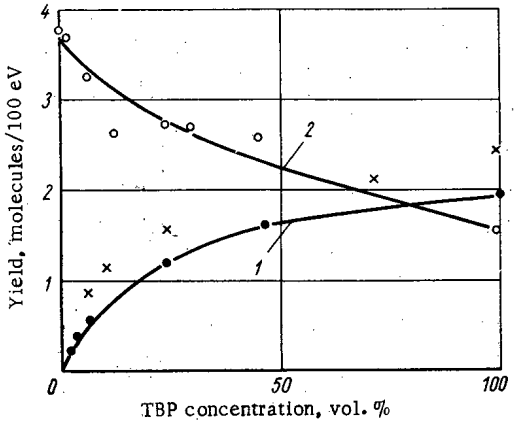

Fig. 1. Dependence of the radiation-chemical yields on the TBP concentration in dodecane. 1) Acid esters (●–data of this work; ×–data of [7]); 2) gaseous products (o).

Influence of Nature of Diluent Upon the Radiation Chemical Stability of TBP

Hydrocarbon	Yield, molecules/100 eV	
	gaseous product	acid product
Dodecane	2.8	1.3
Benzene	0.26	0.31
Toluene	0.34	0.44
Cumene	0.44	0.65
Mesitylene	0.52	0.46
Cymene	0.53	0.50
Monoisopropyldiphenyl . . .	0.19	0.22

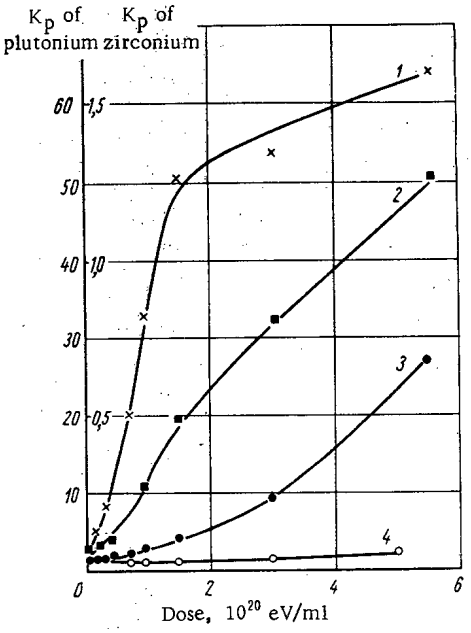

Fig. 2. Influence of nature of diluent on the change in the distribution coefficients during radiolysis of extraction systems. Plutonium: 2) dodecane, 4) cymene. Zirconium: 1) dodecane, 3) cymene.

increases. On the other hand, the yield of gaseous radiolysis products, characteristic to a greater degree of dodecane, decreases with increasing fraction of TBP. Figure 1 also presents the data obtained in [7]. The virtual coincidence of the results indicates that the indirect effect of radiation upon TBP, expressed in an increase in the yield of DBP in dilute solutions of TBP, actually occurs. The energy absorbed by the aliphatic hydrocarbon is partially transferred to TBP by one method or another, which leads to additional decomposition of it.

As can be seen from Table 2, replacement of the aliphatic hydrocarbon in the mixtures by an aromatic hydrocarbon (volume ratio of TBP to hydrocarbon = 1:1) leads to a substantial increase in the stability of TBP, which is expressed in an extremely sharp decrease in the yields of the acid esters and gaseous products, the absolute values of which depend upon the nature of the aromatic substance. The observed increase in the radiation chemical stability can be explained by the transfer of energy from TBP to the aromatic hydrocarbon.

The data obtained are in good agreement with the results of measurements of the distribution coefficients of systems of 20 vol.% TBP + dodecane at 20 vol.% TBP + thymine, irradiated by various doses in the presence of air. From Fig. 2 it can be seen that for the system TBP + dodecane (curves 1 and 2), the change in the distribution coefficients is a nonlinear, increasing function of the dose. The replacement of dodecane by cymene (curves 3 and 4) leads to a sharp increase in the radiation stability: the distribution coefficient of plutonium remains practically constant, while that of zirconium varies little within a broad range of irradiation doses.

In order to evaluate the degree of influence of irradiation of individual components of the extraction mixture upon its extraction properties, the authors of this work subjected TBP, dodecane, as well as solutions containing 20 vol.% TBP + dodecane, to irradiation by identical doses ($5.7 \cdot 10^{20}$ eV/ml). From the irradiated TBP and doecane, solutions corresponding to the nonirradiated components, containing 20 vol.% TBP + dodecane, were prepared by dilution. The extraction properties of the systems obtained are shown in Table 3.

TABLE 3. Influence of Irradiation of Components of the Extraction System Upon the Distribution Coefficients

Extractible element	Dose, 10^{20} eV/ml	Distribution coefficient		
		irradiated system		
		dodecane	TBP	20 vol.% TBP + dodecane
Plutonium	0	-	-	2.0
	5.7	2.03	21.0	32.8
Zirconium	0	-	-	0.032
	5.7	0.032	1.62	1.56

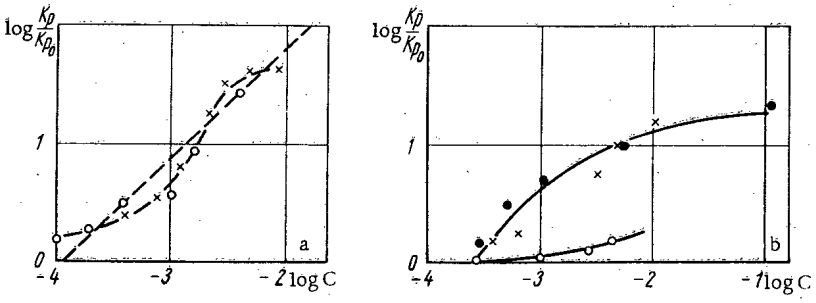

Fig. 3. Dependence of the distribution coefficients on the concentration c of DBP, formed in the radiolyzed system: a) zirconium: (×) TBP + dodecane, (○) TBP + cymene; b) plutonium: (×) TBP + dodecane, (●) data of model experiments [12]; (○) TBP + cymene (K_{p_0} is the distribution coefficient of nonirradiated system).

From the data cited, it follows that extraction is mainly influenced by the irradiation of TBP. This is expressed in a sharp increase in the distribution coefficients of plutonium and zirconium in comparison with the nonirradiated systems. Irradiation of dodecane has practically no effect upon the extraction of plutonium and zirconium. Thus, the change in the extraction properties that occurs when TBP is irradiated in solutions of aliphatic and aromatic hydrocarbons in the cases investigated can be attributed to decomposition of TBP, which, as is shown below, proceeds at different rates in solutions of hydrocarbons of different structures on account of the indirect action.

If we use the formation of DBP as the criterion of the irradiation decomposition of TBP and consider the change in the distribution coefficient of the element as a function of its concentration, then as can be seen from Fig. 3a, this dependence is rather complex in the case of extraction of zirconium; it is described as an S-shaped curve in bilogarithmic coordinates. However, if we attempt to describe this dependence approximately as a simple power function, then the exponent obtained will be equal to one (dotted straight line in Fig. 3a). Precisely such a dependence of the distribution coefficient of zirconium on the DBP concentration was observed in model experiments [10], in which DBP was specially introduced into the solution. As it follows from the experiments of the author of this article, as well as from [11], the nature of the diluent has no influence upon the distribution coefficient in this region of TBP concentrations. It can be seen that the change in the distribution coefficient of zirconium in the radiolysis of a TBP solution in hydrocarbon is determined by the decomposition products of TBP and can be approximately explained by the influence of DBP. In a certain sense, the opposite situation is observed in the case of the action of radiation upon the distribution coefficient of plutonium in the radiation accumulation of acid esters (see Fig. 3b). A comparison of the data on the dependence of the distribution coefficient of plutonium on the radiation chemical accumulation of DBP with the data of model experiments with specially introduced DBP [12] in solutions of aliphatic hydrocarbons gives sufficiently good coincidence of

the results not only on the nature of the change, but also in absolute values of the distribution coefficients of plutonium.

In the case of an aromatic diluent, the distribution coefficients of plutonium measured in systems containing aliphatic and aromatic hydrocarbons do not coincide in the presence of the same concentration of radiolytically formed acid esters. And yet, the change to an aromatic diluent in the model experiments of [11] does not decrease, but rather increases the distribution coefficient of plutonium.

LITERATURE CITED

1. L. Burger and E. Mac-Clanahan, Industr. and Engng Chem., 50, 153 (1958).
2. R. Wagner, E. Kunderman, and L. Taule, Industr. and Engng Chem., 51, 45 (1959).
3. J. Burr, Rad. Res., 8, 214 (1958).
4. F. Williams and K. Wilkinson, Nature, 179, 540 (1957).
5. K. Wilkinson and F. Williams, J. Chem. Soc., 4098 (1961).
6. V. P. Shvedov and S. P. Rosyanov, Zh. Fiz. Khim., 35, 561 (1961).
7. J. Canva and M. Pages, Bull. Soc. chim. France, 5, 909 (1964).
8. V. Cooper and M. Walling, Jr., in the book: Transactions of the Second International Conference on the Peaceful Uses of Atomic Energy (Geneva, 1958). Selected Reports of Foreign Scientists [Russian translation]. Moscow, Atomizdat, 5, p.103 (1959).
9. Mac Lafferty, Analyt. Chem., 28, 306 (1956).
10. V. B. Shevchenko and V. S. Smelov, Extraction. Collection [in Russian]. Moscow, Gosatomizdat, No.2, p.257 (1962).
11. V. B. Shevchenko et al., Radiokhimiya, 3, 281 (1960).
12. V. B. Shevchenko and V. S. Smelov, Atomnaya Énergiya, 5, 542 (1958).

SOLIDIFICATION OF RADIOACTIVE WASTES BY FUSION IN BASALT

Yaroslav Saidl and Yarmila Ralkova

UDC 621.039.7

It is shown that fused basalt is suitable for immobilizing radioactive wastes having high specific activity. It has been found that recrystallization of the vitreous fused basalt phase improves the properties of the material, principally the mechanical strength and the chemical stability. The calculated diffusion coefficients vary from 10^{-15} to 10^{-17} cm^2/sec at temperatures of 30-70°C.

In the removal of radioactive wastes, a special position is occupied by the problem of disposing of the high specific activity wastes resulting from processing irradiated nuclear fuel.

What we are talking about is manipulation involving large quantities of radioactive materials which are very seldom encountered in the form of "exposed radiators." In even a short time, the radiation from these materials destroys all highly developed organisms as well as most of the lower types, and is even capable of producing irreversible changes in inorganic materials. Accordingly, in every case, high-specific-activity wastes have to be strictly isolated from the biosphere. In principle, this can be done in two different ways: by burying the wastes in geological formations which do not come in contact with the biosphere, or by converting them into chemically stable forms and then burying them in some guarded area. The first method is simple as far as the chemical operations are concerned, but it is only suitable for countries containing much desert or unusable territory, and is apt to involve high transportation costs. The second method is very efficient and can be applied to all countries but is quite expensive.

During the last few decades, some experimental work has been done on immobilizing the mixture of fission products in various types of materials using silicon as base [1-4]. These studies were first brought up to the engineering scale in [5].

Under the conditions which exist in Czechoslovakia — a country with a high population density — it is impossible to dispose of high-activity wastes in the soil without first treating them. Accordingly, we made a study of the second method in order to find a suitable material based on the many years of tradition and experience accumulated by the Czechoslovakian glass and ceramic industry. After carefully sampling and classifying the siliceous material available, it was decided to make a study of the types used to produce chemically highly resistant materials.

First of all, a study was made of several kinds of ceramic materials. The materials resulting from fusion had satisfactory properties, but the heat treatment was so complicated that we had to give up the idea of using them. Better results were obtained by the simple method used to make various types of commercial glass [6]. However, their inherently high chemical resistance was impaired after they had been irradiated for a considerable length of time, and their temperature increased as a result of decay of the isotopes that they contained.

Finally, we concentrated our attention on fused minerals of basaltic type, which are noted for their chemical resistance and mechanical strength. Information on commercial fusion of basalt is given [7, 8].

The criteria that we used in choosing the material to be used in our studies were the resistance to hydrolysis and the melting point [9]. Accessibility of the material is no problem, since the supplies of basalt in Czechoslovakia are practically inexhaustible. Out of 14 trials, the most suitable materials

Institute of Nuclear Studies, Czechoslovakian Academy of Sciences, Rzhezh near Prague, Czechoslovakia. Translated from Atomnaya Énergiya, Vol. 21, No. 4, pp. 285-289, October, 1966. Original article submitted April 25, 1966. The scientific research work on this subject is being done under an agreement with the International Atomic Energy Agency.

turned out to be three types of basalt from the deposits in Gelberg, Teshetitsa, and Ogarzhitsa, and olivine basalt from Slapana,* all of which were studied in detail. What was investigated first was whether or not samples of the materials would keep the radioactive isotope in the solid state once it had been introduced. To get some idea of the chemical resistance, systematic observations were made of leaching out an immobilized radioactive isotope (of relatively low specific activity) with water, and the diffusion coefficient of the isotope in the solid was measured as a function of temperature [10-14]. It was found that recrystallizing the vitreous fused basalt phase tends to make it stronger mechanically. The resistance of the material to hydrolysis increases in the process, and the motion of the ions is slowed down many times. The apparent diffusion coefficients calculated from the leaching experiments are in good agreement with the measured values of the diffusion coefficients in the solid. The values for cesium and strontium are low enough (less than 10^{-16} cm^2/sec at 30°C) to meet the safety requirements for long-time storage.

Effect of Ballasting Materials

In mocking up the ballasting compounds, we were guided by the most widely used method of processing irradiated fuel, which is that of dissolving it in concentrated nitric acid. First of all, it is necessary to take into consideration the cations (Na^+) in the neutralizing agent, the cladding material (Al^{3+}), and the corrosion products (Fe^{3+}, Ni^{2+}, Cr^{3+}). Further it was assumed that a large amount of free nitric acid would be present along with an excess of NO^-_3 anion.

Several types of solutions were made up containing either the ions separately or mixtures of them in various proportions. The following table gives the chemical composition of the prototype solutions in moles/liter:

1. $NaNO_3$	4.0	7. Aluminum cladding solution:		9. Purex process (concentrated wastes):		10. Purex process (neutral wastes):	
2. $Al(NO_3)_3$	2.0	$NaAlO_2$	1.2	Na^+	0.5	Na^+	5.1
3. $Fe(NO_3)_3$	2.0	NaOH	1.0	Al^{3+}	0.1	Al^{3+}	0.08
4. HNO_3	5.0	$NaNO_3$	0.6	Fe^{3+}	0.3	Fe^{3+}	0.2
5. $NaNO_3$	2.0	$NaNO_2$	0.9	H^+	5.6	H^+	—
$Fe(NO_3)_3$	0.85	Na_2SiO_3	0.02	OH^-	—	OH^-	0.1
$Al(NO_3)_3$	0.25	8. Stainless steel cladding solution:		NO^-_3	5.8	NO^-_3	5.7
$K_2Cr_2O_7$	0.03			SO^{2-}_4	0.75	SO^{2-}_4	0.56
$Ni(NO_3)_2$	0.03	Na^+	5.3	Si	0.2	Si	0.15
6. $NaNO_3$	3.0	Fe, Cr, Al	0.72				
$Al(NO_3)_3$	0.25	SO^{2-}_4	3.4				
$Fe(NO_3)_3$	0.25	OH^-	0.5				

The solution was mixed with crushed and remelted basalt from the deposits in Ogarzhitsa (grain size > 0.1 mm). After adding a known amount of Cs^{137} together with a carrier, the samples were homogenized, dried (110-220°C) and melted in a Superkantal SM-10 electric furnace at 1250°C. After they were completely melted, the samples were left in the furnace for 24 h with the current turned off. It follows from a comparison of the data on leaching Ce^{137} out with water for a considerable period of time with the results of the experiments that had already been made without any ballasting materials that there was no single case in which the rate at which the cesium leached out of the solid phase into the liquid increased appreciably. This goes to show at the same time that the basic properties of the basaltic material did not get any worse. X-ray structural analysis also showed that the ballasting materials did not, in principle, exert any effect on the crystal structure of the basalt.

Volatilization of Radioactive Isotopes

In even the first experiments on fusing Cs^{137} into basalt, it was observed that the cesium volatilized appreciably, and in some cases it attained more than 30% of the amount originally present. Accordingly, in the rest of the experiments, a study was made of how much various cesium compounds volatilized from different types of surfaces. The maximum amount of volatilization was found at 600°C, after which the amount of cesium carried off became less. When the cesium was put into a melt, further volatilization stopped, as was also the case when the sample was covered with a layer of inactive crushed basalt.

So far, only preliminary experiments have been made with radioactive ruthenium in solutions containing a carrier. The amount of ruthenium that volatilized when the crushed basalt was melted varied over a wide range, depending on the conditions under which the melting took place.

* The olivine basalt from Slapana is used to produce commercial articles. A large amount of waste is produced, consisting of basalt that has been remelted once.

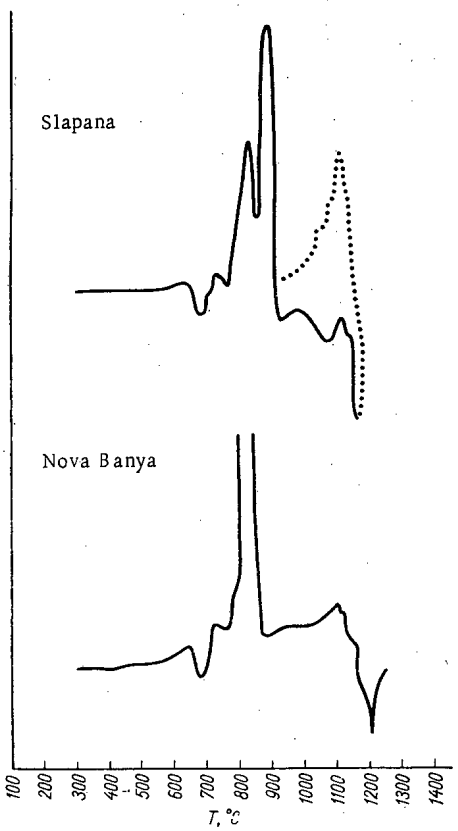

Fig. 1. Thermogram of basalt (the vertical axis gives the magnitude of the exothermic or endothermic effect in relative units).

Radiation Resistance

It is well known that if glass and ionic crystals are irradiated, they become colored, and the Schottky and Frenkel effects show up. If the doses absorbed are large, there may also be a change in the structure of crystalline materials, while in amorphous materials crystallization nuclei may be formed and recrystallization occurs. Macroscopic devitrification of some types of glasses occurs [15].

In order to find what effect irradiation has on the structure of the basalt, the vitreous and recrystallized samples were placed for 300-1500 h in a field with an exposure dose power of $2 \cdot 10^5$ R/h at elevated temperatures. The vitreous samples showed no appreciable changes in physical properties in the range 450-650° C (see Fig. 1). At temperatures of about 700°C, where the vitreous phase starts to recrystallize, a reversible change in the properties of the samples occurs, and they fall apart into irregularly shaped pieces. However, if the sample was recrystallized from the melt by gradual cooling, and was subjected to irradiation at elevated temperatures after recrystallization, it still had the same volume and the same mechanical strength. X-ray measurements showed that irradiation has no effect on the structure of the recrystallized basalt.

At the same time, experiments are being made to find what effect absorbing large doses has on the diffusion of radioactive isotopes in basalt. It follows from the data obtained up to the present time that at temperatures of 450-850° C, irradiation has little effect on the ionic diffusion of vitreous and crystalline basalt.

Discussion

The results obtained show that fused basalt is a good material for immobilizing highly active wastes. The high resistance to hydrolysis that it exhibits is not changed even when relatively large amounts of ballasting materials are added to the initial material. This completely supports Scharles' theory as to what effect water has on the structure of silicates [16]. Of the two reactions:

$$\equiv Si-OM + HOH \rightleftarrows \equiv Si-OH + M^+ + OH^-;$$

$$\equiv Si-O-Si\equiv + HOH \rightleftarrows 2\equiv Si-OH,$$

which might occur during the process, the first reaction is the predominant one, since it is the general scheme for exchange of an alkali ion with hydrogen at a glass-water boundary. Since the alkali ions are only weakly bound to the surface, this reaction is taking place even at the very start of the leaching process. A large amount of leaching out at the start of the process is favored by the fact that the surface is more densely covered with alkali than the inner layers of the solid phase, since, even during melting, the alkali ions penetrate into the surface, in an effort to reduce the surface tension of the melt. The second reaction goes very slowly, as is shown by the fact that silicon is only slightly soluble in water [7]. It is thus probable that of the ballasting cations mentioned, it is only sodium that makes any contribution to the leaching. The rest of the cations, particularly those having a higher charge, take part, in the majority of cases, in building up the silicate lattice, and are thus much more tightly bound. The leaching process, which can only occur at the boundary between the solid and the water phase, will, accordingly, after the first rapid reaction, be regulated by the rate of motion of the moveable ions in the direction of the phase boundary, i.e., by the diffusion in the solid phase.

The amount of leaching cannot increase unless there is a large increase in the surface in contact with the water. This occurs in some glasses when they are subjected to irradiation. As a result of devitrification, the material falls apart into microscopic particles, which are easily cooled off, and, since the surface has been increased many times, they may undergo corrosion from the moisture in the atmosphere. The volume does not change in the case of recrystallized basalt. Since a compact block will heat itself up spontaneously, no moisture can get at it until a substantial part of the radioactive material inside has decomposed.

Another bad feature of glasses is that they soften over a broad temperature range, and have a low melting point. As a result, the block may get out of shape at high temperatures, while recrystallized basalt does not show any changes even up to temperatures of the order of 1000° C.

The volatilization of some of the radioactive isotopes from the fission product mixture that occurs during melting does not seem to be anything insurmountable, nor would it complicate the process very much. If the melting is interrupted, it is only necessary to cover the melt with some inactive crushed material. If the process is continuous, there is no way in which direct volatilization into the surrounding space can occur, since the components that are apt to volatilize out of the heated material will be mainly concentrated in the colder layers on top of the zone that is being heated.

Fused basalt meets all the requirements placed on the materials which are to be used for safe and economically feasible immobilization of high specific activity wastes.

LITERATURE CITED

1. M. Goldman et al. Paper No. 388, presented by the USA at the Second International Conference on the Peaceful Uses of Atomic Energy [Russian translation] (Geneva, 1958).
2. R. Bonniaud, In the book: Treatment and Storage of High Level Radioactive Wastes, IAEA, Vienna, p. 355 (1963).
3. N. I. Bogdanov et al., Paper No. 587, presented by the USSR at the Third International Conference on the Peaceful Uses of Atomic Energy [in Russian] (Geneva 1964).
4. K. Johnson et al. Paper No. 188, presented by Great Britain at the Third International Conference on the Peaceful Uses of Atomic Energy [Russian translation (Geneva 1964).
5. Watson et al., In the book: "Transaction of the Second International Conference on the Peaceful Uses of Atomic Energy." Selected papers by foreign scientists, Vol. 9 [Russian translation], Moscow, Atomizdat, p. 187 (1959).
6. J. Saidl, Jaderná energie, 7, 181 (1961); 8, 341 (1962).
7. A. Pelikán, Tavené horniny, Prague, "Prace." (1955).
8. L. Kopecký and J. Voldán, Krystalisace tavených hornin. ČSAV, Prague (1959).
9. Z. Skranék. Fixace radioaktivních odpadů do skel. Report St. výzkum. ústavu sklář. Hradec Králové (1963).
10. J. Rálková and J. Saidl. In the book: "Treatment and Storage of High Level Radioactive Wastes." IAEA, Vienna, p. 314 (1963).
11. J. Saidl. Kandidát. dissertace. VŠCHT, Prague (1965).
12. J. Saidl and J. Rálková. Technical Digest, 7, 483 (1963).
13. J. Rálková. Kandidát. dissertace. ÚJV ČSAV, Prague (1963).
14. J. Rálková. Glass Technology, 6, 40 (1965).
15. J. Kircher and R. Bowmann, Effect of Radiation on Materials and Compounds. Reinhold Publ., N. Y. (1964).
16. J. Burke. Progress in Ceramic Science. Vol. 1. Pergamon Press. p. 1 (1961).
17. J. Van Lier. Thesis Univ. Utrecht (1959).

ABSTRACTS

INCREASING THE NUMBER OF IONS CAPTURED IN A MAGNETIC TRAP BY PHOTOIONIZATION OF NEUTRAL ATOMS

K.B. Kartashev and E.A. Filimonova

UDC 533.9

This paper discusses the possibility of using the photo-effect to increase the number of ions captured when fast hydrogen atoms are injected into a magnetic trap. The relation is found between the efficiency of the process and the power of two different types of radiators.

It is shown that if a hydrogen atom in a state with principal quantum number n is in a radiation field that follows the Rayleigh-Jeans law, the photoionization probability ξ_n is related to the radiation temperature T by the expression

$$T=\frac{\xi_n h}{8\pi k a_n(\lambda_{max}-\lambda_1)},$$

where h is Planck's constant, k is the Boltzmann constant, λ_1 is the lower limit of the radiation spectrum, λ_{max} is the smaller of the two wavelengths representing either the upper limit of the spectrum or the photoionization threshold of the state in question. In deriving this equation, the photoionization cross section as a function of the wavelength of the radiation was taken to be of the form $\sigma_n(\lambda)=\alpha_n\lambda^3$, where α_n is a coefficient depending on n [1, 2]. For n = 10, the value $\xi_n=10^7$ sec^{-1} occurs at T = 19.3 eV, which corresponds to a radiation power $p=1.4\cdot10^{10}$ W/cm^2.

In the case of monochromatic radiation in a definite direction (e.g., laser radiation), the relation between the radiation power and the photoionization probability is expressed in the form $p=\xi_n hcS/\sigma_n\lambda$ where S is the cross-sectional area of the light beam.

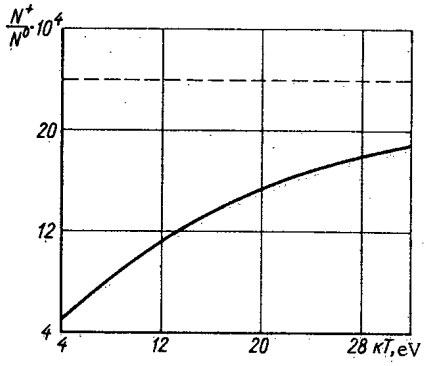

Fig. 1. Proton capture efficiency when fast hydrogen atoms are injected into a magnetic trap as a function of the temperature of a black body radiator ($t = 10^{-7}$ sec, τ_n is the mean statistical value). The dotted line is the limiting case where $kT\to\infty$.

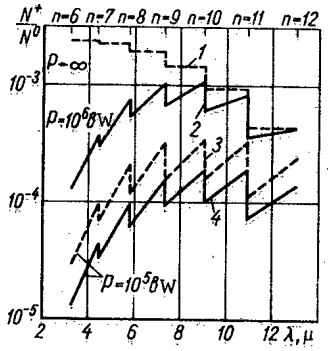

Fig. 2. Proton capture efficiency when fast hydrogen atoms are injected into a magnetic trap as a function of the monochromatic radiation wavelength (τ_n is the mean statistical value): 1, 2, 4 – $\theta=1.25\cdot10^{-6}$ sec; 3 – $\theta=5\cdot10^{-7}$ sec.

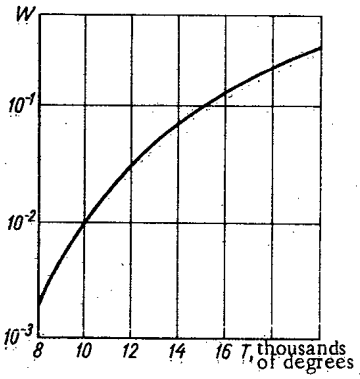

Fig. 3. Photoionization efficiency W of unexcited lithium atoms as a function of the temperature of a black body radiator (spectral range used 2000 $\leq\lambda\leq$ 2300 Å; $t=3.8\cdot10^{-7}$ sec).

Translated from Atomnaya Énergiya, Vol. 21, No. 4, pp. 290-291, October, 1966. Original article submitted March 12, 1966.

Assuming that the occupancy of the excited levels of the hydrogen atoms produced by charge exchange obeys the law an^{-3}, we shall define the capture efficiency as:

$$\frac{N^+}{N^0} = \sum_n \frac{a}{n^3} e^{-\theta/\tau_n} (1 - e^{-\xi_n t}),$$

where τ_n is the lifetime of the excited atom with respect to spontaneous radiation, θ is the time of flight of the excited atom from the point where the charge exchange occurs to the trap, and t is the time of flight of the irradiation zone. Figure 1 shows the results of calculating the capture efficiency for black body radiation with $a = 1$, $\theta = 1.25 \cdot 10^{-6}$ sec, velocity of the atoms $\nu = 4 \cdot 10^8$ cm/sec, and an irradiation zone of length $l = 40$ cm. Photoionization from the ground state was not considered.

Figure 2 is for a monochromatic radiator with a light beam of width $b = 4$ cm and a wavelength of λ for the same values of a, θ, and ν as in Fig. 1.

Clearly, for these values of θ and t, the efficiency increases by a maximum factor of 20 - 25 over the usual case of Lorentz ionization ($N^+/N^0 \approx 10^{-4}$). However, to produce even a 5 - 10 fold effect requires a black body radiator at a temperature of $T = 10$ eV and a total power of $P = 10^{11} - 10^{12}$ or a laser with a power of $10^5 - 10^6$, and the radiator has to act for a time of the order of 1 sec. Radiators of this type are not presently available.*

Figure 3 shows the photoionization probability of lithium atoms as a function of the temperature of a black body radiator. The low ionization potential of lithium (5.39 eV) makes it possible to have ionization directly from the ground state at comparatively low temperatures.

LITERATURE CITED

1. Atomic and Molecular processes, Collected papers. [In Russian], Edited by D. Beits. Moscow, "Mir" (1964).
2. D. P. Grechukhin, É. I. Karpushkina, and Yu. L. Sokolov, Atomnaya Énergiya, 20, 407 (1966).

OPTIMUM COMPOSITION OF HOMOGENEOUS SHIELDS

S. M. Rubanov and L. S. Shkorbatova

UDC 621.039.538.7

This article is devoted to the investigation of the dependence of the thickness and weight of a two-component shield for a nuclear power reactor on the composition of the shielding material.

The calculations are performed by a numerical method which permits taking into account all the components of the total dose outside the shield, including the effect of slow neutron build-up and the production of capture gamma rays.

The contributions made by intermediate neutrons and by capture gamma sources are computed by a seven group age-diffusion calculation [1] of the space and energy dependence of the neutron distribution in the reactor and shield. The method presumes that the spatial distribution of neutrons with energies above 1.5 MeV is known experimentally. The spatial distribution of the total dose is obtained for shields of various compositions.

* These figures are for photoionization of atoms with $n > 1$. The possibility of nonlinear effects occurring during ionization in the electric field of the coherent light beam from a laser has not been discussed.

Translated from Atomnaya Énergiya, Vol. 21, No. 4, p. 291, October, 1966. Original article submitted April 14, 1966.

Weight-Size Characteristics and Optimum Composition of Homogeneous Shields

Composition	ω_x^{min}, %	x_D^{min}, m	ω_G^{min}, %	$G^{min} \times 10^{-3}$, kg/m³
Fe—H_2O	68	1.26	20	6.06
Pb—H_2O	38	1.69	13	4.65
U—H_2O	38	1.24	8	4.37
Fe—polyethylene	72	1.20	25	5.46
Pb—polyethylene	38	1.53	14	4.50
U— polyethylene	38	1.15	10	4.25
Fe—C	25	2.28	20	6.54
Fe—B_4C	64	1.49	25	6.29
Pb—B_4C	40	1.70	16	6.19
U—LiH	35	1.15	11	4.21
LiH (γ=780 kg/m³	—	8.0	—	6.25
CaH_2 (γ=1700 kg/m³	—	4.0	—	6.80
MgH_2 (γ=1400 kg/m³	—	4.5	—	6.30
ZrH_2 (γ=5900 kg/m³	—	1.06	—	6.26
Serpentine concrete (γ=2200 kg/m³	—	3.3	—	7.26
UH_3 (γ=10 900 kg/m³	—	0.92	—	10.00
TiH_2 (γ=3900 kg/m³	—	1.48	—	5.77

In the table are listed minimum values of the thickness x_D^{min} and the weight $G^{min} = \gamma x_D$ (where γ is the density of the shielding material) of a slab shield necessary to reduce the dose rate to the maximum permissible level of 0.6 μ rem/sec, and, in the case of homogeneous two-component shields, the volume fraction of the heavy component insuring minimum thickness ω_x^{min} and minimum weight ω_G^{min}. The radiation source is a hypothetical water-cooled water-moderated 50 MW (thermal) reactor.

On the basis of the calculations performed and by comparison with other data [2,3], it may be stated that for certain optimum weight-size characteristics it is not permissible to neglect the build-up factors for low-energy neutrons and capture gamma radiation from the shield. Discrepancies are observed in the majority of the shielding compositions considered.

LITERATURE CITED

1. D.L. Broder, K.K. Popkov, and S.M. Rubanov, Biological Shields for Naval Reactors, Leningrad, Shipbuilding [in Russian] (1964).
2. G. Thuro, Atomkernenergie, Vol.7/8, 263 (1964).
3. G.A. Lisochkin and F.A. Predovskii, Atomnaya Énergiya, 18, 408 (1965).

EFFICACY OF BORON IN METAL-WATER SHIELDS

M.A. Kartovitskaya, S.M. Rubanov, and L.S. Shkorbatova

UDC 621.039.58

The dependence of weight and size of iron-water and lead-water shields on the boron content and the place where it is introduced into the shield is investigated.

Boration leads to a redistribution of the components of the total dose. This is illustrated in Fig.1 which shows the dependence of the total dose and its components outside the shield on the weight per cent of boron, α_B. Boration gives the largest effect in iron-water shields and in lead-water shields having a high concentration of lead.

Boration of lead-water shields is effective only up to α_B = 0.5 wt% of boron; for ω_{Pb} equal to 0.2 to 0.3, where ω is the volume fraction of the heavy component in a homogeneous metal-water shield, the decrease in shield thickness amounts to 1%, and for ω_{Pb} = 0.7 the decrease is 3%. The saving in shield weight in the case of an axially symmetric arrangement amounts to 1.5 to 2% for ω_{Pb} = 0.2 to 0.3%.

Translated from Atomnaya Énergiya, Vol.21, No.4, p.292, October 1966. Original article submitted May 12, 1966.

Boration is more effective in iron-water shields since the yield of capture gamma radiation from iron is greater than that from lead. For shields with $\omega_{Fe} = 0.5$ the relative decrease in weight is from 5 to 8% and with $\omega_{Fe} = 0.9$ it is 9%. For a lower iron concentration ($\omega_{Fe} = 0.2$) the introduction of 5 wt% boron into the shield leads to a decrease in shield weight of 6%.

The effectiveness of boron as a function of the place it is introduced is determined by a perturbation calculation [1]. The results for the effectiveness of boron in homogeneous shields lead to the conclusion that for a small concentration of the heavy element, the greatest effect is obtained by borating the inner layers of the shield; for $\omega_{Fe} = 0.7$ the boron should be introduced into the outer layer of the shield.

The boration of lead in heterogeneous lead-water shields with $\omega_{Pb} \approx 15$ to 20% does not lead to an appreciable saving in shield weight or thickness. Boration of iron in a heterogeneous iron-water shield with $\omega_{Fe} = 20\%$ leads to a 5% decrease in shield weight. The boration of water leads to a similar result.

Covering iron or lead slabs in a heterogeneous metal-water shield with layers of boron carbide leads to the same result as borating the metal. Cladding a reactor vessel with boron carbide leads to a decrease of 9% in the weight of an iron-water shield with $\omega_{Fe} = 0.2$ and to a 5.5% weight reduction in a lead-water shield with $\omega_{Pb} = 0.5$.

LITERATURE CITED

1. A.A. Abagyan, V.V. Oglov, and G.I. Rodionov, The Physics of Reactor Shielding, Moscow Gosatomizdat [in Russian] p.7 (1963).

STEADY STATE DIFFUSION OF THERMAL NEUTRONS IN MEDIA WITH RANDOM INHOMOGENITIES

A. V. Stepanov

UDC 539.125.52

In studying the propagation of neutrons in inhomogeneous media with parameters which vary rapidly in space, the average neutron density is of practical interest. The averaging performed over an ensemble of diffusing media leads to the mathematical expectation. Examples of inhomogeneous media are a boiling liquid, rocks, etc. An important special case of an inhomogeneous medium to which the statistical description of neutron propagation is applicable is a periodic reactor lattice. In this case the representatives of the statistical ensemble of inhomogeneous media differ from one another in being displaced in space by a "phase shift." In solving such a problem the first step is to replace the real medium with its fluctuating parameters by a moderator with average properties. This correctly takes into account the first moment of the distribution law of the rapidly varying functions $\Sigma_s(r)$ and $\Sigma_a(r)$, the macroscopic neutron scattering and absorption cross sections respectively; the zero moment is determined by the normalization. The next step is to calculate the second moments of the distribution law of Σ_s and Σ_a; to do this there are introduced the correlation functions $(\Sigma_s(r)\,\Sigma_s(r'))$ and $(\Sigma_a(r)\,\Sigma_a(r'))$. This approximation turns out to be satisfactory for small scale fluctuations; a characteristic dimension of an inhomogeneity, l, must be small in comparison with L, the neutron diffusion length in the homogeneous medium. The general form of the equations describing, on the average the propagation of neutrons through media with small scale inhomogeneities was found in previous articles by the author [1].

Translated from Atomnaya Énergiya, Vol. 21, No. 4, p. 292, October, 1966. Original article submitted May 12, 1966; abstract June 13, 1966.

Staying within the framework of the approximations that have been indicated, the present article considers the diffusion of thermal neutrons from a steady source in a medium in which the neutron absorption varies from point to point in a random fashion; the diffusion coefficient D_0 is assumed constant. A medium which is isotropic on the average, and one which is highly anisotropic are considered. An expression is obtained for the relaxation constant of the neutron density in a medium in which the inhomogeneities are in the nature of localized impurities.

LITERATURE CITED

1. A.V. Stepanov, Pulsed Neutron Research, Vol.1, Vienna, IAEA, 1965, p.339; Atomnaya Énergiya, 20, 265 (1966).

SHIELDING PROPERTIES OF FIREPROOF CHROMITE AND MAGNESITE CONCRETES

D.L. Broder, V.B. Dubrovskii, P.A. Lavdanskii, V.P. Pospelov, and V.N. Solov'ev

UDC 621.039.538.7

An experimental study has been made of the shielding properties of fireproof chromite and magnesite concretes, which can be used as thermal shielding in reactors [1, 2]. Fireproof concretes become dehydrated at high temperatures, which changes their shielding properties. In order to make the experimental conditions as close as possible to the conditions under which fireproof concretes operate in actual shield designs, slabs of the materials were given a heat treatment.

The shielding properties of the fireproof concretes were investigated in the 100 mm diameter horizontal hole of the VVR-Ts Reactor at the Lyakarpov Physico-chemical Institute. The neutrons were detected with red phosphorus, indium, and an SNM-3 boron counter. The gamma-dose power was measured with an SBM-10 gamma-dosimeter. To make a comparison under similar conditions, the shielding

Relaxation Lengths in Concrete (numerator) and Thicknesses at which they were Determined (denominator), in cm

Type of concrete	Detector				Extraction length for the fission spectrum	Relaxation length of the γ-dose at a reactor power of:	
	Indium without cadmium	Indium in cadmium	BF_3	P31		0	1 kW
Ordinary concrete	10.4 / 20—120	10.2 / 20—120	12.0 / 50—100	12.5 / 20—80	12.7	9.7 / 20—80	13.75 / 60—120
Chromite	13.5 / 50—120	13.5 / 50—120	14.5 / 50—100	10.4 / 40—80	11.15	8.0 / 20—80	12.45 / 60—120
Magnesite	—	—	19.5 / 50—100	11.0 / 20—80	11.15	8.8 / 20—80	—

Translated from Atomnaya Énergiya, Vol. 21, No. 4, p. 293, October, 1966. Original article submitted February 1, 1966.

properties of ordinary concrete were determined, but the slabs were not given any heat treatment. The experimental values of the relaxation length and the calculated extraction lengths for the fission spectrum are given in the table.

The conclusion is drawn from the data obtained that even in the dehydrated state, fireproof chromite and magnesite concretes make good shielding materials, and are to be recommended for use in building shields to operate under high temperature conditions (up to 800-1700°C).

LITERATURE CITED

1. V.B. Dubrovskii et al., Atomnaya Énergiya, 19, 524 (1965).
2. A.N. Vorob'ev et al., Betonzhelezobeton, No. 2, 11 (1966).

APPROXIMATE DESCRIPTION OF REACTOR KINETICS FOR STABILITY STUDIES

F.M. Mitenkov and V.S. Boyarinov

UDC 621.039.512

In investigating the stability of systems containing a nuclear reactor, a considerable amount of simplification is achieved by replacing the six groups of delayed neutrons in the kinetic equations by one or two equivalent groups.

It is well known that in investigating transient processes it is possible to choose the parameters λ_j^0, β_j^0 of the two equivalent delayed neutron groups in such a way that the change in neutron density is quite accurately described over the time interval in question.

For this purpose, use may be made of the relations:

$$\left.\begin{aligned} \sum_{i=1}^{6}\beta_i=\sum_{j=1}^{2}\beta^0;\ \sum_{i=1}^{6}\frac{\beta_i}{\lambda_i}=\sum_{j=1}^{2}\frac{\beta_j^0}{\lambda_j^0};\\ \sum_{i=1}^{6}\frac{\beta_i}{\lambda_i+\lambda_k^0}=\sum_{j=1}^{2}\frac{\beta_j^0}{\lambda_j^0+\lambda_k^0},\qquad k=1,\ 2, \end{aligned}\right\} \tag{1}$$

obtained from the condition for the minimum value of the integral:

$$J_1=\int_0^\infty\left[\sum_{i=1}^{6}\beta_i(1-e^{-\lambda_i t})-\sum_{j=1}^{2}\beta_j^0(1-e^{-\lambda_j^0 t})\right]^2 dt. \tag{2}$$

However, in system-stability studies, the effective delayed neutron parameters found from Eqs. (1) may result in errors that are too large to tolerate.

It is shown in this paper that if the m parameters of the equivalent delayed neutron groups are determined from the condition for minimum deviation of the corresponding points in the amplitude-phase characteristics, the limits of the ranges of stability calculated using even a single equivalent group are very nearly the same as those calculated using six delayed neutron groups.

Translated from Atomnaya Énergiya, Vol. 21, No. 4, pp. 293-294, October, 1966. Original article submitted January 29, 1966.

The equations for finding the equivalent group parameters, found from the conditions for the minimum value of the integral:

$$J_2=\int_0^\infty\left[\left(\sum_{i=1}^{6}\frac{\beta_i}{T_i^2\omega^2+1}-\sum_{j=1}^{m}\frac{\beta_j^0}{T_j^{0^2}\omega^2+1}\right)^2+\left(\sum_{j=1}^{m}\frac{\beta_j^0T_j^0\omega}{T_j^{0^2}\omega^2+1}-\sum_{i=1}^{6}\frac{\beta_iT_i\omega}{T_i^2\omega^2+1}\right)^2\right]d\omega, \tag{3}$$

are of the form

$$\left.\begin{aligned}&\sum_{i=1}^{6}\frac{\beta_i}{T_i+T_k^0}=\sum_{j=1}^{m}\frac{\beta_j^0}{T_j^0+T_k^0};\\&\sum_{i=1}^{6}\frac{\beta_i}{(T_i+T_k^0)^2}=\sum_{j=1}^{m}\frac{\beta_j^0}{(T_j^0+T_k^0)^2},\quad k=1,2,\ldots,m,\end{aligned}\right\} \tag{4}$$

where T_i is the mean lifetime of the neutron sources for the i-th group, and β_i is the delayed neutron fraction in the i-th group.

The paper gives a comparison of the ranges of stability as found for different numbers of equivalent delayed neutron groups, using different parameters for the groups. The calculations were made for the simplest models of a reactor with automatic control, and of a self-adjusting reactor.

CALORIMETRIC DOSIMETER FOR A NUCLEAR REACTOR

V. M. Kolyada and V. S. Karasev

UDC 614.8:539.12.08:621.039.5

The importance of dosimetric measurements in making radiation material, radiation chemical, biological, and other studies is a matter of general knowledge. However, the use of ionization, chemical, scintillation, and the other common methods for dosimetry of high radiation fluxes in highly loaded reactors has serious fundamental limitations.

In recent years (particularly in foreign countries), wide use has been made of calorimetric dosimetry methods which have the advantages of high accuracy, and reliability, and there is practically no upper limit to the range of measurement.

The review gives a brief description of the methods and apparatus used in calorimetric dosimetry, divided, according to the method of determining the amount of energy absorbed, into three groups, – adiabatic, kinetic, and isothermal. An attempt is made to compare the calorimetric methods and apparatus in question, give their advantages and disadvantages, and determine their range of applicability.

The material presented in the paper will be of aid to scientific and engineering workers engaged in reactor studies, as well as in evaluating the capabilities of calorimetric equipment from the standpoint of use or further improvement.

Translated from Atomnaya Énergiya, Vol. 21, No. 4, p. 294 October, 1966. Original article submitted April 15, 1966.

MICROWAVE RADIATION FROM A QUASISTEADY STATE PLASMA

N. A. Gorokhov and G. G. Dolgov-Savel'ev

UDC 533.9

There are a large number of papers [1-3] dealing with epithermal microwave plasma radiation. However, since there is no suitable apparatus in existence, no careful spectral studies of the signal observed have yet been made, although measurements of this sort are required to find out what the true mechanism is that is exciting the intense electromagnetic oscillations in the plasma medium.

This paper uses a specially constructed piece of apparatus [4] to make a study of the microwave radiation of the high-temperature plasma from equipment of "Tokamak" type [5]. As a result, it was found that a plasma of this type serves as a source of intense electromagnetic radiation lying in the millimeter wavelength range.

A characteristic feature of the radiation is that it is pronouncedly sporadic in nature, and consists of isolated bursts of an intensity corresponding to a surface brightness of the thread of the order of 10^{-3} W/steradian·cm^2. This is more than five orders of magnitude higher than the Bremsstrahlung of a plasma having parameters typical of "Tokamak" equipment (temperature 40 eV, density 10^{13} cm^{-3}, string diameter 30 cm).

The spectrum of the radiation generated (Fig. 1.) was taken with a Fabry-Perot interferometer. It was found that the intensity maximum in the radiation lies in the vicinity of the electronic plasma frequency, and, on the high-frequency side, the spectrum has a comparatively well defined boundary in the upper hybrid frequency region.

A study of how the microwave signal behaves as a function of the discharge parameters showed that radiation does not exist except in those stages of the discharge where the plasma formation is macroscopically stable.

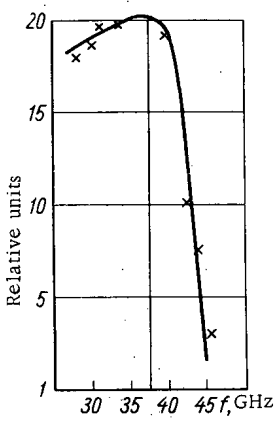

Fig. 1. Spectrum of the radiation.

The fact that electromagnetic radiation of an anomalous intensity exists in "Tokamak" equipment is somewhat unexpected, since, in this case, the electric field in the plasma is obviously less than the critical value required to produce run-away electrons, so that one would not expect intense plasma oscillations to be built up by a fast electron beam. However, a study of the hard x rays with a quantum energy of more than 100 keV produced when the walls of the chamber are bombarded with fast particles has shown that a correlation exists between the instants at which both the microwave radiation and the x rays start and stop.

LITERATURE CITED

1. V. A. Suprunenko, et al., Atomnaya Énergiya, 14, 349 (1963).
2. I. Yu. Adamov et al., Atomnaya Énergiya, 16, 99 (1964).
3. R. Waniek et al., Appl. Phys. Lett., 5, 89 (1964).
4. N. A. Gorokhov and G. G. Dolgov-Savel'ev, Pribory i tekhnika Éksperimenta, No. 1, 126 (1966).
5. V. S. Vasil'evskii et al., ZhTF, 30, 1135 (1960).

Translated from Atomnaya Énergiya, Vol. 21, No. 4, p. 295, October, 1966. Original article submitted April 12, 1966.

TOLERANCES IN LINEAR ION ACCELERATORS WITH QUADRUPOLE FOCUSING OF THE ACCELERATING FIELD

A. P. Mal'tsev

UDC 621.384.62

Quadrupole focusing of the accelerating field (QFAF) [1-3] is one of the varieties of alternating focusing, and, as is the case with any kind of alternating focusing, requires that special attention be given to the accuracy with which the drift tubes are built and suspended. There are a number of special features connected with the problem of tolerances in an accelerator with QFAF.

The high-frequency QFAF lenses are formed between the ends or horns of two neighboring drift tubes. If there are inaccuracies in the way the tubes are arranged or built, the lenses become distorted. For this reason, QFAF differs from focusing with external quadrupole fields, where the tube suspensions have no effect on the lenses.

The most interesting type of QFAF is focusing in a system where there are two gaps in the accelerating period [4]. In this case, the error in any particular lens has less effect on the motion of the particles than with a single gap, but on the other hand there are more lenses.

We shall give more detailed consideration to the problems in question. We shall show that if the displacements of the tubes are small, the deformations in the accelerating and focusing field may be traced back to corresponding displacements of the high-frequency lenses. We shall consider drift tubes with horns [4].

We shall now write the solution of Laplace's equation for an infinitely long lens:

$$\Phi(r, \theta)=\sum_{n=1}^{\infty} r^n (a_n \cos n\theta + b_n \sin n\theta), \tag{1}$$

where $\Phi(r,\theta)$ is the electric field potential in polar coordinates.

In the plane $\theta=(0;\pi)$ let the horn be shifted from the axis by the amount s as a result of displacement of one of the tubes. From the boundary conditions

$$\Phi(R+s, 0)=\Phi(R-s, \pi)=-\Phi\left(R, \frac{\pi}{2}\right)=-\Phi\left(R, \frac{3\pi}{2}\right)=U$$

and from (1) it follows that:

$$\left.\begin{aligned} &a_0=b_0=0; \quad a_1=2a_2 s; \quad a_2=\frac{U}{R^2}; \\ &E_x=-\frac{\partial}{\partial r}\Phi(r, \theta)\Big|_{\theta=0}=2a_2(r+s), \end{aligned}\right\} \tag{2}$$

where U is the voltage at the gap, and R is the radius of the aperture. This means that small displacements of the horns on one of the tubes may be represented as a displacement of the lens as a whole.

We shall assume that the plane of the horns on one of the tubes has been rotated about the axis of the accelerator by the small angle 2χ. From (1), and the boundary conditions:

$$\Phi(R, 2\chi)=\Phi(R, \pi+2\chi)=-\Phi\left(R, \frac{\pi}{2}\right) \quad =-\Phi\left(R, \frac{3\pi}{2}\right)=U$$

it follows that:

$$a_1=b_1=0; \quad a_2=\frac{U}{R^2}; \quad b_2=2a_2\chi.$$

Translated from Atomnaya Énergiya, Vol. 21, No. 4, pp. 295-297, October, 1966. Original article submitted January 21, 1966.

In the deformed field, the particle at the point (r, 0) is acted upon by a force with the components:

$$F_y = -e\frac{\partial}{\partial r}\Phi(r,\theta)\Big|_{\theta=0} = -2era_2;$$

$$F_x = -e\frac{\partial}{r\partial\theta}\Phi(r,\theta)\Big|_{\theta=0} = -2erb_2 = 2F_y\chi. \qquad (3)$$

Exactly the same components show up in an ordinary quadrupole, if it is rotated as a whole through the small angle χ, i.e., rotation of one pair of horns around the axis by the angle 2χ may be represented as rotation of the whole lens by the angle χ.

Any slope of the axis of one of the tubes with respect to the axis of the accelerator may be expressed in terms of the slope of the axis of the lens. This follows directly from Eq. (2), since, if the tubes are only slightly misaligned, the geometric locus of the equilibrium points of the transverse forces will be a straight line having the same slope.

Longitudinal displacements of the tubes produce very little change in the shape of the field. Longitudinal errors include errors in phase, as well as in the lengths of the horns and of the gaps.

Thus, deformations of the accelerating field may be represented in terms of displacements of the high frequency lenses, and the usual methods may be used in calculating the tolerances. We shall estimate the effect of random errors on the output characteristics of the beam from the mean square growth in amplitude of the oscillations:

$$\overline{(\Delta B)^2}_{\text{out}} = \frac{k}{2}\left[\overline{(\Delta x_n)^2} + \frac{1}{\Omega^2_{\min}}\overline{(\Delta\dot{x}_n)^2}\right] \approx \frac{k}{2\Omega^2_{\min}}\overline{(\Delta\dot{x}_n)^2}. \qquad (4)$$

Here, k is the number of focusing periods, $\Omega_{\min}$ is the minimum frequency of the transverse oscillations, and Δx_n and $\Delta\dot{x}_n$ are the deviations of the coordinates and the angle of the particle from the center of the focusing region.

We shall now consider FD and FFDD structures. In the first case the focusing and defocusing gaps simply follow one another, while in the latter case, two focusing periods in the acceleration alternate by two defocusing periods.

The two gaps in the accelerating period may be reduced to a single equivalent gap. The error at the equivalent gap is equal to the sum of the errors at the actual gaps, since the time of flight between the gaps is small:

$$\Delta x_{oe} = \Delta x_1 + \Delta x_2; \qquad \Delta\dot{x}_{oe} = \Delta\dot{x}_1 + \Delta\dot{x}_2,$$

where the subscripts oe, 1, and 2 correspond to the equivalent gap and the first and second gaps in the double gap.

By the use of KFUP transformation matrices, the errors in the equivalent gaps in the focusing period may be converted to the center of the focusing region, which, in the case of an FD structure is at the center of the focusing gap, while in the case of an FFDD structure it is halfway between the focusing gaps. Then, we add up the errors in the individual gaps and average over all the phases and independent sources of error. As a result, we obtain:

$$\overline{(\Delta B)^2}_{\text{out}} = \frac{k}{2\Omega^2_{\min}}[Q_\psi\overline{(\delta\psi)^2} + Q_\varphi\overline{(\delta\varphi)^2} + Q_\chi\overline{\chi^2} + Q_s\overline{s^2} + Q_\xi\overline{\xi^2}], \qquad (5)$$

where $\delta\psi$ is the error in length of the horn, $\delta\varphi$ is the error in phase, χ is the angle by which the tube is rotated around the longitudinal axis, s is the displacement of the tube with respect to the axis of the accelerator, and ξ is the displacement of the ends of the tubes with respect to the axis, produced by the slope of the tube.

The coefficients Q_i may be expressed in terms of the focusing parameters in the following way. (We shall take the best type of focusing: in the double gap, the first gap has a horn, but there is no horn on the second gap. A system resonant on the H-mode is being used.)

For the FD system:

$$\left.\begin{aligned} Q_\psi &= \left(\frac{2B}{T}\right)^2 \left[\left(\frac{\operatorname{tg}\psi}{2}\mu_y + \frac{a\tau\sigma''\cos\varphi}{\sin^2\psi}\right)_1^2 + g\left(\frac{\operatorname{tg}\psi}{2}\mu_x - \frac{a\tau\sigma''\cos\varphi}{\sin^2\psi}\right)_1^2\right]; \\ Q_\varphi &= \frac{B^2}{T^2}\left[\left(\frac{\partial\mu_y}{\partial\varphi}\right)_1^2 + g\left(\frac{\partial\mu_x}{\partial\varphi}\right)_1^2 + (a\tau\cos\varphi)_1^2(1+g)\right]; \\ Q_s &= \frac{1}{T^2}\left[\mu_{y1}^2 + \mu_{x1}^2 g + (a\tau\sin\varphi)_1^2(1+g)\right]; \\ Q_\chi &= \frac{4B^2}{T^2}(a\tau\sigma''\cos\varphi)_1^2(1+g); \\ Q_\xi &= \frac{1}{4}Q_s. \end{aligned}\right\} \quad (6)$$

Here

$$\left.\begin{aligned} \mu_{\binom{x}{y}} &= a\tau\sin\varphi \pm a\tau\sigma''\cos\varphi; \\ g &= \left[1+\frac{1}{2}(a\tau\sin\varphi - a\tau\sigma)_{oe}\right]^2; \\ \sigma &= \sigma'\sin\varphi + \sigma''\cos\varphi; \\ a\tau &= \frac{\pi N\nu U}{2V}; \end{aligned}\right\} \quad (6a)$$

T is the period of the accelerator, N is the drift multiplicity (the ratio between T and the period of the HF oscillations), ν is the efficiency (flight-time factor), and eV is the kinetic energy of the particle. The expressions for the quadrupolarities σ' and σ'' and the efficiency ν of the horned gap are of the form:

$$\left.\begin{aligned} \sigma' &= 0; \\ \sigma'' &= \frac{I_0(k_1R)}{2I_2(k_1R)}\operatorname{tg}\psi; \\ \nu &= \frac{\sin\pi\alpha}{\pi\alpha I_0(k_1R)}\cos\psi, \end{aligned}\right\} \quad (6b)$$

where $I_0(k_1R)$ and $I_2(k_1R)$ are Bessel's functions of an imaginary argument, $k_1 = 2\pi/\beta\lambda$, α is the gap factor (the ratio of the gap length to $\beta\lambda$); and ψ is the length of the horn in k_1 units [4].

In the case of an FFDD, the expressions for Q_i are similar to (6), except that each value of Q_i is multiplied by two, and instead of g we have:

$$h = [1 + (a\tau\sin\varphi - a\tau\sigma)_{oe}]^2.$$

Calculations show that in an accelerator where the focusing is accomplished by the accelerating field, the tolerances under ordinary conditions of acceleration and focusing are of the same order of magnitude as in an accelerator with magnetic quadrupole focusing. But building tubes with accelerating field focusing is considerably simpler than building tubes with magnetic quadrupoles, since no coils have to be mounted in them, the gradients do not have to be adjusted, and the magnetic axis does not have to be aligned with the optical axis.

LITERATURE CITED

1. V.V. Vladimirskii, Pribory i tekhnika éksperimenta, No. 3, 35 (1956).
2. G.M. Anisimov and V.A. Teplyakov, Ibid, No. 1, 21 (1963).
3. F. Fer et al., in the Book Transactions of the International Conference on Accelerators (Dubna, 1963), [in Russian], Moscow, Atomizdat, p. 513 (1964).
4. V.A. Teplyakov, Pribory i tekhnika éksperimenta, No. 8 (1964).

SOME LAWS OF THE DISTRIBUTION OF THE γ-FIELD OF A SOFT EMITTER

O. S. Marenkov

UDC 539.122:539.121.72

Bulatov and Hyodo [1, 2] have carried out experiments on the albedo of γ-quanta from isotropic Co^{60} and Cs^{137} sources situated at the surface of an infinite scatterer. The detector was placed some way from the surface. It was found that the integral intensity of back-scattered γ-rays falls off exponentially with distance from the source.

Applied and engineering physics (e.g., in the γ-γ-method of nuclear geophysics) make extensive use of low-energy γ-sources with $\varepsilon < m_0c^2$. The present author has made a theoretical study of the relation between the integral intensity (number of quanta) of back-scattered radiation and the source-detector distance. The Monte-Carlo method was used, and the γ-sources were Hg^{203} and Ce^{141}.

It is supposed that the half-space $z \geq 0$ is filled with the scatterer, while the half-space $z < 0$ is a vacuum or is regarded as an absolute absorber. The isotropic point source is placed at the origin and the detector at the point $(x, 0, 0)$. We study the integral γ-ray intensity vs. x in the region $z \geq 0$*.

From the generally-accepted Monte-Carlo method, we select the following features:

1. In a statistical simulation of the processes of γ-transfer, we consider Compton scattering and photoelectric absorption; the latter is treated by analytical averaging (the method of conditional probabilities). In limited energy ranges the linear photoelectric attenuation coefficients can be approximated by the formula

$$\tau(\lambda) = \tau_0 + \tau_1\lambda + \tau_2\lambda^2 + \tau_3\lambda^3, \tag{1}$$

where λ is the wavelength in Compton units.

2. The wavelength after the n-th collision, λ_n, is known to be determined from the normalized Klein-Nishini-Tamm distribution:

$$\frac{k(\alpha, \lambda_{n-1})}{k\left(\frac{\lambda_{n-1}}{\lambda_{n-1}+2}, \lambda_{n-1}\right)} = \xi, \tag{2}$$

where ξ is a random number, $\alpha = \frac{\lambda_{n-1}}{\lambda_n}$; and

$$k(\alpha, \lambda) = 0{,}5(1-\alpha^2) + \lambda(\lambda+2)(1-\alpha) + \lambda^2(1-\alpha)\times\alpha^{-1} + (2\lambda^2+2\lambda-1)\ln\alpha.$$

Solving the transcendental equation (2) to get λ_n from the data on λ_{n-1} and ξ is a very uneconomical operation, even with a fast computer. We calculated λ_n by means of an approximate formula due to Carlzon [3]:

$$\lambda_n = \lambda_{n-1} + \frac{\xi\lambda_{n-1} + \xi^3(\lambda_{n-1}+1{,}125)}{\lambda_{n-1}+0{,}5625}. \tag{3}$$

* These geometrical conditions are realized, for example, in selective γ-γ-logging: in this case, the rigidly assembled source-detector system is moved along the surface of the medium under investigation.

Translated from Atomnaya Énergiya, Vol. 21, No. 4, pp. 297-298, October, 1966. Original article submitted March 12, 1966.

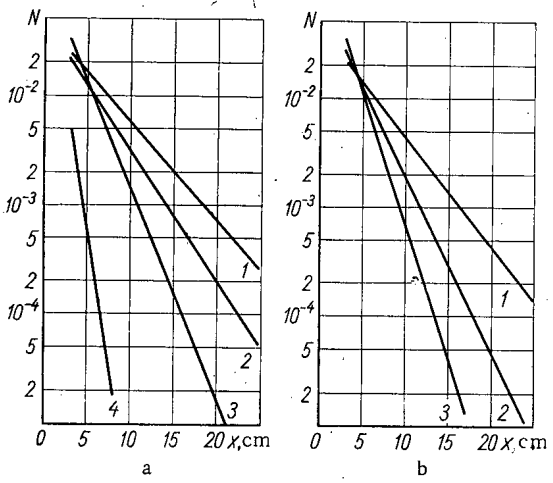

Integral γ-radiation intensity (in relative units) as a function of the source-detector distance; a) Hg^{203} γ-source; b) Ce^{141} γ-source. 1) Water; 2) sand; 3) aluminum; 4) iron.

Leimdörfer [4] has verified (3) and a modification of it in the γ-quantum energy range from 1 to 10 MeV. We have made a similar check in the range from 0.03 to 1 MeV. Equation (2) was converted to an explicit equation for α and was solved by the iteration method. The results of calculations by (2) and (3) were compared for systematic randon numbers ξ, equal to 0, 1/32, 2/32, ..., 32/32. The maximum error in determining λ_n by the Carlson formula occurred in the range $\xi \approx 20/32 \div 30/32$ and was less than 7%.

3. Since the problem does not possess symmetry in the spatial variable, the following modification of the Monte-Carlo method is very effective. The state of a photon is recorded after each collision, and the probability that, owing to the collision, the quantum will reach the detector without further interaction is calculated analytically (by the method of local fluxes). The integral flux of γ-quanta was determined at the same time for five values of x (correlated selection).

The above method of calculation was tested by comparing the results of calculations of the integral albedo (i.e., of the total number of quanta emerging into the half-space $z < 0$) for the Cs^{137} γ-source with the experimental data in [2]:

Scatterer	Theoretical value	Experimental value
Aluminum	0.54	0.59±0.02
Iron	0.38	0.42±0.02
Tin	0.23	0.22±0.02

Satisfactory agreement was found between the theoretical and experimental values.

Calculations were performed for initial source energies of 0.279 MeV (Hg^{203}) and 0.145 MeV (Ce^{141}). The scatterers used were water, quartz sand, aluminum, and iron. The minimum source-detector distance was 3 cm, the maximum 25 cm. The maximum number of quantum "histories" followed was of order 16,000, giving a statistical error of less than 2-3% in the integral flux. Analysis of the theoretical results given in the figure shows that the integral γ-radiation intensity is given as a function of the source-detector distance by the formula

$$N(x) = N_0 e^{-\nu x}.$$

This simple law can be used in applied methodological investigations with soft emitters.

The author would like to thank O. M. Kuznetsov for help with programming the "Minsk-2" computer.

LITERATURE CITED

1. B. P. Bulatov, Atomnaya Énergiya, 7, 359 (1959).
2. T. Hyodo, Nucl. Sci. and Engng, 12, 178 (1962).
3. E. Cashwell and C. E. Everett, A Practical Manual on the Monte-Carlo Method for Random Walk Problems, Pergamon Press (1959).
4. M. Leimdörfer, Nukleonik, 6, 14 (1964).

SOME CHARACTERISTICS OF THE FIELD OF BACK-SCATTERED γ RADIATION IN WORKING PREMISES

N. F. Andryushin, B. P. Bulatov, and G. M. Fradkin

UDC 539.122; 539.121.72; 621.039.58

As a rule, work with radioactive preparations is performed in small rooms. The intensity of radiation at various points in the space is thus determined not only by the primary radiation, but also by the radiation scattered from the walls of the room. In some cases, scattered radiation may appreciably effect the results of measurements. However, until recently there was practically no work in the literature on the quantitative characteristics of radiation inside a closed cavity.

Some information on the dose fields of scattered γ radiation is given in theoretical papers by Leimdörfer [1, 2] and an experimental paper by Andryushin and Bulatov [3].

Work with models has shown, in the first place, that the energy build-up factors for reflection (the ratios of the γ-ray energy flux density measured in the presence of the scatterer to the density measured without the scatterer, $B_{re} = \frac{J_p + J_0}{J_0} = 1 + \frac{J_p}{J_0}$) increase with the size of the cavity, and reach limiting values equal to the build-up factors for reflection from plane barriers with linear dimensions greater than 4-6 times the free path length of the primary quanta in the material of the walls. It was shown that the spatial distribution of scattered radiation inside the cavity is practically isotropic (to within 20-30%).

In this article the authors verify results from model cavities (with sizes less than $50 \times 50 \times 50$ cm) by experiments with an actual room designed for work with powerful γ emitters (the room was $440 \times 320 \times 260$ cm, with concrete walls 100-cm thick).

The scheme of the experiments is shown in Fig. 1. The γ sources (Co^{60} with activity of 1.9 ± 0.1 mCi, and Cs^{137} with activity of 14 ± 0.7 mCi) were enclosed in a cylindrical aluminum ampoule 4×6 mm in size, which was suspended at the center of the room. The detector was a gas-discharge counter tube (type STS-5) with special jackets [4] which ensure practically constant detector sensitivity to γ-radiation flux densities in the energy range from 0.08 to 2.5 MeV. The detector was placed on a light stand at the same height as the source and was moved about between the source and the walls of the room.

To determine the intensity of scattered γ radiation against the background of the primary radiation, we filtered the radiation through lead foils [5, 6]. For this purpose, lead filters 0.18-4.0 mm thick were slipped on to the counter casing, and the energy flux density of the γ-rays was measured at fixed points in the cavity. The scattered radiation is softer than the primary and is easily filtered off. The attenuation increases exponentially with increasing lead thickness; the exponent corresonds to the absorption of primary radiation. A straight line is plotted in semilogarithmic coordinates, and is extrapolated to zero filter thickness, and hence the intensities of the primary and scattered radiation are found. As a by-product of these measurements, we can estimate the spectral composition of the scattered radiation.

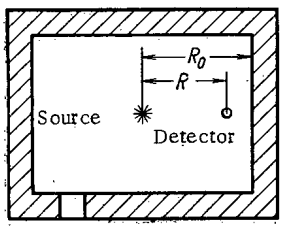

Fig. 1. Scheme for experiment.

Figures 2-4 are semilogarithmic plots of the measured γ-ray intensities versus the thicknesses of the lead filters, for various source-detector distances. The intensity of the scattered radiation was measured to within $\pm$ 15%. From the graphs it will be seen that the γ radiation consists of primary and scattered quanta, which can be characterized by their effective energies. The energy of the primary rays was 0.66 ± 0.09 MeV for the Cs^{137} source and 1.25 ± 0.12 MeV for the Co^{60} source, i.e., the primary rays were attenuated in conditions of "good geometry." The effective energy

Translated from Atomnaya Énergiya, Vol. 21, No. 4, pp. 298-300, October, 1966. Original article submitted April 11, 1966.

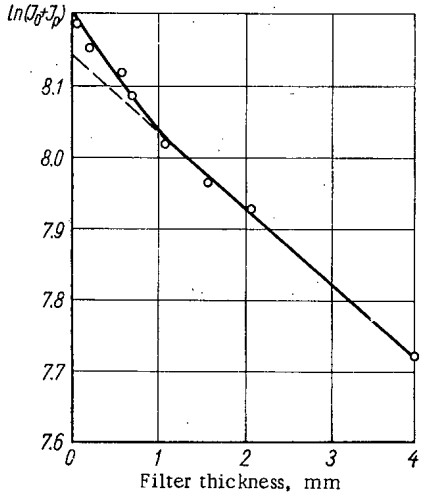

Fig. 2. Intensity of γ radiation versus thickness of filter (Cs^{137} source, R = 143 cm).

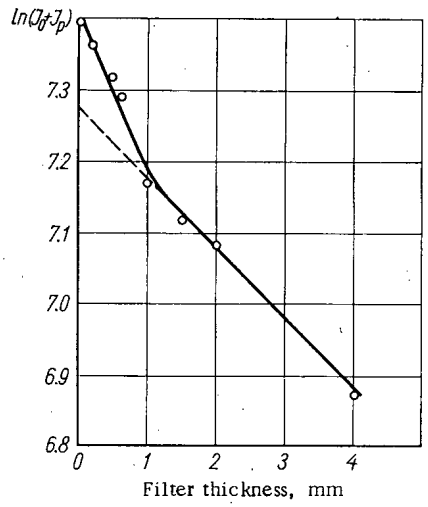

Fig. 3. Intensity of γ radiation versus filter thickness (Cs^{137} source, R = 215 cm).

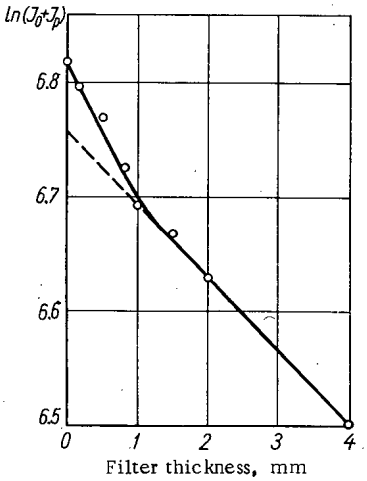

Fig. 4. Intensity of γ radiation versus filter thickness (Co^{60} source, R = 218 cm).

Energy Build-up Factors

Scattering substance	Energy of gamma rays, MeV		
	0.41	0.66	1.25
Water	1.26	1.18	1.088
Concrete	—	1.16	1.07
Aluminum	1.24	1.16	1.085
Iron	1.20	1.12	1.075
Lead	—	1.026	1.012

of the scattered quanta was 0.18 ± 0.02 for the Cs^{137} source and 0.20 ± 0.02 MeV for the Co^{60} source, i.e., the scattered rays consist mainly of quanta which have been scattered once through an angle of nearly 180°. These results agree with those of earlier experiments with narrow beams of γ-rays [5].

As in the experiments on models with small cavities, the energy flux density of the scattered γ-rays was distributed isotropically (to within 20%) through the space in the room, and the energy build-up factors $B_{re} = 1 + J_p/J_0$, found near the walls, were 1.16 ± 0.01 for γ-rays from Cs^{137} and 1.07 ± 0.005 for γ-rays from Co^{60}, in agreement with the results given in [2, 3].

The relative contribution from scattered radiation in the total dose decreases rapidly as we move away from the walls towards the source, since the intensity of scattered radiation is practically constant, whereas that of the primary radiation increases inversely as the square of the distance.

According to the results of this present work and of [1, 3], inside a closed cavity with effective linear dimensions $2R_0$, more that 4 to 6 times the free path of the γ quanta in the material of the walls, the energy flux density can be calculated by a fairly simple formula:

$$J_p = \frac{Q \cdot 3.7 \cdot 10^7}{4\pi R_0^2} \sum_{i=1}^{i=n} E_{\gamma i} \eta_i [B_{rei} - 1] \text{ MeV/cm}^2 \cdot \text{sec},$$

where Q is the activity of the preparation in millicuries, E_{γ_i} is the energy of γ quanta from the i-th line, η_i is the number of such quanta per disintegration, and R_0 is the effective distance from the source to the walls of the room.

For γ-rays from Co^{60}, Cs^{137}, and Au^{198}, this formula takes the simple form

$$J_n = a\frac{Q}{R_0^2}[B_{re}-1] \pm 20\%,$$

where the constant a is equal to $7.4 \cdot 10^6$ for Co^{60}, $1.9 \cdot 10^6$ for Cs^{137}, and $1.2 \cdot 10^6$ for Au^{198}.

Table 1 gives the energy build-up factors for normally incident γ-rays from various substances [7, 8]. The values given refer to "infinitely" thick scatterers.

If the wall thickness d of the cavity is less than 1.5 to 2.0 times the free path λ of the primary quanta in the material of the walls, the build-up factor can be calculated [8] from the formula

$$[B_{re}-1] = [B_{re}-1]_\infty (1-e^{-2\mu d}),$$

where $[B_{re}-1]_\infty$ is the build-up factor for reflection (minus one) for infinite thickness, and μ is the linear attenuation coefficient of the primary quanta in the material of the scatterer.

LITERATURE CITED

1. M. Leimdörfer, Nucl. Sci. and Engng, 17, 357 (1963).
2. M. Leimdörfer, Ibid, p. 352.
3. N. F. Andryushin and B. P. Bulatov, Atomnaya Énergiya, 19, 392 (1965).
4. B. P. Bulatov, Atomnaya Énergiya, 6, 332 (1959).
5. B. P. Bulatov and E. A. Garusov, Atomnaya Énergiya, 5, 631 (1958).
6. B. P. Bulatov, Dissertation, Moscow (1959).
7. M. Berger and J. Doggett, J. Res. of the Nat. Bur. Standards, 56, 2 (1956).
8. B. P. Bulatov and O. I. Leipunskii, Atomnaya Énergiya, 7, 551 (1959).

NEUTRON IRRADIATION AND THE DISTRIBUTION OF CORROSION PRODUCTS OF CONSTRUCTIONAL MATERIALS

D. G. Tskhvirashvili, L. E. Vasadze, and A. S. Tsukh

UDC 621.039.534.4

In the planning and operation of nuclear power stations with boiling-water reactors, it is necessary to know the laws by which corrosion products from the constructional materials, which become dissolved in the water, pass into the steam. Up to the present, the only laws studied have been those governing the partition of cobalt oxide [1] or iron oxides [2, 3] between water and steam in the absence of irradiation. However, the results obtained for iron are contradictory.

The present authors have performed experiments to determine the partition coefficients of the corrosion products of aluminum and carbon steel in experimental apparatus made of 1Kh18N9T stainless steel under neutron irradiation and under a pressure of 78-176 bar. The apparatus was mounted in the process tube of an IRT reactor. Each apparatus (Fig. 1) consisted of a container 1 which was connected to the bubbling unit 8 by means of ascending and descending circulation tubes 10. The apparatus was mounted in the tube opposite the reactor core with shavings of the test material in the container. The bubbling unit had a steam jacket 6 and a sampling tube terminating in a filter 3. The water samples were taken and the make-up water fed in via this tube and T-junction 5. Tube 4 was for taking steam samples. Tube 7 was connected to a manometer. The apparatus was wound with heater and compensation coils. Experiments, performed before mounting the apparatus in the reactor, showed that accurate results could be obtained.

A known amount of bidistillate was placed in the apparatus, which was installed in the reactor tube and subjected to the required conditions, without taking samples. Steam and water samples were then taken. If the activity of the steam sample was greater than the background activity, the experiment was considered to be complete. If not, the apparatus was left in the same conditions. A fairly long time was therefore required to determine the partition coefficient. (N.b.: the partition coefficient is equal to the ratio of the steam sample activity to the water sample activity.)

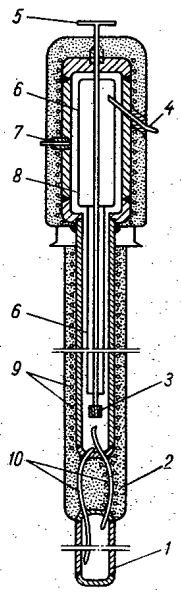

Fig. 1. Diagram of apparatus. 1) Container; 2) thermal insulation; 3) filter; 4) steam sampler; 5) T-junction; 6) steam jacket; 7) tube to manometer; 8) frame; 9) electric heater; 10) circulation tubes.

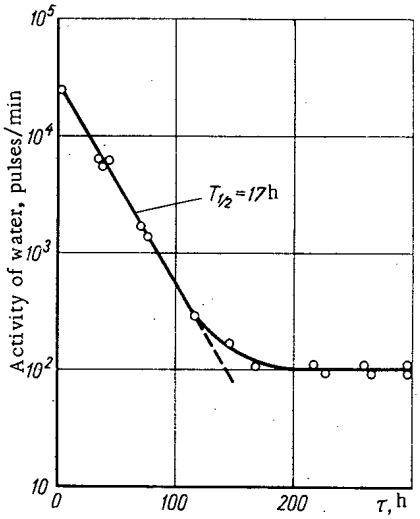

Fig. 2. Decay curve of activity of water.

Translated from Atomnaya Énergiya, Vol. 21, pp. 300-302, 1966. Original article submitted March 12, 1966.

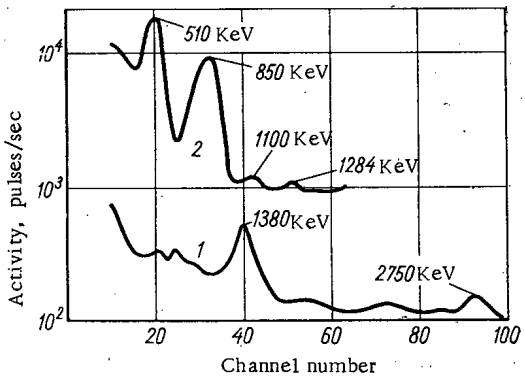

Fig. 3. Energy of γ-radiation from water samples. 1) Aluminum; 2) carbon steel.

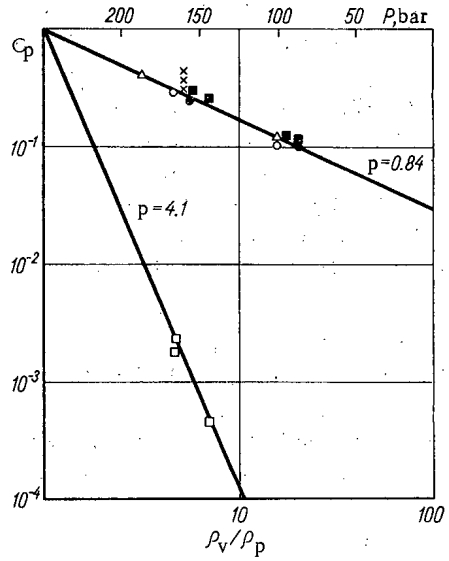

Fig. 4. Partition coefficient versus density ratio of solvent phases. □) Na^{24} (for irradiation of aluminum); ●) Co^{58} and partially Fe^{59} (for irradiation of carbon steel); ×) Fe, data from [2] (pure solution without irradiation); ■) Fe, data by present authors (pure solution without irradiation); △) Cu, data by present authors (pure solution without irradiation); ○) Co, data from [1] (pure solution without irradiation).

In the case of aluminum, the water activity was determined mainly by sodium [reaction $Al^{27}(n, \alpha)$ Na^{24}]. This was discovered by measuring the half-life (Fig. 2) and γ-ray energy (Fig. 3) of the water samples. Figure 2 shows that, in addition to Na^{24}, the water contained a long-lived element which may have reached the water from the material of the test apparatus itself. This conclusion was supported by experience in operating the BORAX, MRT, and EBWR reactors [4]. Consequently, it was impossible to determine the partition coefficients of the aluminum oxides by irradiating aluminum. The partition coefficients of Na^{24} agreed with those of NaOH in the absence of neutron irradiation (Fig. 4).

In the case of carbon steel (see Fig. 3), the water activity was determined by Co^{58} and, to a lesser extent, by Fe^{59}. The partition coefficients found in these experiments were governed more by cobalt than by iron. These values also agree with the results found for pure solutions in the absence of irradiation (cf. Fig. 4). Thus the partition coefficients of compounds in the natural corrosion products agree with those of pure solutions of the same compounds. In boiling-water reactors the main contribution to the activity of corrosion products is known [5] to be made by cobalt, iron and chromium. However, the corrosion products of stainless and carbon steel consist mainly of iron oxides. The only difference is that the products of low-alloy steel are more easily transferred to the water. Thus the partition coefficients of the corrosion products of stainless austenitic steels must be the same as those of the corrosion products of pearlite steels. To confirm this result, Fig. 4 also gives results by the present authors on pure solutions of copper oxide and iron oxides in the absence of neutron irradiation.

The experiments on iron were performed in the bubbling column, inside which was placed a copper structure which prevented corrosion products from the frame of the apparatus itself (stainless steel) from reaching the steam or water phases. On comparing the results (see Fig. 4) it will be seen that the partition coefficients of the corrosion products of the heavy metals are practically all the same, which is due to the similar physico-chemical properties of Fe, Co, Ni, Cu, Mn, and Cr. The crucial characteristics are apparently the molecular and ionic radii, because they are proportional to the coordination number [6] or exponent n. With electrolytes (for which it is mainly ions which cross to the vapor), n depends on the product of the ionic radii [7]. On the other hand, in the case of the largely undissociated molecules of the hydrated oxides of heavy metals, the determining factors will be the molecular radii. The atomic radii of these elements, and hence also the molecular radii of their hydrates, are all practically the same. The coordination numbers must also be the same. Thus the partition coefficients of Fe, Co, and Cu hydroxides are characterized by a single relation with $n = 0.84$. Consequently, there is an appreciable amount of corrosion products reaching the steam, in comparison with other substances present in the reactor's water, at medium as well as super-high pressures (see Fig. 4). The neutron flux has no effect on these phenomena, and therefore data obtained without irradiation can be applied to boiling-water reactors.

LITERATURE CITED

1. M. A. Styrikovich and O. I. Martynova, Atomnaya Énergiya, 15, 214 (1963).
2. A. M. Gryazev et al., In symposium: Water Preparation and Processes inside Boilers, ed. by T. Kh. Margulova, No.3, Moscow-Leningrad, Gosenergoizdat, p.33 (1963).
3. I. Kh. Khaibullin, Energomashinostroenie, No.5 (1964).
4. V. I. Polikarpov et al., Control of Leaks in Fuel Elements, Moscow, Gosatomizdat (1962).
5. E. U. Kramer, Boiling-Water Nuclear Reactors, Moscow, Izd-vo inostr. lit., [Russian translation] (1960).
6. O. Ya. Samoilov, Structures of Aqueous Solutions of Electrolytes and Hydration of Ions, Moscow, Izd-vo AN SSSR (1957).
7. D. G. Tskhvirashvili and V. D. Gotsindze, Trudy Institute Énergetiki AN Gruz SSR, XVIII, 239 (1963).

EFFECT OF NEUTRON IRRADIATION ON THE ELECTRICAL RESISTANCES OF TITANIUM AND CHROMIUM CARBIDES

M.S. Koval'chenko and V.V. Ogorodnikov

UDC 621.039.553

Much material has been accumulated on the effects of neutron irradiation on metals [1]. Interesting mechanisms have been discovered for the formation of various defects [2 - 4], and for radiation and post-radiation annealing of metals [5 - 9]. However, less attention has been paid to the action of radiation on compounds.

We give below the results of a study of the action of neutron irradiation on the electrical resistances of titanium and chromium carbides. These compounds exhibit metallic conductivity, and their conductivities have linear temperature dependences with positive coefficients [10, 11].

Cylindrical samples of TiC and Cr_7C_3 (diameter 8 mm, length 10 - 15 mm) were prepared by hot pressing for 5 min in graphite molds at 120 kg/cm^2, at temperatures of about 0.85 T_m [12].

The residual porosity was 5 - 15%. The samples were irradiated at 100°C in the isotope tunnel of the VVR-M reactor of the Ukrainian Academy of Sciences; the radiation doses were 10^{16} or 10^{20} neutrons/cm^2 (for titanium carbide) and 10^{18} or 10^{20} neutrons/cm^2 (for chromium carbide). The proportion of fast neutrons was about one order of magnitude lower.

The electrical resistances were measured at room and elevated temperatures by means of a special apparatus with the usual potentiometric circuit. The influence of porosity was eliminated by the method of [13]. The irradiated specimens were annealed for 1 h in a tube furnace in argon at 400 - 1200°C (the temperature was varied by 200° steps).

The furnace and resistance meter were placed in a 2KZ shielding chamber, and therefore all the manipulations and measurements were made by remote control.

We found that neutron irradiation markedly increases the electrical resistance of the carbides. For Cr_7C_3, the increase was 35% for 10^{18} neutrons/cm^2 and 60% for 10^{20} neutrons/cm^2. The resistance of titanium carbide showed smaller alterations – 19% and 23% for the above doses, and 14% for 10^{16} neutrons/cm^2. The resistance was measured for five to ten samples at room temperature, before and after irradiation. For each sample, the change in resistance was measured to within ±3%. The scatter for the various specimens was ± 15%. The averaged results are given in Table 1 below.

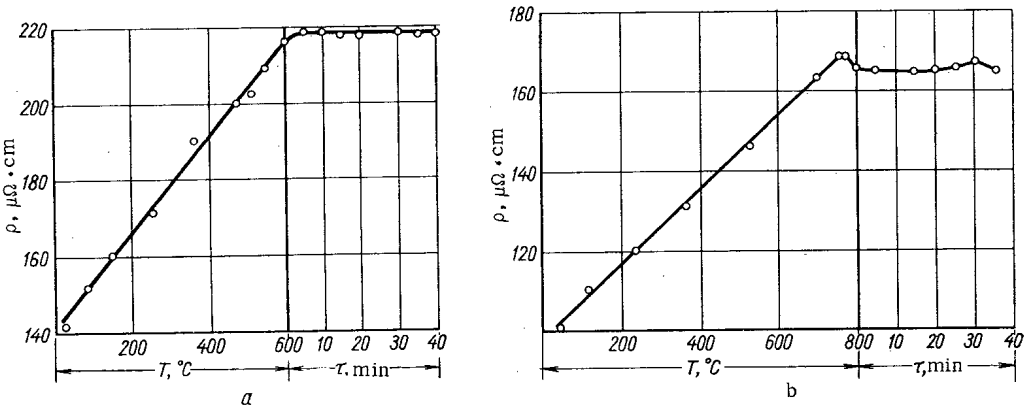

Fig. 1. Temperature dependence of resistance ρ of chromium carbide, irradiated with 10^{18} neutrons/cm^2 and heated to a) 600°C, b) 800°C.

Translated from Atomnaya Énergiya, Vol. 21, No. 4, pp. 302 - 304, October, 1966. Original article submitted May 12, 1966.

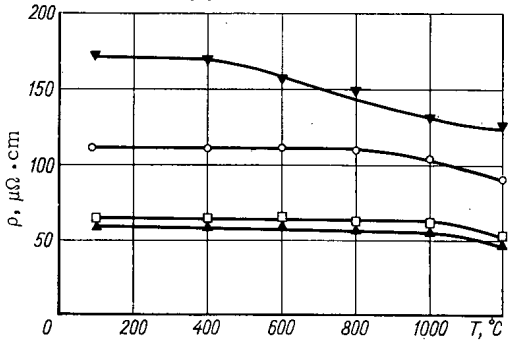

Fig.2. Influence of temperature of isochronous annealing on electrical resistance of irradiated carbides. (▲) TiC, dose 10^{16} neutrons/cm^2; (□) TiC, 10^{20} neutrons/cm^2. (○) Cr_7C_3, 10^{18} neutrons/cm^2; (▼) Cr_7C_3, 10^{20} neutrons/cm^2.

TABLE 1. Effect of Neutron Irradiation on Electrical Resistances of Chromium and Titanium Carbides

Material	Resistance before irradiation μΩ·cm	Integral flux, neutrons/cm^2	Resistance after irradiation μΩ·cm	Increase of resistance, %
Cr_7C_3	110	10^{18}	148	35
		10^{20}	175	60
TiC	52	10^{16}	60	14
		10^{20}	64	23

The electrical resistance was measured during heating at approximately 100° intervals, and then at constant temperature at 5 min intervals. As seen from the graphs in Fig.1, annealing at 600 and 800°C causes no appreciable change in resistance. The temperature dependence of the resistance of Cr_7C_3 after irradiation is linear at low temperatures.

The temperature coefficients of the resistances of the two compounds were $1.05 \cdot 10^{-3}$ and $0.82 \cdot 10^{-3}$ deg^{-1} respectively.

Recovery of resistance by chromium carbide irradiated with 10^{18} neutrons/cm^2 begins at 1000°C, and of chromium carbide irradiated with 10^{20} neutrons/cm^2 at 600°C: a slight reduction in resistance is observed even at 400°C (Fig.2).

For titanium carbide, recovery of resistance begins at 1000°C. Despite the relatively high annealing temperature, recovery of resistance is incomplete for both carbides, as is shown by Fig.2.

These results show that titanium carbide, which has a cubic structure of the NaCl type, is more stable to neutron irradiation than chromium carbide, for which the hexagonal lattice has repeat period a more than three times greater than c. These data serve as additional confirmation of an established fact: the more symmetrical and densely packed a structure is, the greater is its stability to irradiation.

On comparing the temperature coefficients of the resistances of irradiated chromium carbide (10^{18} neutrons/cm^2) with values [14] for nonirradiated material, we find that they are either unchanged or slightly reduced by irradiation. In every case, the results obtained differ from the data given in [14] for titanium carbide, where the temperature resistance coefficient of TiC was found to increase after irradiation by 10^{18} neutrons/cm^2. It is possible that this discrepancy is due to different crystal structures of the compounds.

When chromium carbide is irradiated by 10^{18} neutrons/cm^2 and kept at 600 or 800°C, its resistance is not restored, in agreement with the data on isochronous annealing.

Investigations of healing of radiation defects by isochronous annealing showed that radiation defects in titanium carbide are thermally more stable than those of chromium carbide. This is connected with the fact that the melting point of TiC (3147°C) is higher than that of Cr_7C_3 (1660°C). Appreciable restoration of the resistance of Cr_7C_3 irradiated by 10^{20} neutrons/cm^2 begins at 600°C, while at 400°C there is only a tendency towards decrease of resistance.

Basing our argument on the healing of radiation defects in metals [15] and graphite [16], we can suppose that the point defects (especially vacancies) which arise in TiC and Cr_7C_3 during irradiation are fairly stable. The interstitial atoms are partly annealed during irradiation, owing to the recombination of weakly dissociated Frenkel vapor and capture by traps. In metals, healing of vacancies is observed at $T \approx 0.3 T_m$ (°K). In the carbides studied above, healing of defects takes place at higher temperatures (see Fig.2). The vacancies and interstitial atoms formed by irradiation are removed by self-diffusion at temperatures above $0.4 T_m$ (°K).

LITERATURE CITED

1. A. Seeger, Phys. Verhandl. DPG. 4, 401 (1964).
2. R. Jan, Phys. Stat. Sol., 6, 925 (1964); 7, 299 (1964); 8, 331 (1965).
3. G. Leibfried, J. Appl. Phys. 30, 1388 (1959).
4. M. Thompson, Rend. Sc. internaz. fis. «Enriko Fermi» 1960, vol. 18, N.Y.–Lond., p. 169 (1962).
5. K. Sizman, Res. Group U.K. Atomic Energy Author., NAERE-R4694, 41 (1964).
6. G. Lück and K. Sizman, Phys. Stat. Sol., 6, 263 (1964).
7. K. Dettmann and G. Leibfried, Res. Group U.K. Atomic Energy Author., NAERE-R4694, 39 (1964).
8. W. Frank et al., Phys. Stat. Sol. 8, 345 (1965).
9. A. Damask, Rend. Sc. internaz. fis. «Enriko Fermi» 1960, vol. 18, N.Y.–Lond., p. 555 (1962).
10. G.V. Samsonov and Ya.S. Umanskii, Solid Compounds of Refractory Metals, Moscow, Metallurgizdat (1957).
11. S.N. L'vov et al., Fiz. metallov i metallovedenie, 11, 143(1961).
12. G.V. Samsonov and M.S. Koval'chenko, Hot Pressing, Kiev, Gostekhizdat UkrSSR (1962).
13. V.V. Ogorodnikov, I.M. Fedorchenko, and A.I. Raichenko, Dokl. AN UkrSSR, No. 12, 1603 (1960).
14. I.D. Konozenko and V.S. Neshpor, Poroshkovaya Metallurgiya, No. 1, 60 (1965).
15. H.G. Van Bueren, Imperfections in Crystals, 2nd ed., Wiley (1961).
16. J. Williamson, Graphite in Nuclear Reactors, Papers read at Symposium at the Institute of Metals, London. Khar'kov, Izd. FTI AN UkrSSR [Russian translation] (1962).

DETERMINING THE AGES OF MINERALS BY MEANS OF THE TRACKS OF FISSION FRAGMENTS FROM URANIUM NUCLEI

I.G. Berzina and P.G. Demidova

UDC 539.173.7:539.173.4

A method has recently been developed for determining the ages of minerals by means of the tracks left by fragments from the spontaneous or induced fission of uranium nuclei [1-3]. The crystal lattice defects caused by the fragments are found and measured.

The presence of the Clarke content of the fissile elements in a mineral means that, in principle, we can detect spontaneous fission of these elements from the fission fragment tracks which are observed on the surface of slips of test specimens. Since U^{238} decays by spontaneous fission 23 times faster than U^{235}, while the proportion of U^{235} in natural uranium is only 0.7%, we can assume that most of the fissions are contributed by U^{238}. Fission of U^{238} usually forms two fragments which move in the surrounding substance, losing energy and disturbing the crystal lattice. This disturbance can be detected by etching the mineral with specially chosen reagents, which cause the initial lattice defects to appear as channels of which the cross-section increases with the etching time. If the etching is continued until the channels grow to about 1000 A, they will become resolvable under the microscope.

The number of tracks from spontaneous fission fragments is a function of the age of the specimen. The main difficulty in calculating the mineral's age lies in determining the uranium content in the same volume of substance as that used to count the tracks. This prblem is solved by a method given in [2] for determining the uranium concentration from the tracks due to induced fission. The age T of the mineral is given [3] by the formula

$$T=\frac{\rho_1 n\sigma J^{235}}{\rho_2 \lambda J^{238}}, \quad (1)$$

where ρ_1 and ρ_2 are the densities of tracks due to spontaneous and induced uranium fission, respectively, λ is the spontaneous decay constant of U^{238}, n is the dose of thermal neutrons, σ is the fission cross section of U^{235} for thermal neutrons, and J^{235} and J^{238} are the isotopic quantities of U^{235} and U^{238} in the mineral. Equation (1) is valid for $T \leq 10^9$ yr.

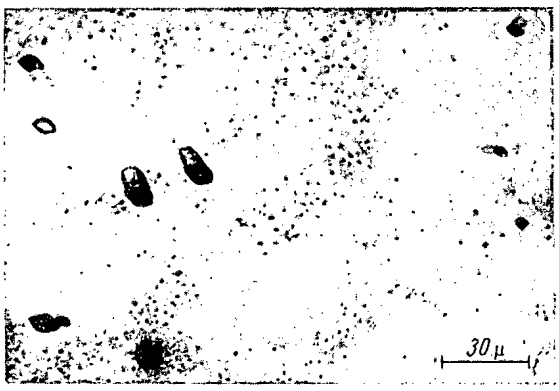

Fig. 1. Tracks from fragments due to spontaneous and induced fission of uranium nuclei in muscovite (double etching).

TABLE 1. Ages of Minerals, Measured by Means of Uranium Fission-Fragment Tracks and by the Potassium-Argon Method

Specimen No.	Taken from:	Age, in millions of years	
		From uranium fission-fragment tracks	From potassium-argon method*
1	Quartz-wolframite vein	122±19	132±5
2	Quartz-wolframite vein	117±15	131±5
3	Pegmatite vein	122±18	138±7

* The potassium-argon analysis of the mica was performed in the Absolute Age Laboratory of the Institute for Geology of Ore Deposits, Petrography, Mineralogy and Geochemistry of the Academy of Sciences of the USSR, under the direction of L.L. Shanin.

Translated from Atomnaya Énergiya, Vol. 21, No. 4, pp. 304 - 306, October, 1966. Original article submitted May 12, 1966.

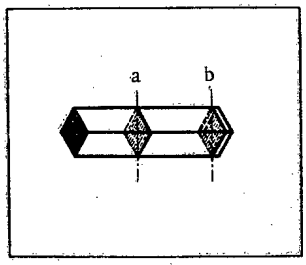

Fig.2. Rupture of fission-fragment track when mica is split along its cleavage.

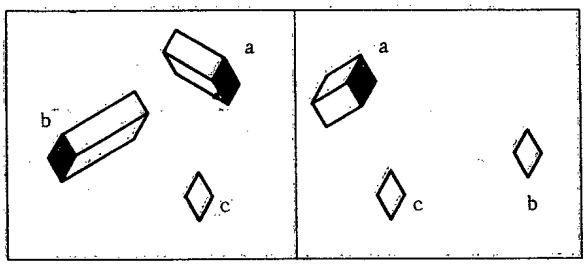

Fig. 3. Various possible appearances of tracks due to fission fragments on opposite cleavage faces of mica. a) Paired extended tracks; b) extended and flat tracks; c) paired flat tracks.

The above method was used to determine the ages of minerals from rare-metal deposits in Eastern Transbaikal', which, according to general geological data, have not been subjected to high temperatures since the time of their formation. In particular, specimens 1 and 2 (see Table 1) were taken from the central parts of quartz-wolframite veins, after which the only later formations were veins and veinlets of low-temperature chalcedony-like quartz.

In the experiments, plates of the mica were immersed in 48% hydrofluoric acid for 20 h at 20°C. The density of spontaneous-fission tracks on the etched surfaces was measured, and the specimens were then coated with polyethylene film to prevent contamination and irradiated with thermal neutrons in a reactor. They were then again etched in the same conditions as before, and the density of tracks due to induced fission was measured.

Figure 1 shows typical tracks due to fission fragments in the mineral, revealed by double etching with hydrofluoric acid before and after irradiation with thermal neutrons. The cross sections of the tracks are rhombic in shape.

On etched opposite cleavage faces of mica we found three types of fission-fragment tracks — paired extended, extended and flat, and paired flat tracks [5]. Figure 2 shows the rupture of a track due to splitting of the mica along a cleavage plane. If the cleavage plane intersects the track far from its ends, then two extended tracks will be observed on opposite etched cleavage faces (see Figs. 2 and 3a). If the cleavage plane intersects the track near one end, the opposite cleavage faces will display one extended and one corresponding flat track (see Figs. 2 and 3b). Tracks of the third type (see Fig. 3c), as shown in [5], represent tracks which have been 'healed up' by high temperature annealing. In our case, the contribution of flat defects represents less than 7% of the total number of fission-fragment tracks used in determining the age of the mineral. The very small number of "healed" tracks can be regarded as evidence for the absence of periods of thermometamorphism at any time during the geological history of the test specimens. Fleisher et al. [4] have shown that the action of moderate temperatures (of order 150°C) on mica does not lead to "healing" of tracks, even if continued for a very long time.

The Table gives results of determinations of the ages of minerals from fission-fragment tracks and by the potassium-argon method. There appears to be a systematic error in the results of the first method, which tend to be too low: this may be mainly due to errors in determining the neutron fluxes, because the statistical errors were reduced to a minimum (3%) by multiple measurements.

These experiments confirm the feasibility of using the above method to determine the absolute age of mica which has not been subjected to thermal metamorphism. This method might be applied to minerals which have undergone prolonged heating at above 100 - 150°C in order to find out how long ago the metamorphosis has occurred; this cannot be estimated by existing methods, but is of much interest for the solution of several geological problems.

The above method has the advantage over other geochronological methods that it can be used to find the age of any mineral from small pure samples (e. g., thin mica plates with areas of 1 mm^2).

In conclusion, the authors would like to thank G.N. Flerov for suggesting the research topic, and also Yu. S. Shimelevich for helpful discussions on the results.

LITERATURE CITED

1. M. Maurette, P. Pellas, and R. Walker, Bull. Soc. franç. mineral. et cristallogr., 87, 6 (1964).
2. P. Price and R. Walker, Appl. Phys. Letters, 2, 23 (1963).
3. P. Price and R. Walker, J. Geophys. Res., 68, 4847 (1963).
4. R. Fleisher et al., Science, 143, 349 (1964).
5. Ya. E. Geguzin, I. G. Berzina, and I. V. Vorob'eva, Izv. AN SSSR, ser. geol., No. 6, 21 (1966).

ENERGY CHARACTERISTICS OF X-RAYS WITH MAXIMUM VOLTAGES OF 40-120 kV

R. V. Stavitskii

UDC 621.386.7:621.386.86

In designing and testing shielding against direct and scattered x-radiation with maximum tube voltages of 40-120 kV, account must be taken of the energy characteristics of both forms of radiation. We have used an indirect method of determining these characteristics, based on single and double measurements of half-attenuation layers Δ, followed by determinations of the effective energy by means of tables given in [1]. This method cannot be regarded as absolute, as the spectral composition of the radiation changes in the half-attenuation layer itself. However, for purposes of practical dosimetry, a knowledge of the effective energies of the radiation is considered quite sufficient [2, 3].

The half-attenuation layer was measured for three media — (1) water, which is a tissue-equivalent material; (2) brick (density 1.6 g/cm^3); (3) concrete (2.3 g/cm^3). The radiation fields were 4 × 4 and 20 × 20 cm. It was assumed that the first case corresponded to narrow-beam geometry and the second case to wide-beam geometry. To allow for the different effective energies of the radiation in irradiated objects of different thicknesses, the measurements were made twice — once in a tissue-equivalent medium of thickness 5 cm, and once in 20 cm. We used a capacitor-type dosimeter with a thin-walled ionization chamber of sensitivity 9-250 mR, accuracy not worse than ±5%, and energy range 30-200 keV.

We first measured the relation between the half-value attenuation layer and the tube voltage, in free air (Fig. 1). There was a significant difference between Δ_1 and Δ_2, the first and second half-attenuation layers, over practically the entire range of tube voltages: this indicates that the radiation was very inhomogeneous (with 40 kV max., Δ_2/Δ_1 = 1.21; with 80 kV max., 1.33; with 120 kV max., 1.38). Consequently, to reduce the absorption of radiation in the surface layers of the irradiated substance, the additional filtering must be augmented, beginning from tube voltages of 60-80 kV max. or over.

Figure 2 shows the energy characteristics of the primary x rays after passage through 5 or 20 cm of water. The natures of the curves for a narrow beam show that the effective energy increases uniformly, and the homogeneity of the radiation is approximately constant. The effective energies are practically independent of the thickness of the water layer, i.e., with 5-cm water layers there is fairly good filtration of the radiation. Further increase in the thickness of the absorbing medium has practically no effect on the energy characteristics of the radiation. Comparison of the characteristics of the wide and narrow beams for both thicknesses of the absorbing media reveals a certain difference, even for tube voltages of 40-80 kV max. At higher voltages the difference is even more marked. The closeness of the results for a wide beam for both absorbing-layer thicknesses is explained by the fact that low-energy quanta, entering the absorbing medium or formed in its first 15 cm, are totally absorbed by the remaining water layer. We can reckon that the spectral composition of the radiation remains practically constant, in this range of effective primary-radiation energies, for absorbing media 5 cm or more in thickness.

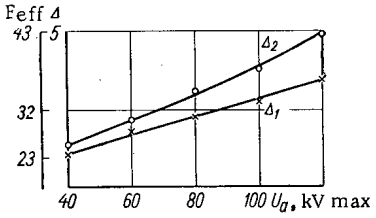

Fig. 1. Half-attenuation layer Δ and effective energy Eeff of x-radiation, versus tube voltage U_a, measured in air (additional filter – aluminum, thickness 2 cm). Δ_1 and Δ_2 are the first and second half-attenuation layers, respectively.

For tube voltages lower than 80 kV max. the effective energy of a wide beam of x rays falls off sharply, reaching a value less than that of the narrow beam by a factor of 1.5-2.0. The coefficient of homogeneity is equal to 1.2 for 100 kV max., and 1.3 for 120 kV max. This phenomenon is clearly due to Compton scattering.

The energy characteristics of scattered radiation were measured and analyzed as follows: the tube voltage was 40-120 kV max., the

Translated from Atomnaya Énergiya, Vol. 21, No. 4, pp. 306-308, October, 1966. Original article submitted April 12, 1966.

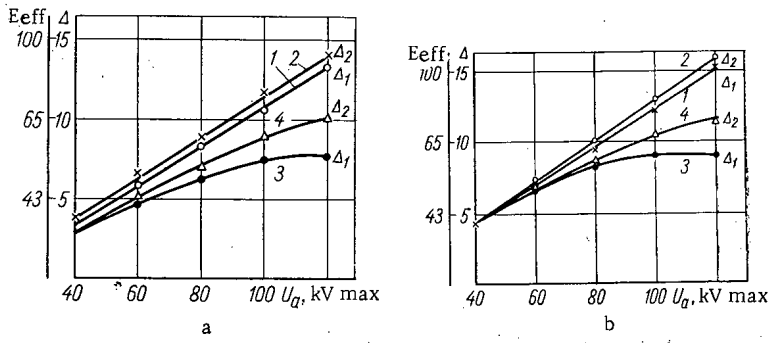

Fig. 2. Comparison of half-attenuation layers Δ and effective energies E_{eff} of wide and narrow beams of x rays for water layers with thicknesses of 5 cm (a) and 20 cm (b), versus tube voltage U_a. (1), (2) Radiation field 4 × 4 cm (narrow beam); (3), (4) 20 × 20 cm (wide beam).

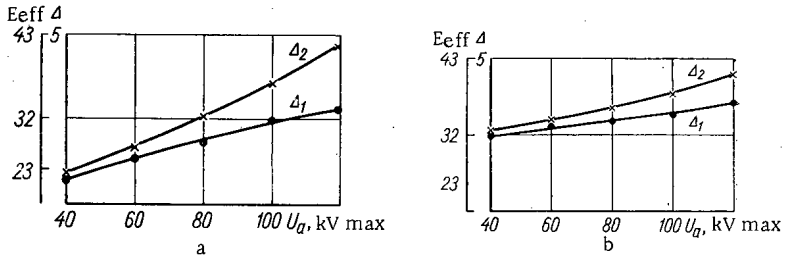

Fig. 3. Half-attenuation layers Δ and effective energy E_{eff} of scattered radiation in water, versus tube voltage U_a, for various distances between radiation field and side surface: (a) 1 cm; (b) 10 cm.

thickness of the scattering water layer 20 cm, the cross section of the primary beam at the surface of the irradiated medium 20 × 20 cm, and the angle of scattering 90°. The half-value attenuation layers were measured twice-with the edge of the radiation field 1 cm and 10 cm from the side surface of the vessel containing the water. This arrangement made it possible to assess how the thickness of the absorbing layer influenced the energy characteristics of the scattered radiation. The results are plotted in Fig. 3.

With a radiation field located near the edge, for tube voltages more than 80-90 kV max., we observed a fairly sharp reduction in the yield of radiation with low energies. This is most probably due to an increase in the yield of quanta which have undergone Compton scattering. The contribution made by characteristic x radiation cannot be large, because for low tube voltages (below 80 kV max.) the degree of homogeneity of the scattered radiation is relatively large (Δ_2/Δ_1 = 1.1 at 40 kV max. and 1.22 at 60 kV max.), despite the fact that these voltages are higher than those which excite characteristic radiation for water and oxygen.

Removal of the beam away from the edge leads to increased homogeneity in the scattered radiation. It must be remarked that in this case there is relatively little increase in the effective energies of scattered radiation throughout the range of tube voltages.

Our investigation of the energy characteristics of primary and scattered radiation passing through water has thus shown that for tube energies of 40-120 kV max. (additional filter — aluminum, 2 mm thick), (1) the effective energy of a wide beam of x rays is 40-60 keV, that of a narrow beam 40-95 keV; (2) the effective energy of radiation scattered through 90° is close to that of the primary beam in free air (23-34 keV), though the homogeneity is somewhat less.

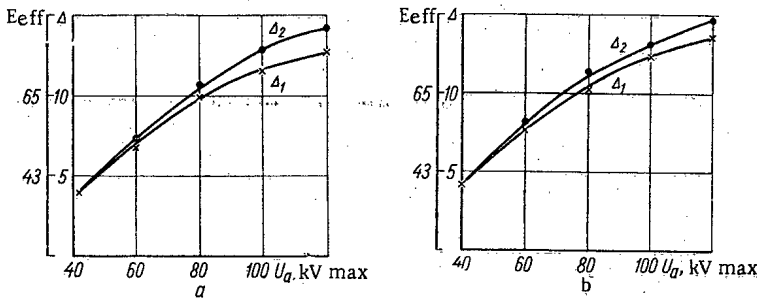

Fig. 4. Attenuation half-value layer Δ and effective energy Eeff of wide beam of x rays passing through a 12.5-cm layer of brick (a) or a 12-cm layer of concrete (b), versus tube voltage U_a.

The energy characteristics of x rays passing through layers of concrete and brick were studied only for wide x ray beams. The results are shown in Fig. 4. The curve for the first half-attenuation layer versus tube voltage practically coincides with that for the second layer. For voltages lower than 80-90 kV max. the degree of homogeneity is very high, but falls somewhat on increase of voltage, without exceeding the limit 1.1. This means that the long-wave part of the spectrum of radiation passing through the shielding has a low intensity, because low-energy quanta formed in the first few layers of shielding are wholly absorbed in the deeper layers. The radiation scattered in the last layers of concrete or brick shielding is of low intensity, since this radiation has practically no effect on the qualitative characteristic. It must be pointed out that 12 (12.5) cm thicknesses of concrete (brick) have inadequate shielding properties at tube voltages of 80-120 kV max., if we regard them as permanent shields for offices or laboratories where x rays are used. Nevertheless, analysis of the energy characteristics of radiation which has passed through these thicknesses of concrete or brick shows that, for high enough homogeneity of the radiation, the effective energy is about 3/4 of the absolute tube voltage. In particular, this enables us to solve the problem of choosing an energy range in which to operate dosimetric devices for monitoring the efficiency of shielding.

LITERATURE CITED

1. A. N. Krongauz, In book: Some Aspects of X-ray and Nuclear Radiology, Moscow, Medgiz, p. 119 (1961).
2. A. V. Frolova, Ibid., p. 93.
3. A. V. Frolova et al., Vestnik rentgenologii i radiologii, No. 1, 49 (1961).

ANALYSIS OF INTEGRAL β- SPECTRA BY THE HARLEY-HALLDEN METHOD

L. I. Gedeonov, G. V. Yakovleva, and I. M. Eliseeva

UDC 543.52

In laboratory practice it is often necessary to determine or check the radiochemical purity of a β-emitter. To identify a radioactive isotope, and as a criterion of its radiochemical purity, the present authors have used the shape of the integral β-spectrum, measured by means of a scintillation spectrometer. Registration of the integral spectrum increases the sensitivity of the method and makes it possible to determine the energy of the β-rays from weakly-active preparations. The method was used both for infinitely thin preparations and for sources with thicknesses up to 100 mg/cm^2.

Present methods [1-6] of analysing the spectra of β-emitters by means of scintillation spectrometers are based on the use of a crystal with a well, or double crystals between which is placed a source of negligible weight deposited on a thin backing. The recorded differential simple spectrum of the β-emitter has, to a first approximation, a shape which can be represented by a Curie straight-line graph. However, with scintillation detectors we get an instrumental spectrum which is badly distorted at low and high energies, owing to the poor resolving power of scintillation β-spectrometers, the finite thickness of the preparations, and reverse scattering of β-particles by the substrate and the crystal itself. The effects of the inadequate resolving power of the spectrometer can be partly avoided by introducing complicated corrections [7-9], calculated from the shape of the lines of the given spectrometer. With the best scintillation β-spectrometers, it is possible to get rectilinear Curie graphs up to 50 keV. Unfortunately, this method, besides being complicated, is quite inapplicable to the measurement of substances with low specific activity. In this case, the shape of the spectrum is distorted owing to self-absorption of β-particles in the source, and the Curie graph becomes nonlinear throughout the spectrum.

The scintillation β-spectrometer which we used consisted of a crystal (stilbene, diameter 30 mm, height 15 mm), a photomultiplier, a cathode follower, a discriminator amplifier and a counting circuit. The measured integral spectra of thin preparations (on colloid films) were analyzed by the Harley-Hallden method [10]. The integral β-spectrum of Y^{91} with E_{max} = 1.5 MeV was used as reference standard, and the β-spectra under investigation were compared with it. For the test and reference specimens we determined the ratio of the integral number of pulses, N, for a given

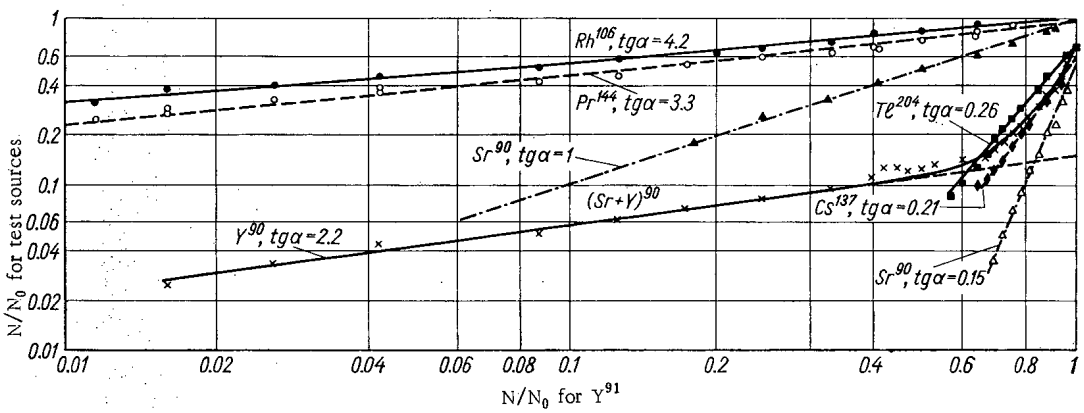

Fig. 1. Integral β-spectra of various radioactive isotopes (thin sources), relative to the integral β-spectrum of Y^{91}.

Translated from Atomnaya Énergiya, Vol. 21, No. 4, pp. 308-311, October, 1966. Original article submitted March 2, 1966.

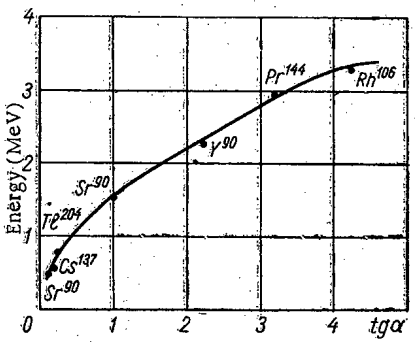

Fig. 2. Slope of straight line versus limiting energy of β-spectrum.

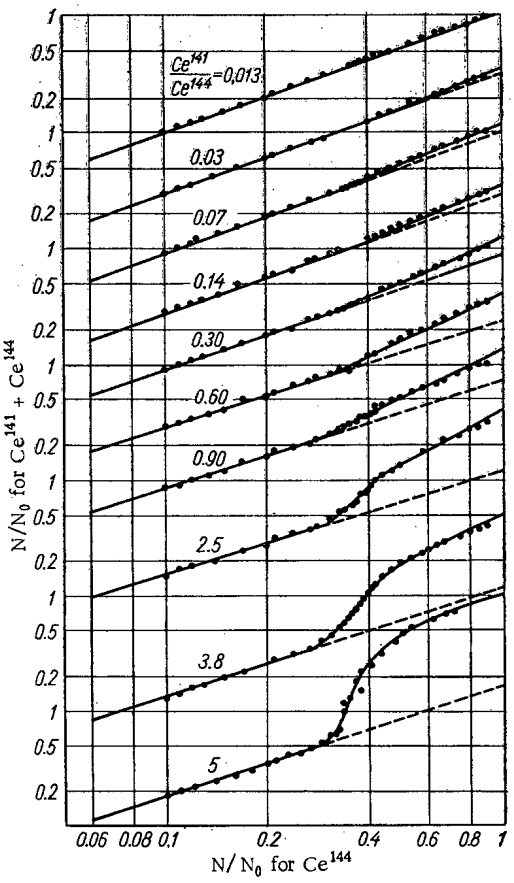

Fig. 3. Spectrum of $Ce^{141} + Ce^{144}$ (thin films), relative to spectrum of Ce^{144}.

displacement of the discriminator, to that, N_0, without displacement. The values found were plotted in logarithmic coordinates. Figure 1 shows that in this form the integral spectrum of simple β-radiation is a straight line with a slope which depends on the limiting energy of the β-spectrum. No difference was observed in the slopes of the integral β-spectra for the two positions of the source (1 and 25 mm from the crystal).

Figure 2 plots the energy dependence of the gradient of the straight-line graph. It can be expressed analytically as

$$E = 0.85\,\mathrm{tg}\,\alpha + 0.70 - 0.05\,\mathrm{tg}^2\alpha.$$

This empirical relation enables us to determine the limiting energy of the β-spectrum of an unknown isotope, to within ~10%. The time required to identify a β-emitter with an activity of 10^{-8} Ci is about 10 min, and is inversely proportional to the activity of the preparation. The lowest activity necessary for the use of the above method is about 10^{-9} Ci.

The method was also applied to preparations of Sr^{89}, Ce^{144}, and $Sr^{90} + Y^{90}$ with thicknesses up to 100 mg/cm^2 (tablets of 5 mm diameter, pressed on a lead substrate). From measurements with $E\beta > 150$ keV it was shown that the slopes of graphs of the integral spectra of Sr^{89} do not depend on the weight of the preparation up to 70 mg/cm^2 (or for Ce^{144} or Y^{90} up to 100 mg/cm^2), owing to the high limiting energies of these spectra. In the soft range, the integral spectrum of $Sr^{90} + Y^{90}$ depends on the weight of the preparation, owing to the low energy of β-radiation from Sr^{90} (500 keV). Therefore, to test the radiochemical purity of $Sr^{90} + Y^{90}$ we have to compare their spectra with that of a reference $Sr^{90} + Y^{90}$ source of similar density.

The method described above was also applied to two-component mixtures of β-emitters.

Figure 3 shows the β-spectra of thin preparations of $Ce^{141} + Ce^{144}$ for various relative isotope contents. In this case the reference standard was Ce^{144}. It will be seen that the spectrum of the cerium isotope mixture consists of two parts. The hard part of the spectrum corresponds to Ce^{144}; the gradient is equal to unity. The low-energy part (below 0.5 MeV) corresponds to Ce^{141} and has a steeper slope. The ratio of the points of intersection of the dashed and solid lines with the vertical axis gives the ratio between the activities of C^{141} and Ce^{144} in the mixture. The activity of Ce^{141} found from the curves in Fig. 3 is somewhat less than the true figure, because part of the soft β-radiation from the Ce^{141} is cut off by the displacement of the discriminator required to cut off the noise from the photomultiplier. This fraction is determined by using the spectrometer to make direct measurements of the count rate of β-rays from Ce^{141} of known absolute activity.

Figure 3 also shows that a 1% admixture of Ce^{141} in Ce^{144} is undetectable. A 3% admixture of Ce^{141} can just be detected, and quantitative determination of the activity of each component can begin at 7% Ce^{141}. This method not only enables us to determine the quantitative composition of a mixture of

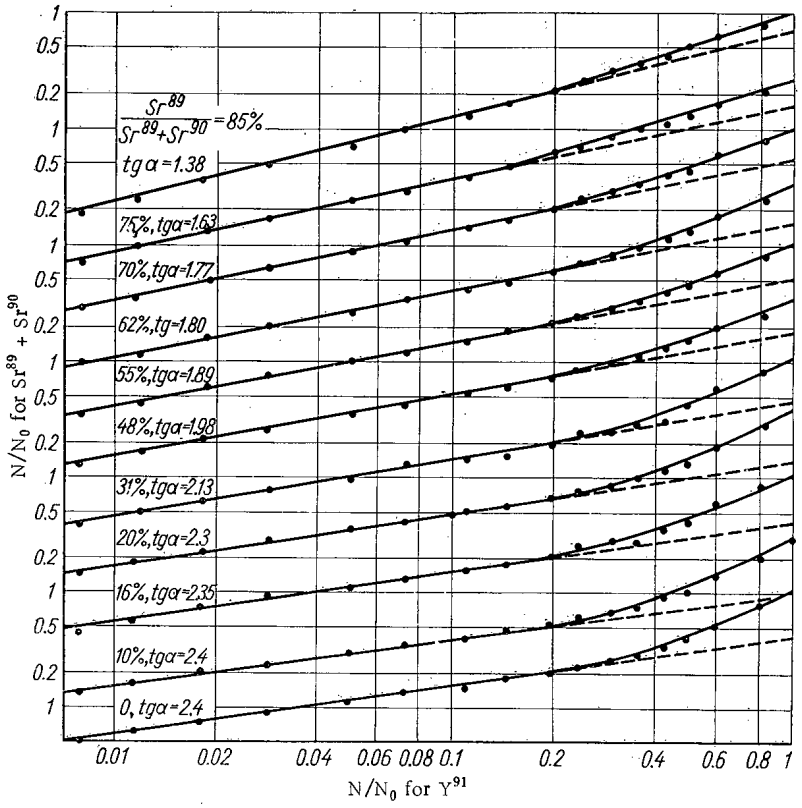

Fig. 4. Spectra of $Sr^{89} + Sr^{90}$ (thin sources) relative to spectrum of Y^{91}.

$Ce^{141 + 144}$, but also makes it possible to establish the radiochemical purity of cerium. Exact similarity between the shapes of the integral spectra was also observed for preparations of $Ce^{141} + Ce^{144}$ with weights up to 100 mg/cm^2. In this case the count rate determined by each cerium isotope is also found from the ratio of the initial ordinates of the solid and dashed curves.

Figure 4 gives the β-spectra of thin specimens of $Sr^{89} + Sr^{90}$ of various compositions. It was established that any preparation of Sr^{89} always contains a little Sr^{90}. For this reason, the reference standard used for strontium isotope mixtures was of Y^{91}, for which the β-spectrum is similar to that of Sr^{89}. From Fig. 4 it will be seen that the hard section of the β-spectrum of $Sr^{89} + Sr^{90}$ is rectilinear, and that its gradient depends on the percentage content of Sr^{89} in the mixture. Since the energy of β-rays from Y^{90} is close to that of Sr^{89}, no bend is observed in the hard section of the spectrum, in contrast to the case of $Ce^{141} + Ce^{144}$. Analysis of the experimental relation between the slope of the integral spectra of $Sr^{89} + Sr^{90}$ and the proportion of Sr^{89} showed that the minimum detectable proportion of Sr^{89} is 10%. The mean error in determining Sr^{89} by this method is about 10% when its activity constitutes > 20% of the total. If the Sr^{89} content is lower, the accuracy is somewhat worse.

The time required to analyse a two-component radioactive mixture with total activity of 10^{-9} Ci is about 2 h.

This method can be used for activities about ten times lower than those required for analysing the absorption curves for β-radiation. It also requires much less time than that required to analyse the decay curves of long-lived isotopes, being about a thousand times more rapid.

LITERATURE CITED

1. B. Ketell, Phys. Rev., 80, 758 (1950).
2. J. Hopkins, Phys. Rev., 77, 406 (1950).
3. R. Davis and P. Bell, Phys. Rev., 83, 483 (1951).
4. D. Gardner and W. Heinke, Internat. J. Appl. Radiat, and Isotop., 3, 232 (1958).

5. R. Ricci, Physica, 23, 693 (1957).
6. R. Johnson, O. Johnson, and L. Langer, Phys. Rev., 102, 1142 (1956).
7. G. Owen and H. Primakoff, Phys. Rev., 74, 1406 (1948).
8. G. Owen and H. Primakoff, Rev. Scient. Instrum., 21, 447 (1950).
9. M. Freedman, T. Novey, and F. Porter, Rev Scient. Instrum., 27, 716 (1956).
10. J. Harley and N. Hallden, Nucleonics, 13, No. 1, 32 (1955).

EAST GERMANY'S FIRST WHOLE BODY COUNTER

K. Poulheim

UDC 539.107.43

Construction of the SZS whole body counter, East Germany's first such facility, began in 1963. The recording system presently in use was completed by late 1964, calibration and regular measurements began in January, 1965.

The whole body counter built at the State Center for Ionizing Radiation Shielding is designed to measure the content of radioactive materials present in the human organism in the wake of accidents and exposures, to rate neutron dosage by the activity of Na^{24} formed in the human organism after exposure to neutron radiation, and for experimental research. It also provides dosimetric monitoring of exposure of personnel working with radium light-sensitive compounds of fixed composition — the first facility of this kind. After a second whole body counter, which is now the planning boards, has been build, this counter facility will be relegated to use on experimental animals.

All of the materials and instruments used in the fabrication of the counter were produced by East German industry (with the sole exception of the scintillation measuring probe). The shielding includes 50 tons of gypsum, and the measurements chamber is built from a section of iron ductwork (diameter 145 cm, length 200 cm, wall thickness 1.5 cm) fabricated in 1925. The measurement chamber is lined with lead plates 6 mm thick and 150 cm long, thinning out the background in the low-energy portion of the spectrum (down to 500 keV). The lead, a product about half a century old, was studied for its own content of radioactive materials before being set in place in the measurement chamber. The lead plates were coated with electrolytic copper sheet of 3 mm thickness to absorb the characteristic K-radiation.

The earlier Tl-activated NaI crystal (diameter 100 mm, height 70 mm) scintillation measurement probe [1] was later replaced with a new Nuclear Enterprises measuring probe. The latter featured

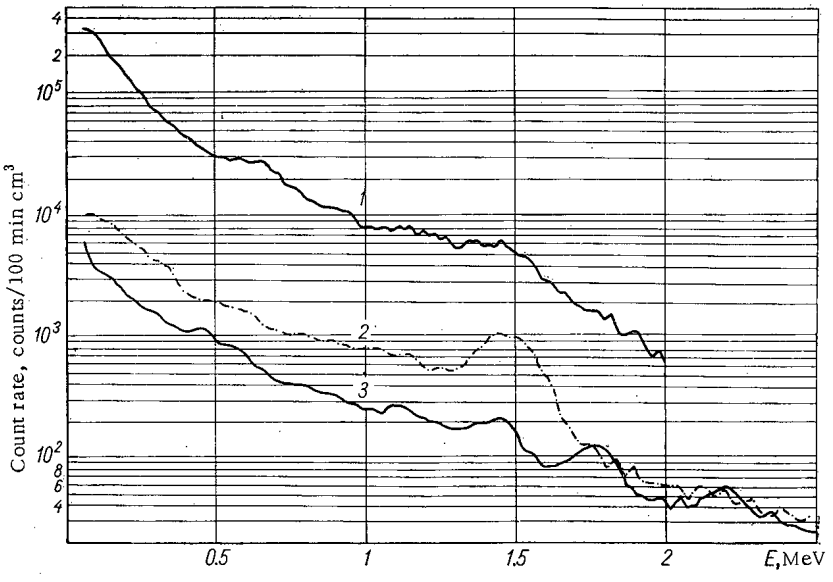

Fig. 1. Spectral scan of background in SZS experimental whole body counter. 1) Unshielded, crystal ∅ 100 ×70 mm; 2) gypsum shield in place, same crystal; 3) gypsum shield in place, crystal ∅ 125 ×100 mm.

State Center for Ionizing Radiation Shielding, Berlin-Feidrichshagen, Deutsche Demokratische Republik. Translated from Atomnaya Énergiya, Vol. 21, No. 4, pp. 311-312, October, 1966. Original article submitted April 12, 1966.

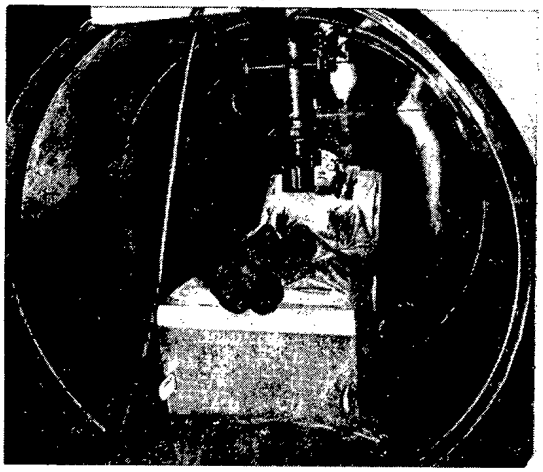

Fig. 2. Patient in position in SZS measuring chamber.

Gypsum Shield; γ-Ray Attenuation Factors

Crystal size, mm	Background in 0.09-3 MeV range, normalized to 1230 cm³ volume, in pulses/min	Attenuation factor for		
		0.1 MeV	1 MeV	1.5 MeV
⌀100 × 70	2595	30	11	5
⌀125 × 100	860	83	34	28

a NaI (Tl) crystal ϕ 125×100 mm optically coupled to an EMI-9530 QA photomultiplier tube of 127-mm cathode diameter; these components had an exceptionally low background. The measuring probe had a low potassium content (10^{-4}% to $2 \cdot 10^{-4}$% in the crystal; quartz-window photomultiplier tube) and excellent energy resolution. An aluminum window 50 μ thick allowed γ radiation through, so as to detect low-energy γ radiation and bremsstrahlung. An energy resolution of 9.1% was obtained, with the aid of a point source, for the Cs^{137} photopeak (661 keV). Voltage pulses taken from the photomultiplier output were passed through a transistor preamplifier and impressed across the input of a wideband amplifier, whose output pulses were presented in turn to a 100-channel pulse height analyzer fabricated by the Central Nuclear Research Institute (Rossendorf). The information so obtained was stored in a ferrite memory coupled to an automatic recorder.

The counter background spectra appear in Fig. 1. Spectra taken with crystals of different sizes were normalized with respect to data for the measuring probe with the ϕ 100×70 mm NaI (Tl) crystal. The count rates in different channels were converted to equal crystal volume (550 cm^3).

Attenuation factors for γ radiation in different energy regions are tabulated for both measuring probes. The integrated background is 0.71 pulses/min · cm^3 in the 0.090 to 3 MeV energy range. In contrast to the results of the first studies, peaks ascribable to γ emitted by RaC, a Ra^{226} daughter, were recorded in the background scans after the gypsum shield was set in place. The discrepancy in the data clearly imply an exceptionally low Ra^{226} content in the water used initially. Distilled water is therefore recommended for an additional gypsum shield. The restricted volume of the measuring chamber and the use of only one detector are determining factors in the measurement geometry. In general, either multiposition geometry [2] or inclined-chair geometry [3] can be resorted to. In most cases the inclined-chair geometry will be used in research studies. The distance from the crystal center to the back of the chair is 42 cm, or 41 cm to the seat of the chair. The chair was made of wood, to avoid the use of recently fabricated steel tubes. The placement of the chair in the measuring chamber produces no background enhancement, A view of the measuring chamber appears in Fig. 2.

The whole body counter described was fabricated to measure potassium and Cs^{137} after K^{42} calibration, on ten volunteers [4], and was then tried out on an anthropomorphic phantom filled with Cs^{137} solution. Potassium content and Cs^{137} content in the human organism was measured on over a hundred subjects.

LITERATURE CITED

1. K. Poulheim and H. Hoesselbarth, Health Physics, 11, 52, (1965); Atomnaya Énergiya, 19, 488 (1965).
2. C. Miller, Health Physics, 10, 1065 (1964).
3. C. Miller, Proc. of Second United Nation Intern. Conf. on the Peaceful Uses of Atomic Energy, Geneva, Unit. Nat., Vol. 23, p. 113 (1958).
4. K. Poulheim, H. Hoesselbarth, and V. Lossner, Determination of Natural Potassium Content in the Human Organism with the Aid of the SZS Experimental Whole Body Counter. Report delivered to the X Congress of the Medical Science Society of the German Democratic Republic (Leipzig, October 20-23 1965).

TEN YEARS OF THE DUBNA JOINT INSTITUTE FOR NUCLEAR RESEARCH

V. Biryukov

The Tenth Aniversary Session of the Learned Council of the Joint Institute for Nuclear Research was held May 31 through June 4, 1966; this was the XX session of the Learned Council. A full ten years have elapsed since the signing of the agreement in Moscow to set up this international scientific research center serving the socialist countries. Leading scientists of member-nations of the Joint Institute for Nuclear Research and diplomatic representatives of a number of countries were on hand for the XX session at Dubna.

Academician N. N. Bogolyubov, director of the JINR, surveyed the work of the Institute in the ten years of its existence in a report to the solemn anniversary session. At the time of its organization in 1956, the Institute comprised two laboratories of the Academy of Sciences of the USSR: the Nuclear-Problems Laboratory with its existing proton accelerator, the 680 MeV synchrocyclotron, and the High-Energy Laboratory, which at that time was working on adjustment of a new accelerator, the 10-GeV proton synchrotron (the "synchrophasotron"). A decision was soon made to set up three new laboratories: the Theoretical-Physics Laboratory, the Nuclear-Reactions Laboratory, and the Neutron-Physics Laboratory. The first half-decade saw the solution of the basic problems confronting the installation of large experimental facilities. The proton synchrotron began operating in 1957, and a powerful cyclotron accelerating multiply charged ions was commissioned in 1960. A pulsed fast reactor went into operation in the same year. The second half-decade of the Institute saw the successful implementation of and further improvements in experimental techniques and the development of experimental information processing systems incorporating electronic computers.

In ten years, the Joint Institute has become a major scientific center of worldwide renown, with many discoveries to its credit, and a program of diversified front-line research in experimental physics and advanced theoretical physics.

Scientists on the staff of the Nuclear-Problems Laboratory have made important contributions to the knowledge of nuclear forces through their many years of research on elastic and inelastic nucleon-nucleon scattering. The study of interactions involving π-mesons and nucleons has yielded highly reliable proofs of charge symmetry and charge invariance of nuclear forces. Synchrocyclotron experiments have confirmed the validity of the causality principle, of major importance for modern theory, down to distances on the scale of 10^{-13}cm. A proof of muon-electron symmetry was obtained and the validity of the principal tenets of the modern theory of universal weak interaction have been confirmed. Scientists working in this laboratory have establised the possibility of the existence of an electron neutrino and a muon neutrino, and have suggested an experiment to detect the latter. Some interesting effects were noted in the study of π-mesoatomic and μ-mesoatomic phenomena. Over 40 new nuclides have been discovered by research in nuclear spectroscopy and radiochemistry. The advances achieved by the laboratory in the theory and practive of high-current accelerators are widely acknowledged. It was in this laboratory that the first cyclotron with spatially varied magnetic field was built. The laboratory, which is the oldest one in the Institute, is directed by V. P. Dzhelepov, corresponding member of the USSR Academy of Sciences.

The second largest scientific body at Dubna is the High-Energy Laboratory, formerly headed by the late Academician V. I. Veksler. The production of particles of "cosmic" energies under laboratory conditions has placed in the hands of physicists a tool capable of greatly expanding and deepening research on the properties of elementary particles at high energies. A research program of wide scope on the production of mesons, nucleons, and hyperons, has led to some intriguing inferences on the

Translated from Atomnaya Énergiya, Vol.21, No.4, pp.313-315, October, 1966. Tenth Anniversary Session of the JINR Learned Council at Dubna.

nature of those reactions, and on the properties of particle interactions. The regularities established in the experiments have since been accounted for within the framework of several theoretical models. A new particle, the antisigma-minus-hyperon, has been discovered in proton synchrotron experiments, and its discovery has validated general theoretical predictions on the properties of particles. Many research projects have centered on the study of new particles, or resonances, some of which were first discovered by scientists attached to the High-Energy Laboratory. Subtle experimental techniques for studying nucleon structure have been elaborated here. Interest focuses particularly in a series of experiments on scattering of nucleons and π-mesons by nucleons at limiting small angles, and on back-scattering of π-mesons by nucleons, at angles close to 180°. The results provide experimental confirmation of fundamental points in modern theory.

Later on, N. N. Bogolyubov presented an account of the foundation and subsequent activities of three new laboratories in the Institute complex. As a result of efforts of member-nations of the JINR, in sending their scientists to Dubna for concentrated work, one of the largest centers in theoretical thought has materialized — the Theoretical Physics Laboratory. This laboratory is exerting a substantial influence on the development of this sector of world science. Scientists on the staff of this laboratory are working in the front line of contemporary theoretical physics. The staff is currently headed by D. I. Blokhintsev, corresponding member of the USSR Academy of Sciences.

A rigorous derivation of dispersion relations was arrived at Dubna, followed by concrete applications of dispersion relations, and experimental verification of the findings provided an answer to the basic question on the correctness of the fundamental concepts of current field theory. Research on particle interactions at high energies, one of the laboratory's activities, relies heavily on the general tenets of field theory. Experimental work connected with the development of a phenomenological theory have played an important role in the planning and interpretation of accelerator experiments. Many investigations by theoretical physicists have been related to the study of space-time geometry in the microcosmos, and to field-theory models and particle models. Attempts to make headway in the complicated problem of the enormous number of presently discovered particles have been undertaken in particle systematics research. Application of the theory of symmetries to particle structure have been notably successful in recent work. Great advances in nuclear theory have been achieved by laboratory scientists in these years. This research, based on the application of physical and mathematical techniques developed earlier in the theory of superfluidity and superconductivity to the study of complex nuclei, shed new light on many experimentally observed properties of nuclei.

Some important lines of research, such as the study of nuclear transformations induced by heavy ions, are being conducted at the Nuclear-Reactions Laboratory, which is headed by G. N. Flerov, corresponding member of the USSR Academy of Sciences. A major facility of this laboratory, the three-meter cyclotron, generates beams of different multiply charged ions (from boron to argon). In a short time span the staff scientists have completed some significant research, and have uncovered new physical phenomena. A significant advance was registered in the area of fusion and in the study of the physical and chemical properties of the far transuranium elements. New isotopes of elements 102 and 103 were synthesized in this laboratory. The new element 104 was discovered, and both physical and chemical identifications were achieved. Heavy ions were employed in the discovery of a new mode of radioactivity: proton decay of nuclei. The laboratory scientists have provided a theoretical basis for the concept of nuclei overrich in protons which emit a proton on decaying, and have since synthesized such nuclei. A new and intriguing phenomenon has been discovered: and abrupt increase (over 10^{20}-fold) in the probability of spontaneous fission of nuclei in an isomeric state. Many investigations involve studies of coulomb excitation of nuclei bombarded by heavy ions, as well as evaporation reactions and nucleon group transfer, fission reactions, and other topics.

The Neutron-Physics Laboratory is headed by I. M. Frank, corresponding member of the USSR Academy of Sciences. The pulsed reactor has proved a valuable research tool in the discovery of new experimental data on atomic and magnetic structure, in the study of the dynamics of liquids, crystals, and molecules with the aid of slow neutrons. This new tool has aided physicists in studying many interesting phenomena in liquids and crystals. Pulsed fast flux from the IBR reactor combined with long path lengths now set up conditions favoring the solution of various problems in the neutron spectrometry of nuclei. Research of broad scope and versatility has yielded unique information on the properties of levels of excited nuclei, and has smoothed the way for experiments with fissionable elements, for example. Physicists on the laboratory staff have had great success in attempts to develop an effective method for producing a polarized neutron beam by transmission of neutrons through a polarized proton

target. An electron accelerator (a microtron) has been built at the Neutron-Physics Laboratory in a collaborative undertaking with the Institute of Physics Problems of the USSR Academy of Sciences. It is now being employed as an injector adjunct to the reactor, increasing the accuracy of neutron spectrometric measurements ten-fold. Complex experimentation is being facilitated by a measurements center set up as adjunct to the laboratory, and capable of processing a huge volume of experimental information.

New experimental and theoretical research techniques in modern nuclear physics call for automation of experiments and the use of electronic computers to handle mathematical calculations of the utmost complexity. Direct coupling between physical analyzing facilities and computers has been successfully achieved in many cases. The measurements centers now in existence or being set up as laboratory adjuncts are now backed up by a Computing Center equipped with electronic computers. E. P. Zhidkov is in charge of the Computing Center. A lot of attention has been given to the development of automated experimental information processing methods and facilities at the Joint Instute.

In his concluding remarks, N. N. Bogolyubov gave an account of the international collaboration of the Joint Institute with nuclear research centers in many countries. Over the decade the Institute has published over 2500 brochures on the results of various scientific research projects and has sent them out to a mailing list of over 1000. Papers by scientists attached to the Institute have been dispatched to 36 countries throughout the world and have been published in many periodicals. The Joint Institute for Nuclear Research has entered into collaboration with scientific bodies in the member-nations of the Institute in carrying out about a hundred experimental and theoretical research projects. Each year, 200-odd specialists from member-nations of the Institute travel to Dubna to carry on joint work and to exchange experience. Physicists and engineers on the JINR staff travel to member-nations of the Institute to deliver lectures and conduct discussions on joint work projects. Each year, the Institute organizes over ten workshops on current topics in nuclear physics. JINR scientists participate in many international and national conferences. The scientific liaisons of the JINR with such leading scientific centers as CERN (Geneva), the Niels Bohr Institute (Copenhagen), the research centers Saclay and Orsay in France, are being continually expanded. A heavy value is placed on the developing collaboration between the Joint Institute at Dubna and the Institute of High Energy Physics at Serpukhov.

"The great international experiment begun at Dubna ten years ago has," in the words of N. N. Bogolyubov, "fully confirmed the correctness of the idea of combining the forces of scientists in the socialist countries."

A report by a group of scientist on the staff of the Nuclear Reactions Laboratory, presented a report to the XX session of the learned Council: I. Zvara, "Chemical properties of element 104 and confirmation of the discovery of element 104 by chemical methods" (I. Zvara et al., Atomnaya Énergiya, 21, 83 (1966)). The fact has been publicized that a team of physicists headed by G. N. Flerov first synthesized element 104 in this laboratory in 1964. Some delicate chemical research on the properties of the new element were completed here in 1966, employing an original high-speed procedure for continuous separation of the nuclear interaction products in high-temperature rapidly flowing gas streams. This method made possible a study of the chemical properties of the element using a small number of available 104 atoms, in a fraction of a second. The Learned Council awarded the JINR special first prize to the authors of this paper. Following the proposal of the Nuclear-Reactions Laboratory, the Learned Council passed a resolution assigning the name of I. V. Kurchatov to element 104 in memory of the outstanding services of Academician I. V. Kurchatov to the development of Soviet and world nuclear physics.

The Learned Council of the JINR confirmed the decision of the contest panel on the competition for JINR prizes on the most outstanding work on research and techniques in 1965. Ten research projects at the Institute were nominated for prizes. First prize was awarded for a cycle of papers on "The theory of polarized target reactions and the complete experiment," and two other prizes were awarded for "Synthesis and investigation of the properties of isotopes 102^{254} and 102^{256}," and "Experimental and theoretical research on the properties of K_2^0 -mesons." In addition, first and second prizes were awarded jointly for the study on technique entitled "Cycle of research on enhanced intensity and longer duration of the internal beam in the JINR synchrocyclotron," and the paper "The IBR [fast reactor] – microtron system."

THE THIRD ALL-UNION SEMINAR ON REFRACTORY COATINGS

N. N. Popov

The Third All-Union Seminar on Refractory Coatings, organized under the sponsorship of the I. V. Grebenshchikov Institute of Silicate Chemistry of the USSR Academy of Sciences, was held May 27-31, 1966 in Leningrad. 400-odd representatives from over 130 organizations took part in the proceedings, and 50 papers were heard and discussed.

New theorectical developments on physicochemical processes in the fabrication of protective coatings from melts and gaseous media were announced in papers by V. P. Elyutin, N. N. Rykalin, A. A. Appen, M. A. Maurakh, M. Kh Shorshorov, and others.

A report by A. I. Avgustinik and G. I Zhuravlev on the thermal stability of ceramic coatings was interesting from both theoretical and practical standpoints. There is a need for preliminary evaluation of the thermal stability of ceramic coatings because this property is one of the decisive factors in the choice of coating, and since many components and articles have to function under nonstationary heat conditions. The most correct approach, in the view of these authors, is to calculate the temperature fields in the coatings, and then to find the thermoelastic stresses and stress relaxation brought about by those fields through creep deformation of the materials. Solution of these basic problems opened the way for obtaining formulas with which to calculate temperature fields, stresses, and the allowable heating rate for refractory-coated articles.

Most of the papers submitted dealt with protective coatings applied to cast iron, steels, and chromium-nickel base alloys by a variety of methods (hardfacing, diffusion saturation of the metal surface, vapor deposition), determination of the corrosion resistance of coatings, and studies of the effect of coatings on the mechanical properties of steels and alloys.

G. V. Karpenko et al. described a pilot facility and procedure for diffusion-bonding coatings on steels by a vapor-phase technique in a hydrogen and HCl medium, determined the thermal stability of diffusion-bonded layers at various temperatures, demonstrated the effect of diffusion chrome-plating, vanadizing, calorizing, on the fatigue strength of 45 steel at room temperature and at elevated temperatures, and studied the change in the thermal conductivity of steel coated in any of the ways mentioned.

L. D. Svirskii and N. P. Sobol' performed some interesting studies on refractory coatings on unalloyed steels. They were able to produce a coating which offers decisive protection against oxidation on a long-term basis at 800°C temperature and which forms at a relatively low temperature; this coating was produced by exploiting the polyalkaline effect and a similar effect occurring when alkali earths are simultaneously introduced into enamel (ZnO: BaO = 1: 2.8).

E. A. Antonova showed that the strength of cermet coatings on Kh18N9T applied by enameling techniques is far higher for protection against scoring under dry friction conditions at 20° and 300°C than the strength of stellite G or stellite Ts. For example, scoring did not appear on the cermet coatings after 300 cycles had been completed, at 25 kg_{force}/cm^2 specific pressure and 300°C, whereas scoring appears on stellite Ts after only 100 cycles.

The effect of cermet coatings on the mechanical properties of steels (such as ÉI415 and ÉI572L steels) was discussed in a paper presented by V. N. Fedorov. The tensile strength of ÉI572L steel was pushed from 32.2 to 42.4 kg/mm^2 at 650°C by applying a cermet coating, i.e., a 25% increase. Tests for long-term strength at 650°C and $\sigma = 25$ kg/mm^2 showed that time to failure in unprotected steel and protected steel is 124 h and 5090 h respectively. The ceramic coating improved the fatigue strength of the steel 25% (for 10^7 cycles) and improved the thermal stability four-fold, i.e., it improved the performance of the steels at elevated temperatures.

A. A. Appen and S. S. Kayalova, by introducing nichrome powder into glass, were able to form a protective coating on steel which is superior to ordinary enamel coating in impact strength.

Translated from Atomnaya Énergiya, Vol. 21, No. 4, pp. 316-317, October, 1966.

M.V. Sazonova showed that coatings consisting of $MoSi_2$, SiC, and silicate adhesive, designed for protection of nonmetallic materials, exhibit excellent thermal stability of 1500°C in air. At the same time they are quite stable in certain aggressive media, such as boiling solutions of HCl, HNO_3, H_2SO_4, in an aluminum melt at 800°C, in H_2, N_2, and in superheated sulfur vapour at 1100°C. Glass-silicide coatings are stable in an NH_3 atmosphere at 1380°C. The external form of the coatings and their microstructure after protracted tests in these media undergo virtually no change.

Corrosion protection of piping was discussed by N.S. Gorbunov, T.M. Koval'chuk, et al. A coating which resists corrosion better than coatings applied by vapor-phase techniques was obtained by heat treating diffusion-bonded wet-process zinc coatings. Piping with exceptionally high corrosion strength was obtained by diffusion vacuum thermal chromizing.

Reports by N.S. Gorbunov, S.A. Klevtsur, Yu.V. Hrdina, et al. dealt with protective coatings applied to the surfaces of refractory metals and graphite. Protection of graphite and high-melting metals is achieved by coating the surface with a scale-resistant refractory compound ($MoSi_2$, SiC, Cr_3C_2, etc.)

Organosilicate materials are widely used in stress measurements for stress coatings, thanks to recent work by N.P. Kharitonov and colleagues, in protection of structural elements for current sources operated at high temperatures, for insulating thermoelectrode leads in microthermocouples measuring temperatures to 1000-1200°C. Thermography, thermogravimetry, mass spectroscopy, gas chromatography, and other research techniques have enabled N.A. Toropov, N.P. Kharitonov, V.A. Krotikov, et al. to establish the temperature range of basic transformations occurring in organosilicate materials at different temperatures (anywhere from 20° to 1600°C). It was shown that polyorganosiloxane molecules become grafted onto the surface of silicate particles in the fabrication of organosilicate materials, as a result of mechanical and chemical effects on the system. Organosilicate material acquires a spatial structure in which the inorganic components are bonded to the polymer base not by Van der Waals forces but by the formation of chemical linkages (this occurs in the 150-300°C range). Degradation of the framework of the polyorganosiloxane binder occurs at higher temperatures, as do some other processes, which nevertheless do not bring about mechanical destruction of the material. G. S. Pisarenko, V.E. Gorbatenko, and L.I. Gotlib provided information on various methods of testing coatings.

A decision was taken at the concluding session to publish the proceedings and to hold an anniversary All-Union seminar on refractory coatings which will be dedicated to the Fifty-Year Anniversary of Soviet power, in Leningrad May 1967.

SEMINAR ON APPLICATIONS OF RADIOISOTOPE TECHNIQUES AND RADIOISOTOPE DEVICES IN PROCESS CONTROL AND MONITORING IN THE PAPER, PULP, AND LUMBER INDUSTRY

V. Sinitsyn

The All-Union Combine Izotop, in collaboration with the Ministry of the Lumber, Paper and Pulp, and Wood Processing Industries of the USSR, and other organizations, sponsored a seminar in Riga, in May, 1966, on applications of radioisotope techniques and devices in monitoring and automatic control of technological processes in the paper and pulp and wood processing industries. The seminar attracted 270 representatives of industrial plants, research institutes, and production and design organizations. 22 reports were delivered, discussing various trends in the use of radioisotope techniques and instruments, certain aspects of radiation chemistry, and experience in the use of radioisotope techniques at individual plants.

A report on applications of radioisotope techniques and instrumentation in process control and monitoring in industry was given by V. I. Sinitsyn, engineer-in-chief of the All-Union Combine Izotop. E. P. Fesenko, representative of the Ministry of the Lumber, Paper and Pulp, and Wood Processing Industries of the USSR, reported on the positive experience gained in the use of radioisotope devices at various plants such as the Krasnogorod experimental paper combine, the Yuglavsk paper mill, the Lignums plywood plant in Riga, the "Riga" furniture works, and others.

Seminar participants manifested interest in a report by B. Ya. Varshava on shielding techniques in handling radioactive materials and radioisotope devices, on rules for the proper operation of radioisotope facilities, and on storage requirements for radioactive items.

Radioisotope neutralizers for eliminating charges of static electricity in the paper and wood processing industries were reported on by K. D. Pismannik, F. G. Portnov, B. M. Kashlinskii, and E. K. Ventskuz. Some papers discussed engineering data on the RRV radioisotope device designed for monitoring and control of a square meter of paper and cardboard sheet, and production-line experience with this device in the paper industry of the Latvian SSR.

V. I. Pankratov told of the outlook for applications of radioactive isotopes and radioisotope techniques in the paper and wood processing industries in the coming half-decade, and cited technical data and design details of instruments for measuring a square meter of paper and carboard sheet (the RBV-2 instrument).

Representatives of several paper plants shared experiences in using radioisotope weight control devices (RRV type for one square meter of paper sheet) and other radioisotope devices at their plants. All of them rated the RRV device very highly, stressing its simple design, ease of operation, reliable performance, and low cost. Tentative data supplied by the Krasnogorod experimental paper combine indicate that regular use of the RRV-63 isotope device on a single papermaking machine will save 58,000 rubles annually.

V. A. Yanushkovskii, director of the Riga branch of the All-Union radiation techniques research institute, delivered a report on a modularized system of radioisotope relay type gages (the AUS RRP line). The reporter cited examples of the use of the AUS RRP system in automatic process control and monitoring in the paper and pulp and wood processing industries.

E. P. Shpalte reported on a device with the combined function of measuring the weight of 1 m^2 of paper and cardboard sheet and measuring its moisture, for application in a wide variety of high-speed paper and cardboard manufacturing machines. A device capable of handling a maximum sheet width of 8.5m scans the width of the sheet to sense and measure moisture and weight per square meter. The device has a built-in computer for calculating the dry weight of the paper and cardboard sheet. The

Translated from Atomnaya Énergiya, Vol. 21, No. 4, p. 318, October, 1966.

components of the instrument are mounted on the control panel of the papermaking machine they service. Large-size square-meter weight and moisture gages can be mounted outboard.

Several reports dealt with radiation-chemical processes in the production of wood and plastic materials. V. L. Karpov mentioned some wood-plastic composites made from inexpensive grades of lumber and monomers which show enhanced compressive strength and hardness, take up water at a markedly slow rate, and as a result are recalcitrant to change induced by ambient conditions. The reporter cited comparative characteristics of ordinary and modified lumber.

Operating experience in the use of radioisotope instrumentation in paper and pulp plants and in wood processing plants was divulged by I. T. Zhuk.

The participants of the seminar adopted a resolution stressing the important place of radioisotope techniques and instruments in the solution of automatic process control and monitoring problems encountered in the paper and pulp and lumber industries.

THE RG-1 GEOLOGICAL RESEARCH REACTOR

Yu. M Bulkin, A. D. Zhirnov, L. V. Konstantinov,
V. A. Nikolaev, I. A. Stenbok, V. S. Lobanov,
and A. M. Benevolenskii

The RG-1 pool type reactor, 5 kW(th), was built as a radioisotope production reactor (producing isotopes with different half-lives), and is also designed for activation analysis on technological samples and geological specimens, and for evaluation of the absorbing properties of solids, liquids, and alloys.

New engineering research techniques employing radioactive isotopes can be developed on the basis of a complex of laboratories housed in a typical RG-1 reactor building (facilities included in the complex are: a radiochemical laboratory, a laboratory for precision radiometric measurements, the reactor hall, and miscellaneous specialized rooms).

The RG-1 reactor lends itself to research purposes. There is a choice of several core and reflector arrangements differing in composition, geometry, or both.

Figures 1 and 2 show longitudinal and transverse cross sections through the RG-1 reactor.

The reactor core, 450 mm in diameter and 500 mm high, can accommodate as many as 72 graphite-reflected fuel assemblies. The assemblies consists of seven standard rod type fuel elements, aluminum-clad and 10 mm in diameter. The fuel meat is UO_2 (10% enrichment), and the critical charge is 2.6 kg U^{235}

The graphite reflector is assembled from separate aluminum-jacketed graphite blocks. The core -reflector complex rests on the bottom of the water-filled aluminum vessel. The vessel diameter is 1500 mm and the height is 3500 mm. The vessel is covered on top by a cast iron shield plug 460 mm thick.

The reactor control rod elements are four hollow cylindrical boron steel rods (two scram rods, one automatic control rod, one manual control rod).

The following accessories are available for experiments: 1) pneumatic rabbit shuttle: two channels (one for thermal neutron work, the other for fast neutronwork); 2) a centrally placed experimental channel 39 mm in diameter with thermal flux of 10^{11} neutrons/cm^2 sec; 3) an experimental channel on the core periphery, 39 mm in diameter with thermal flux $6 \cdot 10^{10}$ neutrons/cm^2 sec; 4) two channels 72 mm in diameter and four channels 52 mm in diameter embedded in the graphite reflector, with thermal flux $2 \cdot 10^{10}$ neutrons/cm^2 sec; 5) one experimental channel 72 mm in diameter situated in the second row of graphite reflector blocks.

At 5 kW, the Na^{24} capacity of the RG-1 reactor with the two core experimental channels charged with standard capsules (diameter 28 mm, height 125 mm) filled with saturated NaCl solution is 120 mCi (two capsules) in six-hour runs; the Na^{24} capacity can be stepped up to 290 mCi (six capsules) by using Na_2CO_3 solution. The Mn^{56} capacity is 2600 mCi (eight capsules) when saturated $KMnO_4$ solution is employed; the activity of a single capsule can run to 400 mCi.

A special transfer system connecting the headroom above the reactor to the laboratory is provided for safe and rapid delivery of isotopes or specimens from the experimental channels to the laboratory; the specimens or isotopes are discharged in specially designed glove boxes where the specimens can undergo further processing.

A remote-controlled handling grip, transport container, and rotating plug are used to open the experimental channels and for transfer of irradiated specimens to the reloading and discharge unit; these operations are carried out underneath the shield slab. A special lead glass viewing window is mounted on the rotating plug for visual monitoring of the specimen transfer process; the core can be

Translated from Atomnaya Énergiya, Vol. 21, No. 4, pp. 319-321, October, 1966.

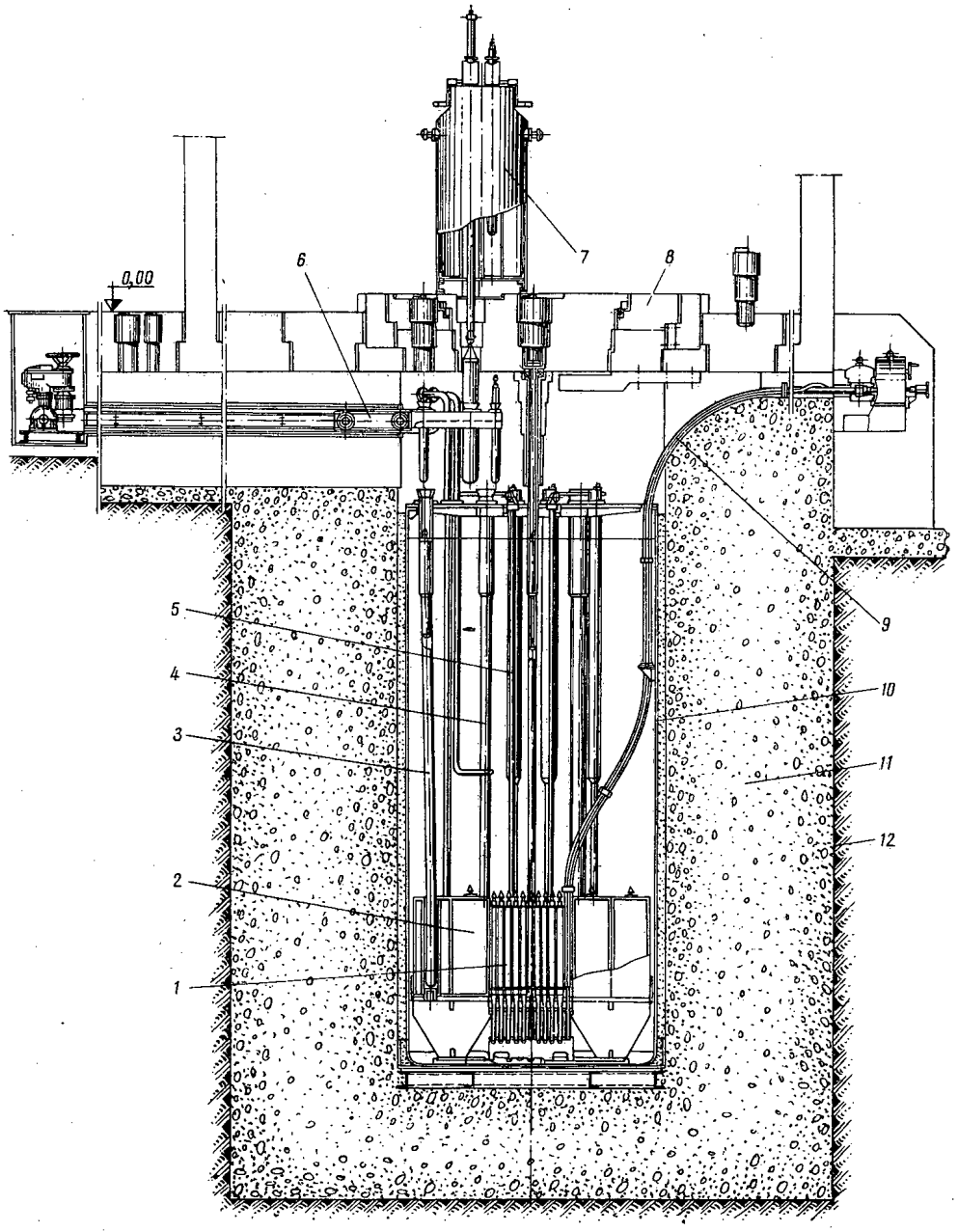

Fig. 1. Longitudinal section through the RG-1 reactor. 1) Core; 2) graphite reflector; 3) experimental channel; 4) ionization chamber channel; 5) control rod channel; 6) reloading and discharge unit; 7) fuel transport container; 8) shield slab; 9) pneumatic rabbit shuttle; 10) reactor pressure vessel; 11) biological shield; 12) hydraulic seal.

kept under observation while the reactor is in operation, if necessary, and two luminaires are positioned in the reactor tank beneath the shield slab, for underwater illumination.

The experimental channels with automatic pneumatic devices allow transfer of specimens to the highest neutron flux zone and back to a receiving vessel.

Planned reactor shutdowns are carried out manually by an operator at the control panel, by inserting poison rods into the core. The rods can be inserted automatically in a scram situation.

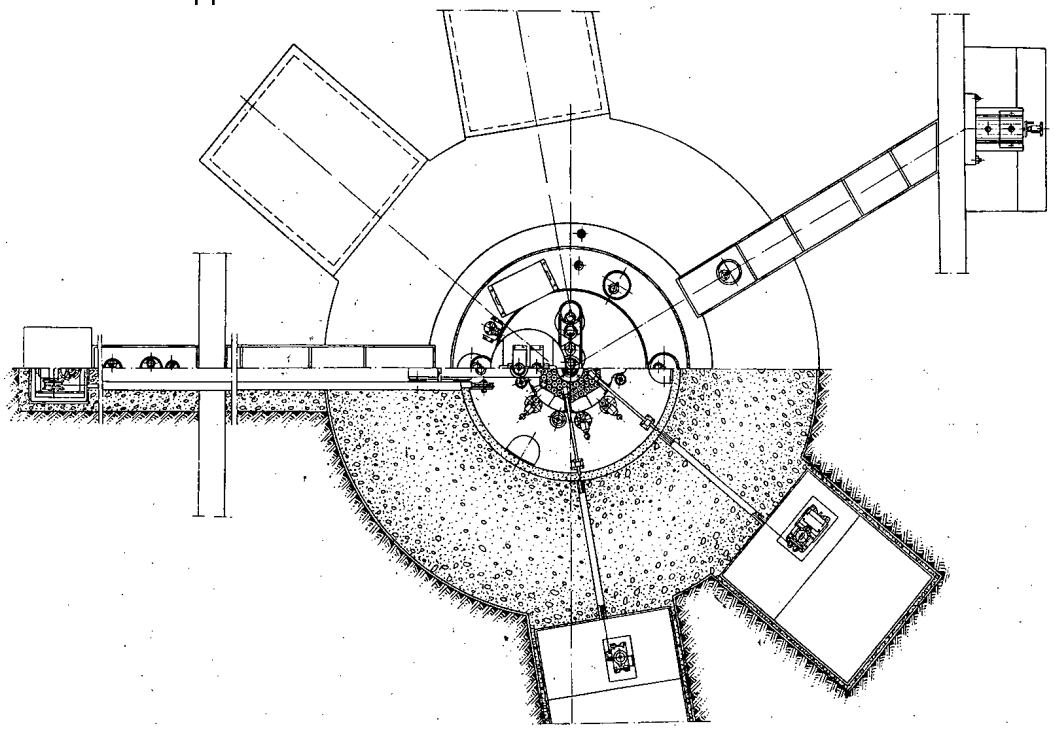

Fig. 2. Transverse cross section (view from above) through the RG-1 reactor facility.

The negative temperature coefficient of reactivity is responsible for ease of reactor self regulation and intrinsic reactor safety, while the control rod system assures safe and reliable operation.

THE SO-1 NEUTRON BOOSTER

Yu. M. Bulkin, A. D. Zhirnov, L. V. Konstantinov,
V. A. Nikolaev, I. Kh. Ganev, V. S. Lobanov
and B. S. Poppel'

There are many reasons for the recent intensification of interest in neutron boosters, which are subcritical nuclear facilities. The neutron booster makes its possible to organize activation analysis studies of isotopes in different materials, liquids, solutions, and other substances. Activation analysis can be used, as one example, to determine trace impurities of certain elements in semiconducting materials.

The neutron booster is particularly suited to geological work in prospecting and exploration of ore deposits, in prospecting and exploration of oil fields and natural gas fields, and in some other branches of the national economy where neutron fluxes on the order of 10^7 to 10^8 neutrons/cm^2 sec are useful in research.

Subcritical nuclear facilities of this type are also capable of meeting various needs in industry and agriculture, in medical institutions, geological field crews, cases where short-lived radioisotopes needed in the work are currently expensive or altogether unavailable, as is most often the case.

The diagram shows a longitudinal section through a neutron booster built by the present authors. A team headed by N.V. Zvonov and T.A. Lopovok has done similar design work on neutron boosters.

The basic physical and engineering parameters of a movable homogeneous solid subcritical SO-1 booster using thermal neutrons are:

Power	0.5 W
Effective neutron multiplication factor	0.996
Core center peak flux:	
thermal flux:	$2.5 \cdot 10^7$ neutrons/cm^2 sec
fast flux:	$7 \cdot 10^7$ neutrons/cm^2 sec
Thermal flux at experimental devices	10^7 neutrons/cm^2 sec
Fuel	Uranium dioxide dispersed in polyethylene matrix
Charge (U^{235})	900 g
Uranium enrichment	36%
Neutron moderator	Polyethylene
Neutron reflector	Graphite-polyethylene composite
Biological shield	Lead, paraffin with 5% boron carbide and water
Experimental devices	Three vertical channels 52 mm in diameter, one 51 mm diameter horizontal channel equipped with pneumatic shuttle
Control	65 mCi Po-Be neutron source; one boron steel rod

Translated from Atomnaya Énergiya, Vol. 21, No. 4, pp. 321-322, October, 1966.

Dimensions:	
diameter	2025 mm
weight	4650 mm (with reloading mechanism rod in extreme position; rod travel 1360 mm)
Weight	
in stationary position	11 tons
in transport position (minus water)	8 tons
maximum weight of any one component assembly	not more than 2 tons

The core of the SO-1 neutron booster consists of fuel elements shaped as cylindrical disks 270 mm in diameter. The center of a disk 240 mm across is occupied by a uranium-polyethylene mixture, and the periphery is made of pure polyethylene. Each fuel element is jacketed in a leaktight polyethlyene film to keep the uranium-polyethylene fuel composition isolated from the surroundings.

The neutron booster core formed of these fuel elements is placed in a specially fabricated aluminum vessel.

A vertical channel 24 mm in diameter is located at the geometric center of the core vessel, and its function is to hold in place isotope neutron sources and an absorbing rod rigidly coupled to it.

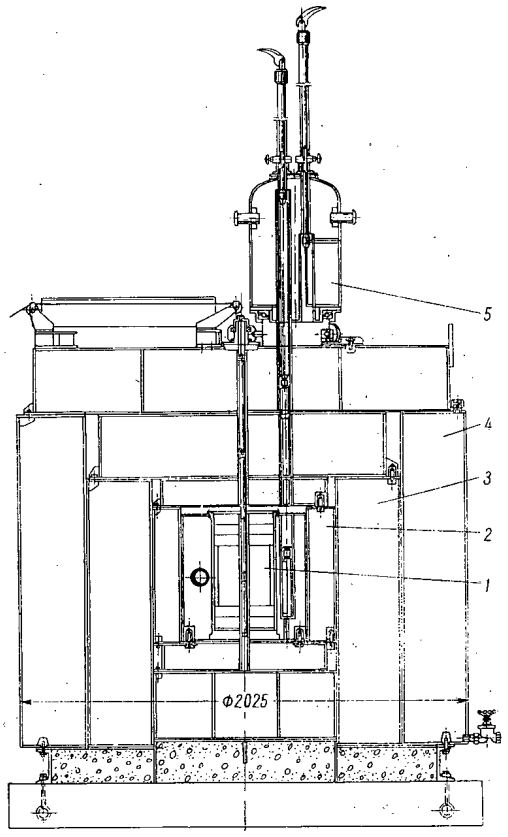

Longitudinal cross section through SO-1 neutron booster. 1) Core; 2) lead shield; 3) paraffin shield; 4) water shield; 5) reloading mechanism.

The multiplying section of the core is surrounded on all sides by a neutron reflector. The SO-1 reflector is made of graphite-polyethylene composite to raise the thermal neutron emission level at points where experimental devices are positioned. The total reflector thickness is 150 mm. The first reflector layer, 15 mm thick, is the peripheral polyethelene annulus around the fuel element. The second reflector layer is graphite 115 mm thick, and the third layer is polyethylene in aluminum cladding for ease in assembly and dismantling.

All of the experimental devices belonging to the neutron multiplier are situated in the graphite reflector zone. This arrangement is due to the presence of a weakly varying thermal neutron field in this zone. A special sample loading and unloading device servicing the vertical experimental channels is mounted above the biological shield so that samples can be transferred while the neutron booster is in operation.

A horizontal channel outfitted with a pneumatic rabbit shuttle is available in the reflector zone for production of short-lived isotopes. By changing the direction of flow of compressed gas through actuating a pneumatic distributor valve, a sample placed in a special shuttle can be passed automatically along the transfer channel to the reflector, and, after being irradiated, can be shuttled back to the receiver. The extreme shuttle position in the pneumatic tube is fixed by a microswitch. This sends an electric signal to the control panel, where a signal lamp is flashed on.

Samples can be irradiated by either thermal or fast

neutrons in the pneumatic shuttle channel. This is accomplished by using some shuttles clad with aluminum and the remaining ones clad with cadmium on the inside.

The SO-1 neutron booster is controlled by an operator stationed at the control panel where he has convenient access to all the necessary monitoring and control apparatus.

The neutron radiation level in the SO-1 critical facility can be varied by remote control from the control desk by moving the neutron source in the core and with it the absorbing rod rigidly coupled to it (this operation is done manually with the aid of a small capstan).

Neutron radiation in the SO-1 facility is measured by two ionization chambers placed in the reflector region in two special sealed suspension mounts. Two microammeters measure the ionization chamber currents.

The modular design of the SO-1 neutron booster and its compact size recommend it for use in practically any heated enclosure suitable for work with radioactive radiations. The air temperature in the room or enclosure can be from 5° to 40°C at up to 80% air humidity. When required, the SO-1 neutron booster facility can be transported in its entirety on a truck of not less than 10 tons carrying capacity, or on several trucks of lesser capacity.

Its simple control features, the elimination of any possibility of runaway during operation, mobility, and , no less important, the ease with which it can be fabricated, give it great promise as a workhouse tool in many areas of the national economy.

RADIOACTIVE ISOTOPES IN MACHINE-TOOL WORK

V. Sinitsyn

The USSR Ministry of construction, highway, and civil engineering machinery, in collaboration with the All-Union "Izotop" Organization, sponsored a seminar in Moscow in June, 1966 on applications of radioisotope techniques and devices in automatic process control and monitoring in the fabrication and operation of construction machinery, highway machinery, and public works machinery. The seminar attracted over a hundred representatives of industrial plants, research institutes, and design organizations. The seminar audience heard 13 reports.

A report by V. A. Nikiforov, representing the Ministry of construction, highway, and civil engineering machinery of the USSR, took note of the use of radioactive isotopes by research organizations and industrial plants in this branch of industry, a practice which already has a ten-year history. Over 40 plants under the Ministry's jurisdiction are already making successful use of radiation techniques in their work. A considerable expansion of research work in this area is scheduled for 1966, and plant operations will be followed up to pinpoint those sectors where installation of radioisotope equipment could yield impressive engineering and cost benefits.

A report on the status and future outlook of the use of radioisotope techniques and instruments in scientific research, and in automatic process control and monitoring in machinery design and fabrication was delivered by V. I. Sinitsyn (All-Union "Izotop").

A. G. Sul'kin (All-Union Radiation Techniques Research Institute) informed the seminar audience of new developments in γ-ray equipment for nondestructive testing, and experience in γ-ray flaw monitoring and detection in machine manufacture.

A radioactive tracer study of wear on parts, with measures to lengthen the service life of internal combustion engine parts, was reported by D. G. Tochil'nikov (Leningrad waterworks institute).

G. I. Gil'man ("Ekonomaizer" boilerworks, Leningrad) shared his plant's experience in the utilization of radioactive level gases in a foundry pneumatic conveying system which is automated. A. E. Artes, a representative of the Moscow machine-tool institute , discussed applications for radioisotope devices in press and die metalworking production.

V. A. Rikhter (All-Union research institute for construction and highway machinery) shed light on some promising applications of quantity-manufactured radioisotope instruments, in his report entitled "Applications of radioisotope techniques and instruments in highway and construction machinery systems." The reporter mentioned γ-ray electronic relay gages of all types, designed to record the presence or absence of material in the space monitored, and also as tools in automating loading and discharge of free-flowing materials and fluids. γ-ray gages can be used successfully in automated monitoring of charge level in stone crushing equipment, in automation of movement of materials on belt conveyor lines, level gaging of material in hoppers and closed vessels of different geometrical dimensions and configuration. γ-ray electronic conveyor scales can be used in continuous contactless weighing of non-ore materials on belt conveyors.

V. V. Misozhnikov reported on experience in the use of radioisotope techniques and devices at the Moscow carburator plant. M. I. Tolokonnikov cited some data on production-line use of radioisotope equipment at the Likhachev automative plant in Moscow.

In their discussion, the participants noted that radioisotope devices are effective tools for raising labor productivity, cutting down on the number of servicing personnel, and curtailing the amounts of raw materials going into production.

Translated from Atomnaya Énergiya, Vol.21, No.4, pp. 325-326, October, 1966.

Plants were also encouraged to make use of radioisotope devices and techniques in automation and monitoring of such industrial processes as loading charge in cupola furnaces, distributing molding sands and molding mixes to appropriate points in foundries, maintaining electrolyte level constant in electroplating baths, stocktaking and inventorying, contactless thickness monitoring of nonmetallic materials in coating processes (coating applies to nonmetallic base), in metal plating and application of paints and surface coating finishes, continuous weighing and automatic batching of free-flowing bulk materials, and other applications. Radioisotope techniques and devices have a special role cut out for them in improving the reliability and lengthening the operating life of earthdigging machinery, in studies of the nature and degree of wear on cutting edges of tools biting into soils of different classes, and in improving the design of excavating machinery.

11TH SESSION OF TEAM NO. 1, PERMANENT COMMISSION OF THE COUNCIL FOR MUTUAL ECONOMIC AID [COMECON] ON PEACEFUL USES OF ATOMIC ENERGY

A. Moskvichev

The 11th session of team No. 1 (on nucleonic instrumentation) of the COMECON Permanent Commission of Peaceful Uses of Atomic Energy was held in Warsaw, April 12-18, 1966.

In accordance with the agenda adopted, the Commission discussed specialization in the production of radioisotope instruments, standardization of methods for testing radioisotope relay-type devices, and standardization of components in gas-discharge counters.

The following materials were prepared for the regularly scheduled session of the COMECON Permanent Commission: 1) a list of technical parameters for suggestions on specialization in the fabrication of radioisotope devices, 2) recommendations on standardization of methods for testing radioisotope relay type gages, 3) recommendations on standardization of gas-discharge counter components (flexible leads, lead caps, coaxial base and socket for connecting up counters), 4) recommendations on standardization of outer diameters of cylindrical detector units for work with ionizing radiations.

The session also discussed the outline and format of a consolidated catalog of nucleonic instruments manufactured in COMECON countries. Specialists in the German Democratic Republic will work on publication of this catalog, in collaboration with the COMECON secretariat.

Translated from Atomnaya Énergiya, Vol. 21, No. 4, p. 326, October, 1966.

ITALIAN POWER REACTOR AND NUCLEAR POWER PLANT SPECIALISTS VISIT THE USSR*

A delegation of Italian specialists in the field of power reactors and nuclear-fueled power generating stations visited the USSR May 23 through May 29, 1966. The delegation included Professors M. Silvestri, A. Pedretti, F. Pierantoni, D. Foganogliolo, S. Villani, I. Casagrande, and D. Naschi.

The delegation visited the Obninsk Power Physics Institute, the Atomic Reactor Research Institute in Melekess, and the I. V. Kurchatov Beloyarsk nuclear power station in the Sverdlovsk district.

The guests were familiarized with the BR-5 fast experimental reactor, the physical critical assembly for investigating the neutron physics characteristics of the BFS line of fast reactors with the BR-1 reactor, and the sodium laboratory at the Power Physics Institute.

At Melekess, the Italian specialists visited the experimental power facility with its VK-50 boiling water reactor and critical test loop, where many reactor physics studies are in progress.

At the Beloyarsk power station, they visited the central hall, the machine hall, and inspected the control panel and the health physics monitoring panel.

The Italian scientists had a chance to converse with Soviet scientists and specialists in their fields, and contributed some interesting information in general discussions on the work they are now conducting in Italy in power reactor design. The Soviet colleagues also showed interest in the experience accumulated in Italy in the operation of the Italian nuclear power stations Garigliano (river), Trino-Vercellese, and Latina.

The Italian guests were very much interested in the current fast reactor research in the Soviet Union, and in future plans along those lines.

BELGIAN AND NETHERLANDS SPECIALISTS ON RESEARCH REACTORS VISIT THE USSR*

E. Karelin

A delegation of Belgian and Dutch scientists working in the field of nuclear research reactors visited the Soviet Union in June 1966, under the terms of an agreement arrived at between the USSR State Committee on Peaceful Uses of Atomic Energy and reactor research centers in Belgium and the Netherlands. The delegation was headed up by G. Snepvangers.

In the course of their visit, the members of the delegation stopped at the I. V. Kurchatov Institute of Atomic Energy and the Institute of Theoretical and Experimental Physics in Moscow, the Atomic Reactor Research Institute in Melkess, the Power Physics Institute in Obninsk, the Leningrad Physics and Engineering Institute, and the Joint Institute for Nuclear Research. The guests inspected the SM-2, MR, IBR reactors, the "Romashka" facility, and the construction site of the MIR reactor.

The members of the delegation paid close attention to the question of utilization of research reactors in the USSR, with particular interest in test-loop investigations of fuel elements, and in power reactor materials. The Belgian and Dutch scientists displayed keen interest in research on fast reactor fuels and structural materials.

* Translated from Atomnaya Énergiya, Volume 21, No. 4, p. 326, October, 1966.

Fruitful discussions on various aspects of reactor design, utilization of research reactors, neutron physics research, and related topics, were held in the course of visits to various reactor centers in the USSR.

Members of the delegation were deeply impressed by the volume of research in progress at the SM-2 and MR reactor facilities. They took special note of the rapid progress in construction of experimental test loops at the MR reactor facility, and the swift pace of construction and rigging work at the MIR site.

They expressed high opinions of the redesigned IRT reactor at the Institute of Atomic Energy, and showed a favorable response to the work going on in the heat transfer laboratory of the Power Physics Institute.

The advantage in doing away with reactor containment shells, as is the USSR practice, was stressed in the discussions. Note was made of the stringent radiation safety requirements, their observance in all facilities and research centers. The delegation expressed approval of further development in collaboration in the field of research reactors and their utilization.

In his remarks at a talk at the end of their stay in the USSR, G. Snepvangers, speaking in the name of all members of the delegation in a reception at the State Committe on Peaceful Uses of Atomic Energy, expressed great satisfaction with the visit, and took special note of the hospitality of their Soviet colleagues and of the benefit they gained from the discussions.

BIBLIOGRAPHY

G.E. Brown. Unified Theory of Nuclear Models. Amsterdam, North-Holland, 178 p, 1964. *

G. E. Brown, a renowned specialist on the theory of the nucleus, now working at the Niels Bohr Institute in Copenhagen, has written a book based on a lecture course which he has been giving in recent years in various nuclear physics schools and universities, discussing the various nuclear models from a unified point of view. The shell model, the collective model with nucleon pairing effects taken into account, and the optical model are discussed. An extension of the Hartree-Fok method to the theory of the nucleus lies at the basis of his treatment. Many topics are discussed in this book, and in our view the author has been successful in getting across the ideas underlying the models of the nucleus enumerated.

The author has shown the way to a systematic application of the concepts of the self-consistent field expressed in terms of the Hartree-Fok method. Single-particle excitations of the nucleus are discussed, vibrational degrees of freedom of the nucleus are described, and another topic covered is the ground states of nonspherical nuclei as constructed by the Hartree-Fok method. Moments of inertia are calculated. A special chapter takes up pair correlations in nuclei. Finally, the author discusses the optical model of the nucleus and attempts to sketch out its range of applicability.

The bibliography supplied by the author must be supplemented with references to the innumerable contributions by Soviet authors on the theory of the nucleus.

On the whole, the book will be a useful reference stating a definite viewpoint on the theory of the nucleus.

E. N. da C. Andrade. Rutherford and the Nature of the Atom. N. Y., Anchor Books, Doubleday, 218 p, 1964. *

This book, written by one of Rutherford's disciples, is a scientific biography of the founder of the modern model of the atom. The chronological treatment is combined with a fairly thorough lucid description of the essence of Rutherford's scientific contributions in different periods of his life. The book ends with a subject and author index.

The Discovery of Radioactivity and Transmutation. Edited and Commented on by A. Romer. N. Y., Dover, (Classics of Science, Vol. 2), 234 p, 1965. *

This book is a collection of original papers of Becquerel, Pierre and Marie Curie, Rutherford, Soddey, and others, published in the 1896-1905 decade. The range of material in this second volume in

* Translated from Atomnaya Énergiya, Vol. 21, No. 4, p.327, October, 1966.

the recently initiated "Classics of Science" series covers the discovery of radioactivity and of families of naturally radioactive substances. All the papers are published in English, whatever the original language. The collection is prefaced by a brief introduction more in the nature of a historical reference. Articles are accompanied by the necessary scientific commentary. The book ends with a subject and author index.

J. M. Daniels. Oriented Nuclei. Polarized Targets and Beams. N. Y., Academic, XII + 278 p. 1965. *

The seven chapters of this book present a detailed treatment of the present state of the problem of production of nuclei oriented preferentially in one position (in terms of spin direction). A brief introduction (Chapter 1) is followed by Chapter 2 on methods of orienting nuclei through thermal equilibrium. Chapter 3 discusses nonthermal equilibrium methods, and Chapter 4 deals with the requisite experimental technique (emphasis placed on cryogenic techniques). Methods of producing beams of polarized neutrons, protons, deuterons, tritons, and γ-rays are dealt with in Chapter 5. Chapter 6 describes sources of polarized ions for use in modern charged particle accelerators. The book ends with apparticularly extensive section (Chapter 7) on experiments with oriented nuclei.

Appendices offer a detailed list of literature (covering 16 pages of text), plus a subject index and authors index.

K. G. Steffen. High Energy Beam Optics. Monographs and Texts in Physics and Astronomy. Vol. XVII. N. Y., Interscience, 212 p, 1965. *

This review book consists of four parts of approximately equal volume devoted respectively to calculations of the trajectories of individual high-energy charged particles in quadrupole systems (Chapter 1, 42 references), deflecting magnets (Chapter 2, 21 references), multilayered systems and spectrometers (Chapter 3, 32 references), and the behavior of multiparticle beams in focusing devices (Chapter 4, 34 references). A concise subject index is appended to the monograph.

* Translated from Atomnaya Énergiya, Vol.21, No.4, p.327, October, 1966.

Industrial Atomic Energy Uses, Hazards and Controls,* Vols. 1-3. N. Y., Rider Publ., Vol. 1, 1965. Development and Basic Concepts. 142 p, Vol. 2. Instrumentation, Biological Effects and Radiation Protection. 166 p, Vol. 3. Impact on the Community. 116 p.

This three-volume set is intended for engineers who have no special training in nuclear physics. The first volume provides information on the development of nuclear power and applications of nuclear energy in industry and in science. Reactors and accelerators are described in popular style. The second volume is a manual on radiation shielding. Basic rules for safety, critical exposure levels for personnel, and radiation control measures are included and explained. The third volume offers the reader data on the possible effects of a large-scale nuclear facility on the surounding region and proper measures for radiation monitoring and protection. This volume gives special attention to disposal of radioactive wastes from nuclear reactors. Each volume ends with glossary and subject index. The third volume offers an extensive list of recommended literature.

D. O. Woodbury. Atoms for Peace.† N Y., Dodd, Mead, 276 p, 1965.

This is a book on nuclear power and on various aspects of the utilization of radioactive isotopes, written by a well-known American popular science writer.

S. J. Pearson. Spravochnik po interpretatsii dannykh karotazha. Russian translation [of: Manual for Interpreting Well Logging Data]. Moscow, Nedra press, 414 p. 1966. †

A brief systematic description of modern techniques for oil field and geophysical studies of profiles in oil wells and gas wells is given in this book. Chapter 15 gives the reader information on γ-ray well logging (measurements of natural radioactivity of rock over the well profile), Chapter 16 gives information on γ-γ well logging (measurements of scattered radiaition from a Co^{60} source lowered down a well with a detector shielded from direct radiation).

Several types of neutron logging methods are outlined in the quite detailed Chapter 17. Chapter 18 cites data on nuclear magnetic logging.

---

* Translated from Atomnaya Énergiya, Vol.21, No.4, pp.327-328, October, 1966.

† Translated from Atomnaya Énergiya, Vol.21, No.4, p. 328, October, 1966.

R. W. Bassard and R. D. Delaner. Fundamentals of Nuclear Flight. N. Y., McGraw-Hill, 454 p. 1965.*

This book is based on a lecture course given by the authors at the University of California, and consists of seven chapters. A short introduction (Chapter 1) describing various principles underlying the utilization of atomic energy in rocket propulsion is followed by Chapter 2 on the principles underlying calculation of the motion of bodies of variable mass. Heat transfer and mass flow are the subject matter of Chapter 3. Chapter 4 on physical processes in reactor cores follows. Chapter 5 treats penetrating radiations and shielding. Chapter 6 gives information on spacecraft materials. Chapter 7 discusses the design principles of reactors and spacecraft nuclear power plants. Appendices list useful physical constants, tables of Bessel functions, and multigroup constants, for reactor calculations. The book ends with a subject index.

R. P. Haviland and C. M. House. Handbook of Satellites and Space Vehicles. Princeton, New Jersey, Van Nostrand, XVI+457 p, 1965.*

The handbook deals with various aspects of the design, building, and shielding of artificial satellites. Section 8, "The space surrounding the earth," contains information on primary cosmic radiation and the radiation belts encircling the earth. Section 11, "Spacecraft materials," give data on the radiation stability of materials used and on principles for shielding against ionizing radiations. Section 17, "Man in space," lists values of doses of ionizing radiation responsible for specified biological effects, and critical tolerance exposure doses based on USAEC rules.

J. J. Scavullo and F. J. Paul. Aerospace Ranges Instrumentation. Princeton, New Jersey, Van Nostrand, XVI+458 p, 1965. *

This book, one of a series entitled "Design principles of guided missiles," gives a detailed description of the instrumentation on artificial satellites and spacecraft. A brief introduction leads into the seven basic chapters of the monograph. Chapter 1 contains information on design principles and applications of the various instruments. Chapter 2 concentrates data on optical systems and photographic techniques. Instruments for telemetering analysis and monitoring of flight performance are described in Chapter 3. Chapter 4 offers the reader exhaustive data on electronic equipment used in measuring the elements of a trajectory. Methods for processing information are covered by Chapter 5. Chapter 6 discusses information on telecommunication systems. The concluding Chapter 7 deals with precision in measurements, when using instruments remote from the observer. A detailed subject index is appended.

---

* Translated from Atomnaya Énergiya, Vol.21, No.4, p.328, October, 1966.

Space Exploration and the Solar System.* Proceedings of the Enrico Fermi International School of Physics. Course XXIV. Edited by B. Rossi. N. Y., Academic, 312 p, 1964.

This book constitutes the complete text of a lecture course on space physics given and published at the famous Enrico Fermi International School of Physics in Italy. In addition to a brief preface by B. Rossi, organizer of the course, the book publishes nine papers by front-rank investigators. The first two papers give an introduction to plasma physics and a mathematical description of the motion of charged particles in a magnetic field. The next three papers provide information on the structure of the inner planets in the solar system, on phenomena occurring in the photosphere, chromosphere, the solar corona, and in the interplanetary medium. A paper by J. Van Allen, written in collaboration with V. Lean, on results of observations of solar cosmic radiation from October 1959 through February 1961, with the aid of the Explorer VII satellite, takes up a lot of space. The two last sections of the book contain lectures on the atmospheres and high-energy emissions of the moon and of the other planets in the solar system.

Space Exploration.† Edited by D. P. Le Galley and J. W. McKee. N. Y., McGraw-Hill, 468 p, 1964.

This is a consistent treatment of physics and engineering problems to be resolved in conquering outer space. It consists of 15 chapters written by a panel of specialists. The monograph opens with a chapter on the scientific and engineering results of artificial satellite launchings and space rocket launchings in the USA and the USSR. The second section surveys cosmology and relativity briefly and lucidly. Data on the earth's nearest planetrary neighbors, Mars and Venus, appear in Chapter 3. Chapter 4 on the effects of solar flares on the radiation environment of the earth and on radiation in interplanetary space is of special interest. Astrodynamics, including orbit calculations and navigation problems, are covered in Chapter 5. Spacecraft control and maneuvering are covered later on (Chapter 6), followed by a survey of the conditions confronting humans inhabiting a restricted closed space (Chapter 7). Orbit maneuvers (including rendezvous and docking maneuvers) are described in Chapter 8. The reader will find a description of how meteorite hazards are analyzed in Chapter 9. Materials selection problems in designing a heat-stable casing for space vehicles and for re-entry, a problem of unusual complexity, is given close attention in the extended Chapter 10. Concise information on radiation shielding of space vehicles to handle ionizing radiations is found in Chapter 11, and information on propulsion nuclear reactors is found in Chapter 12. Scientific problems resolved with the aid of artificial satellites and space rockets are considered in detail in Chapters 13-15. The book ends with a list of symbols and notation, plus a copious index of subjects and authors.

---

* Translated from Atomnaya Énergiya, Vol.21, No.4, p.328, October, 1966.

† Translated from Atomnaya Énergiya, Vol.21, No.4, pp. 328-329, October, 1966.

Space Research, V. Proceedings of the Fifth International Space Science Symposium. Edited by D. G. King-Hele et al. Amsterdam, North-Holland, 1248 p, 1965. *

The book contains the proceedings of the V international conference on space research convened by COSPAR (international committee on space research) in Florence, in May 1964. A review lecture by B. Rossi (USA) on x-ray astronomy and γ-ray astronomy is followed by the texts of the 154 papers, distributed over 12 sections. All the papers appear in English, no matter what the original language, but some of them have abstracts in Russian. The first section, "Interaction of high-energy particles with the atmosphere," contains 17 papers; the second section, "Ionospheric processes and anomalies," contains 13 papers; the third section, "Effect of high-energy particles on polar aurorae," contains 10 papers; the fourth section, "Radiation belts," contains 16 papers; the fifth section, "Solar radiation and the interplanetary medium," contains 15 papers; the sixth section, "The ionosphere," contains 13 papers; the seventh section, "Structure and composition of the atmosphere," contains 15 papers. Three reports on galactic x-ray astronomy appear in section 8. The next sections on observation and dynamics of satellites offer ten and eight papers respectively. Section 11 gathers together miscellaneous papers (21 in all) not particularly related in subject material, and touching on some phase of IGY research. In this case attention is centered on the results of ionosphere observations and on studies of the earth's environment. Section 12 on studies of upper-lying layers of the atmosphere with rocket-borne and satellite-borne equipment contains 13 papers. A list of authors is appended.

Scientific Research in Space. (Eight lectures delivered at the University of London). London, Elek Books, 194 p. 1964. *

Here we have a lecture course given by leading British specialists at the University of London. The first lecture formulates the basic problems to be resolved through launching artificial earth satellites and space vehicles, and a brief description of appropriate techniques and means is included. Instruments mounted on board satellites are discussed in the second lecture. Then follows a lecture on orbits of artificial bodies near the earth and the moon, and between planets of the solar system.

A good deal of factual material is provided in the fourth lecture, on the earth's atmosphere (above and below 120 km above sea level). The fifth lecture analyzes the effect of solar electromagnetic radiation on the earth's ionosphere. Corpuscular space radiation and the interplanetary medium are discussed in the rather detailed sixth lecture. The moon and the planets are teated in the seventh lecture, which is as detailed as the sixth. The list of literature for these lectures (articles in the periodical literature for the most part) lists 25-27 titles. The book ends in a lecture on astronomical observations carried out on artificial satellites.

---

* Translated from Atomnaya Énergiya, Vol.21, No.4, p.329, October, 1966.

Space ... The New Frontier.* Washington, National Aeronautics and Space Administration, 74 p, 1964.

This NASA brochure, a popular science approach, is richly illustrated with both black/white and color photographs. There are 10 sections in the album; 1) space research and society; 2) history of space flight; 3) the solar system; 4) artificial satellites; 5) unmanned artificial satellites; 6) unmanned space vehicles for lunar exploration, and interplanetary probes; 7) manned space vehicles; 8) rocket vehicles; 9) biological space research; 10) space research techniques.

The book ends with an extended glossary of terms used in astronautics and aeronautics.

Space Radiation Effects.* (Presented at the 66th Annual Meeting of the Amer. Soc. for Testing and materials). Phila., ASTM Special Technicial Publication No. 363, 158 p, 1964.

The book contains the texts of papers and stenographic records of discussions at a symposium on the effects of space radiation on various materials; the symposium was held in June 1963; in Atlantic City. Twelve papers are grouped in two sections: a) space radiation and methods of simulating space radiation under experimental conditions; b) effects of space radiation on components and systems. The second section centers attention on radiation damage to semiconductor detectors and transistor circuitry.

The Science of Ionizing Radiation.† Edited by L. E. Etter. Springfield, Illinois, C. C. Thomas, 788 p, 1965.

The book consists of articles by leading specialists in different lines of work, and is published in the form of an encyclopedia designed to offer a general impression of advances in practically all fields of utilization of ionizing radiations. The volume contains 14 sections, each of which offers up to three articles of somehow related subject material: 1) historical reviews; 2) equipment; 3) radiation physics; 4) photographic recording techniques; 5) chemistry; 6) radiobiology; 7) application of ionizing radiations to the human organism; 8) applications in industry; 9) crystallography; 10) paleontology and archaeology; 11) anthropology; 12) radiography and graphic images; 13) applications in agriculture; 14) radiation shielding, The book is liberally illustrated with drawings, graphs, and photographs. Appendices offer a generous subject and name index.

---

* Translated from Atomnaya Énergiya, Vol.21, No.4, p.329, October, 1966.

† Translated from Atomnaya Énergiya, Vol.21, No.4, pp.329-330, October, 1966.

Chemical Oceanography. Vol. 1. Edited by J. P. Riley and G. S. Harrow, New York, Academic, 712 p, 1966. *

The first and fifth parts of this book contain data on the concentration of naturally radioactive elements in ocean water, and chapter 7 ("Dissolved gases") contains some information on radiocarbon included in CO_2 dissolved in water.

J. H. Lawrence, B. Manowitz, and R. S. Loeb. Radioisotopes and Radiation. (Recent advances in medicine, agriculture, and industry). N.Y., McGraw-Hill, XII + 134 p. 1964. *

This book, written by prominent American specialists in nuclear energy and applications, consists of a brief foreword and eight chapters. Chapter 1 describes research on medical diagnostics involving radioisotope techniques, in detail. Chapters 2 and 3 take up results of the application of ionizing radiations in medical therapy and veterinary science. Chapter 4 acquaints the reader with applications of radioactive isotopes and radioactive radiations in agriculture. Chapter 5 is devoted to radiation-induced sterilization of foodstuffs and medical instruments. The synthesis of chemical compounds is the subject of Chapter 6. Results of investigations on ionizing radiations and their applications in radiography, thickness measurements, analysis of wear, and other areas are concentrated in Chapter 7. The book ends with Chapter 8, on the utilization of radioactive isotopes in hydrology and in criminology. The monograph, along popular science lines, is splendidly illustrated with photographs.

Obmen radioizotopov v zhivotnom organizme. [Radioisotope turnover in animals]. Proceedings of the Institute of Biology of the Ural branch of the USSR Academy of Sciences, No. 46. Sverdlovsk, 160 p. 1966. *

This collection of 13 papers discusses various aspects of the metabolism in ingestion of radioactive materials by animals. Various pathways for the introduction of isotopes (intravenous, subcutaneous, intraperitoneal, orally, through the lungs) are considered, as well as the effect of a variety of physiological (age, sex, species, diet, hormonal activity, etc.), chemical, and physico-chemical factors (complexons [sequestrating agents], diuretics, sorbing colloids, cation exchange resins, etc.), on metabolism where radioactive materials are ingested, are studied. Experiments performed on an unseparated mixture of fission fragments of uranium, cesium, strontium, yttrium, cerium, zirconium, niobium, ruthenium, the whole range of rare earths, and plutonium, are described. Mice and rats were the experimental animals in this study.

* Translated from Atomnaya Énergiya, Vol.21, No.4, p.330, October, 1966.

M.D. Kamen. A Tracer Experiment. N.Y., Holt, Rinehart, & Winston, 128 p, 1964. *

This book is written in popular science style by a leading American specialist in radiometry, the author of the fundamental monograph "Radioactive isotopes in biology."

Nuclear Safety Research and Development Program (Summary Report). Washington, USAEC, 170 p, 1964. *

This report comes in five parts. A brief introduction leads into a detailed description of findings in a series of experiments studying reactor kinetics at SPERT type facilities, chemical reactions between metal and water, fission product yield from molten fuel, and testing of containment shells in simulated accidents involving total coolant loss. The third part gives the reader information on testing of reactors of the KIWI series and on the SNAPTRAN experiments simulating re-entry of radioisotope generators into the earth's atmosphere from outer space.

The fourth section contains brief reports summing up work in reprocessing, disposal, and burial of radioactive wastes in a variety of physico-chemical states. The last part analyzes the reasons and consequences of pressure vessel failure in simulated nuclear reactor safety experiments. The report is liberally illustrated.

Operational Accidents and Radiation Exposure Experience. Washington, USAEC, V+155 p, 1965. *

This report contains five chapters. The first chapter briefly runs through USAEC principles for organizing safety research, the second lists definitions of terms in use in the subsequent text. Chapter 3 offers ample statistical data on the causes of accidents which have occurred anywhere in the country and in USAEC plants. Chapter 4 systematizes this material from the standpoint of damage to materials and plant. This chapter also presents detailed tabular data on major accidents occurring in the USA in the 1963-1964 period, and information on supercriticality accidents in USAEC facilities. The short Chapter 5 contains information on USAEC plants distinguished by long-term accident-free operation. Appendices give information on all mortalities and overexposures (>15 r) suffered in the USA in radiation work.

---

* Translated from Atomnaya Énergiya, Vol.21, No.4, p.330, October, 1966.

Biological Effects of Magnetic Fields. Edited by Madeleine F. Barnothy, N.Y., Plenum Press, 324 p., 1964.

Reviewed by Yu. V. Sivintsev

Written by a large panel of specialists (31 authors in all), this book offers a consistent presentation of topics pertaining to biological effects of magnetic fields. The first part of the book analyzes these phenomena theoretically. A voluminous introduction is followed by a description of simple theoretical models of the interaction between a magnetic field and biological structures (Chapter 2), and the basic concepts applying to magnetic fields and magnetic susceptibility (Chapter 3). The short Chapter 4 presents data on the vectorial nature of the magnetic field and magnetic field gradient, and the possible application of these concepts to biomagnetic experimentation in space flight. Relationships between the magnetic field and rates of chemical reactions, and the role played by this effect in biomagnetism, are taken up in Chapter 5. The short Chapter 6 considers variation in chemical bond angle in response to applied magnetic fields. The possible effect of magnetic fields on the genetic code is analyzed in Chapter 7.

The second part of the book collects, and discusses critically, experimental data on the effect of high magnetic fields on experimental animals in vivo. In Chapter 1 of part two, the reader finds information of young mice, and in Chapter 2 information on the inhibition by a magnetic field of malignant tumors transplanted in mice; in Chapter 3, information on magnetogenic hematological changes in mice. Chapter 4 briefly presents some particularly interesting information on reduced mortality in animals exposed to ionizing radiations when they are exposed first to the effects of magnetic fields. Chapter 5 considers this effect in connection with the prolonged lifespan of animals suffering from malignant tumors and so treated, and Chapter 6 deals with tissue regeneration and wound healing in magnetically treated animals. Chapter 7 goes into particular detail on magnetic-field effects on drosophila flies and on sarcoma tumor cells, and the possible mechanisms at work in these reactions. Detailed material on magnetotropism can be found in Chapter 8. The next section (Chapter 9) analyzes experimental data on the relationship between plant growth rate and magnetic field strength. Chapter 10 offers a brief resume of data on magnetic field effects on the central nervous system. Part II concludes with Chapter 11, which describes experiments on survival of various animal species in magnetic fields of 140,000 Oe intensity.

Part III presents material on the effects of strong magnetic fields on biological objects in vitro. Respiration of tissues (Chapter 1), agglutination of human blood stream erythrocytes (Chapter 2), inhibition of bacterial growth in paramagnetic fields (Chapter 3) and in homogeneous fields (Chapter 4), stepped-up chemical activity of intact trypsin (Chapter 5) and of partially inhibited trypsin (Chapter 6), are discussed.

The fourth part of the book publishes information on the biological effects of very weak magnetic fields: Chapter 1 on the orientation of animals with respect to magnetic lines of force, Chapter 2 on a possible relationship between the "magic wand" (the Dowser) of underground water diviners and weak magnetic field gradients, and Chapter 3 on proposed mechanisms operative in the navigation of migrating birds.

The bibliographical section (part five of the book) occupies 15 pages of text in great detail. The literature cited is grouped by topics in several sections. The monograph ends in notes of information on the authors and a detailed subject index.

Translated from Atomnaya Énergiya, Vol.21, No.4, pp.330-331, October, 1966.

Physical Processes in Radiation Biology. Edited by L. Angenstein et al. New York, Academic 378 p, 1964. *

Reviewed by Yu. V. Sivintsev

The book publishes reports given at the May 1963 international symposium on the subject at the University of Michigan. Most of the volume is taken up by 20 review papers prepared by leading specialists in biophysics and radiobiology. The thematic content of these papers is quite broad: from primary processes of absorption, excitation, and transfer of energy in solids to scintillation properties of liquids and the photodynamic effects in biological systems. The last part of the book consists of a stenogram of a general discussion at the symposium. The book ends with subject index and authors index.

Radiation Accidents and Emergencies in Medicine, Research, and Industry. Edited by L. H. Lanzl, J. H. Pingel, and J. H. Rust. Springfield, Illinois, C. C. Thomas, 328 + XIV p, 1965. *

Reviewed by Yu. V. Sivintsev

This volume contains the proceedings of a symposium on radiation accidents in medicine, science, and industry held under the auspices of the North American Society for Radiation Safety, in Chicago, December 1963.

A brief introduction leads into the texts of 28 papers grouped in eight sections: accidents involving ionizing radiations or radioactive materials (2 papers); initial operations in accidents (4 papers); first aid to accident victims (4 papers); deactivation of buildings and equipment (4 papers); special problems: radiation monitoring, dosimetry, allowable radiation levels (4 papers); administrative problems in radiation accidents (4 papers); governmental services and regulations (4 papers), and ethical problems (2 papers). The book ends with detailed subject index and an authors index.

Radioactivity in Man. Proceedings of second symposium sponsored by Northwestern University Medical School and American Medical Association. Edited by G.R. Meneely and J. M. Linde. Springfield, Illinois, C. C. Thomas, 616 p + 48 p. *

Reviewed by Yu. V. Sivintsev

This book contains the proceedings of the II interamerican (actually international) symposium on methods for measuring activity in the human body and the effect of γ-ray emitters deposited in the human body on the health of the organism. The book comprises eight sections, the first of which includes a list of participants and introductory remarks by the chairmen of the 17 symposium sessions (48 pages). The basic content of the book consists of 44 papers distributed over seven sections: instruments, techniques for measurement and calibration (13 papers); composition of body tissues and potassium content (7 papers);

* Translated from Atomnaya Énergiya, Vol.21, No.4, p.331, October, 1966.

cobalt metabolism (5 papers); iron metabolism (4 papers); miscellaneous topics (3 papers); fission fragment metabolism (9 papers); social and industrial aspects of deposition of radioactive isotopes in the human body (3 papers). Illustrated with a large number of graphs and photographs, the book ends with a list of authors (10 pages) and a systematic subject index (21 pages).

Proceedings of Conference on Mechanisms of the Dose Rate Effect of Radiation at the Genetic and Cellular Levels.* Oiso, November 4-7 1964. Osaka, the Genetics Society of Japan, 280 p, 1965.

The book presents 19 papers by Japanese and American radiobiologists delivered and discussed at the November 1964 conference at Oiso (Japan). Results of investigations on plants, drosophila, spermatogonia of mice and mammalian cells, with x-rays, γ-rays, and neutrons, are reported. The quantitative criteria studied are such factors as inactivation of bacteria, chromosomal aberrations, survival rate of spermatogonia populations, recovery of the entire organism from radiation injury, etc. A list of participants, the conference agenda, and a resolution adopted are appended to the text. The most timely scientific research on the mechanism at work in the effect of the dose rate of ionizing radiations at the genetic and molecular levels is pointed out in the resolution adopted.

Handbuch der medizinischen Radiologie.† Band 1, Teil 2. Physikalische Grundlagen und Technik. [Handbook of Medical Radiology. Volume 1, part 2. Physical Fundamentals and Techniques]. Berlin, Springer Verlag, 346 p, 1965.

This is a basic handbook forming part of a multivolume edition handbook series on medical radiology, prepared and compiled by a group of prominent German specialists in x-ray techniques and radiology. The monograph comprises three large sections: 1) methods for generating x-radiation (84 pages); 2) methods for generating ultrahard x-radiation (40 pages); 3) techniques for medical utilization of x-radiation (200 pages). Each of these sections is generously illustrated with photographs and appended with a list of recommended literature. Detailed indexes of authors and subjects are accompanied by a German-English glossary of terms employed in the text.

---

* Translated from Atomnaya Énergiya, Vol.21, No.4, pp.331-332, October, 1966.

† Translated from Atomnaya Énergiya, Vol.21, No.4, p.332, October, 1966.

G. J. Plaatz. Medical X-Ray Technique. Eindhoven, Philips Technical Library, XII + 484 p, 1965. *

The third edition of this handbook is extensively revised and expanded. In this new edition comprising 24 chapters, a slight appendix, and a detailed subject index, the first two chapters deal with the design and varieties of x-ray tubes, and the third chapter covers the properties of x-radiation. Methods of forming projections and laws governing them are discussed in Chapter 4. The fifth chapter presents information on the perception of detail in an x-ray plate or image. Methods for improving acutance and contrast are analyzed in Chapters 6 and 7. Qualitative characteristics of fluoroscopic screens and x-ray photographic emulsions are covered in Chapter 8.

The next chapter presents recommendations on photographic laboratory and plate development techneques and equipment. Irradiation is discussed in detail in Chapters 10-12, and general and special radiographic techniques in Chapters 13 and 14. Equipment for diagnostic plates is described in Chapters 15 and 16. Information on biological effects of irradiation can be found in Chapter 17. The next sections deal with general problems of dosimetry (Chapter 18) and concretely x-ray dosimetry (Chapter 19). Different methods in the therapeutic use of x-radiation take up 3 chapters, covering exposure of superficial layers of the body (Chapter 20), depth exposures (Chapter 21), and contact exposure (Chapter 22). Chapter 23 furnishes information on therapy by means of radioactive substances, and Chapter 24 deals with radiation hazards and measures of protection taken when using x-radiation for diagnosis and therapy. The appendix lists data on image brightness enhancement and on applications for television in x-ray work.

Radioactive Fallout, Soils, Plants, Foods, Man. Edited by Eric B. Fowler. Amsterdam, Elsevier, Publ. Co., 318 p, 1965.

The 11 chapters of this book trace the path of intake of radioactive materials originating in nuclear weapons tests into the human organism. The first chapter characterizes contamination of the biosphere of uranium fission fragments (predominantly Sr^{90} and Cs^{137}). The next two chapters deal with these same emitters in soils: Chapter 2 considers the ion exchange properties of soils with respect to Sr^{90} taken up by plants, and Chapter 3 deals with general interrelations of soils, flora, and radioactive isotopes. Chapters 4 and 5 discuss pathways of intake of radioactive materials through the roots or foliage of different plants. These chapters contain a wealth of factual material and supply extenisve bibliographies (78 and 72 titles, respectively).

The book focuses particular attention on the results of investigations of foodstuffs. Four chapters are reserved for this point. Chapter 6 presents a broad survey of work on the content of naturally radioactive substances in food products (212 references). Chapter 7 offers data on radioactive contamination in milk, and Chapter 8 deals with the influence of various transfer mechanisms on radioactive contamination. Chapter 9 contains a review of information available on the ingestion of radioactive materials into the human organism from consumed foodstuffs (141 references). Chapter 10 on radioactive substances present in the human body is quite detailed and informative. The book ends with Chapter 11 on methods for measuring trace quantities of fission fragments in different samples. A glossary and subject index are appended to the text.

---

* Translated from Atomnaya Énergiya, Vol.21, No.4, p.332, October, 1966.

STUDIES OF NUCLEAR REACTIONS

"Trudy" Volume 33 of the Lebedev Physics Institute Series

Edited by Academician D. V. Skobel'tsyn

Director, Lebedev Physics Institute
Academy of Sciences of the USSR

Translated from Russian

Contains nine articles prepared by leading research workers at the Lebedev Physics Institute, one of the largest research centers of the Soviet Union, on such topics as the elastic scattering of charged particles on some light nuclei, interactions of protons and tritium, and inelastic scattering of neutrons on light and medium nuclei. Other articles deal with quantum mechanics and the theory of particle interactions, scattering, and nuclear reactions.

CONTENTS: Investigation of the interaction of protons with tritium at energies below the threshold of the (p,n)-reaction, *A. B. Kurepin* • Investigation of elastic scattering of charged particles on several light nuclei at low energies, *Yu. G. Balashko* • Analysis of the *p*—T interaction above the threshold of the T (p,n) He^3 reaction, *Yu. G. Balashko and I. Ya. Barit* • Investigation of inelastic scattering of 14 Mev neutrons on light and medium nuclei, *B. A. Benetskii* • Theory of nuclear reactions and the many-body problems, *G. M. Vagradov* • Quantum-mechanical fundamentals of the theory of nuclear reactions, *V. I. Serdobol'skii* • On the phases of the elastic n—d-scattering process, *V. N. Efimov and S. A. Myachkova* • Method of time correlation functions in the description of the interaction of various particles with a complex system, and its applications, *M. V. Kazarnovskii* • Some possible ways of increasing the yield of nuclear reactions, *L. N. Katsaurov*.

222 pages 1966 $22.50
87 ill., 28 tables

Previously published in the Lebedev Physics Institute series:

Volume 25: Optical Methods of Investigating Solid Bodies
188 pages 1965 $22.50

Volume 26: Cosmic Rays
254 pages 1965 $27.50

Volume 27: Research in Molecular Spectroscopy
205 pages 1965 $22.50

In preparation:

Volume 28: Radio Telescopes
173 pages 1966 $22.50

Volume 29: Quantum Field Theory and Hydrodynamics
Approx. 240 pages 1967 $27.50

Volume 30: Physical Optics
Approx. 250 pages 1966 $27.50

Volume 31: Quantum Radiophysics

Volume 32: Plasma Physics

Volume 34: Photomesonic and Photonuclear Processes

Volume 36: Photodisintegration of Nuclei in the Giant Resonance Region

Volume 37: Electrical and Optical Properties of Semiconductors

---

OF INTEREST TO: nuclear physicists and theoretical and mathematical physicists investigating nuclear interactions.

CONSULTANTS BUREAU 227 West 17th Street, New York, New York 10011

A DIVISION OF PLENUM PUBLISHING CORPORATION

Declassified and Approved For Release 2013/03/12 : CIA-RDP10-02196R000700040004-0